# Southeastern Geology: Volume 24, No. 3 November 1983

Edited by: S. Duncan Heron, Jr.

**Abstract**

Academic journal published quarterly by the Department of Geology, Duke University.

# SOUTHEASTERN GEOLOGY

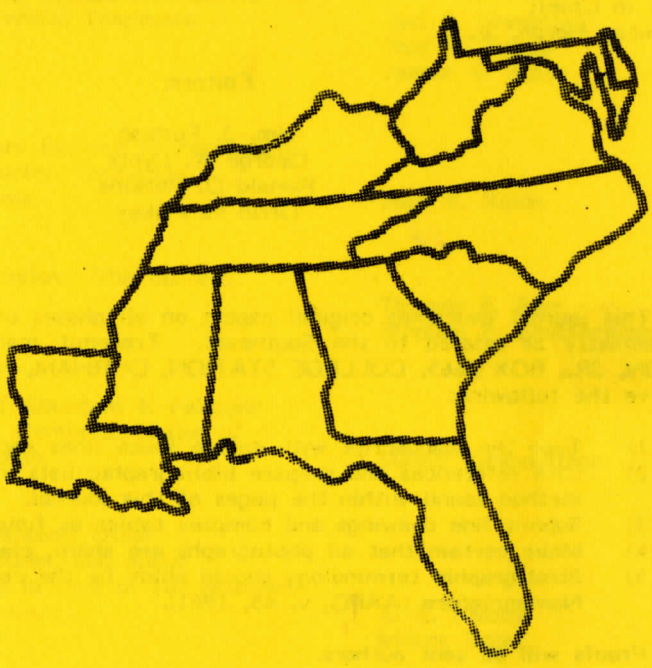

PUBLISHED AT DUKE UNIVERSITY DURHAM, NORTH CAROLINA

VOL. 24, NO. 3 NOVEMBER, 1983

SOUTHEASTERN GEOLOGY

PUBLISHED QUARTERLY

AT

DUKE UNIVERSITY



This journal welcomes original papers on all phases of geology, geophysics, and geochemistry as related to the Southeast. Transmit manuscripts to S. DUNCAN HERON, JR., BOX 6665, COLLEGE STATION, DURHAM, NORTH CAROLINA 27708. Observe the following:

1) Type the manuscript with double space lines and submit in duplicate.
2) Cite references and prepare bibliographic lists in accordance with the method found within the pages of this journal.
3) Submit line drawings and complex tables as finished copy.
4) Make certain that all photographs are sharp, clear, and of good contrast.
5) Stratigraphic terminology should abide by the code of Stratigraphic Nomenclature (AAPG, v. 45, 1961).

Proofs will be sent authors.

Reprints must be ordered prior to publication; prices available upon request. Subscriptions to Southeastern Geology are $8.00 per volume (US and Canada) $10.00 per volume (foreign). Inquiries should be sent to: SOUTHEASTERN GEOLOGY, BOX 6665, COLLEGE STATION, DURHAM, NORTH CAROLINA 27708. Make checks payable to: Southeastern Geology.

SOUTHEASTERN GEOLOGY

Table of Contents

Vol. 24, No. 3

November, 1983

1. Geochemistry of the Chattanooga Shale, DeKalb County, Central Tennessee — Joel S. Leventhal, Paul H. Briggs, James W. Baker — 101

2. Geochemical Factors Related to Formation of Coals in the Norton Formation, Southwestern Virginia — Jack E. Nolde — 117

3. Barrier Island Dynamics: The Eastern Shore of Virginia — Thomas E. Rice, Stephen P. Leatherman — 125

4. The Significance of Abundant K-Feldspar in Potassium-Rich, Cambrian Shales of the Appalachian Basin — Vishnu Ranganathan — 139

5. The Clingman Lineament, Other Aeromagnetic Features, and Major Lithotectonic Units in Part of the Southern Appalachian Mountains — A. E. Nelson, Isidore Zeitz — 147

# GEOCHEMISTRY OF THE CHATTANOOGA SHALE, DEKALB COUNTY, CENTRAL TENNESSEE

JOEL S. LEVENTHAL
PAUL H. BRIGGS
JAMES W. BAKER

*U.S. Geological Survey, Federal Center, Denver, Colorado, 80225*

## ABSTRACT

The Upper Devonian Chattanooga Shale of Tennessee is of interest because of its unusual enrichment in trace elements, especially uranium. A new chemical analysis of major, minor, and trace elements is presented. Stable isotopes of carbon (organic) show $\delta^{13}C \sim -29$ °/00 and for total sulfur show -21 to -27 °/00 $\delta^{34}S$. The organic matter was found to range from dominantly marine (Dowelltown Member) to dominantly terrestrial (Gassaway Member) by extraction-column chromatography-gas chromatography and also by prolysis-gas chromatography of kerogen. Trace elements, U, Mo, Co, Zn, Cu, Ni, V, As, and Hg are enriched in the organic- and sulfide-rich units. This enrichment can be related to a euxinic depositional environment, to a very slow sedimentation rate (~2mm/1000 years), to type of organic matter that varied from mainly marine to terrestrial, and to source of the metals that shows abundance variations and that was, at least in part, from volcanic ash layers.

## INTRODUCTION

The Chattanooga Shale of central Tennessee was last intensively studied 20-25 years ago (Swanson, 1953; Conant and Swanson, 1961; Breger and Brown, 1962, 1963; Bates and Strahl, 1957; Strahl, 1958) principally as a possible source of uranium, before the sandstone ore deposits of Wyoming, Texas, and New Mexico were evaluated. Since 1976, new attention has been given to the Devonian shales of the Appalachian basin (Oliver and others, 1969) as a source of natural gas (Schott and others, 1978). These shales also have been studied for sources of energy and minerals either by surface or *in situ* processing (Matthews, 1982).

Despite this interest in black shales, among which the Chattanooga is generally mentioned, no modern detailed chemical analysis of the Chattanooga Shale is available in the literature. This paper reports new chemical analyses and a geochemical interpretation of the genesis of the Chattanooga Shale based on set of analyses from a core sample taken in 1953 in the Youngs Bend area, DeKalb County, Tennessee. The Chattanooga Shale is a unit that is related stratigraphically to the New Albany Shale, Ohio Shale, Olentangy Shale of Kentucky and Ohio, and Java, West Falls, Sonyea and Genesee Formations of New York (Oliver and others, 1969). The Chattanooga Shale is unique in that it represents much slower rates of deposition than the other units. These chemical data can be compared with similar data for stratigraphically equivalent rocks from other parts of the Appalachian, Michigan, and Illinois basins (Leventhal, 1978, 1979b, 1980).

## SAMPLES

The samples reported here are from the remaining quarter of core YB-15 (35° 55' N., 85° 45' W.), DeKalb County, Tennessee, which was from one of 21 holes drilled on a 5 by 30 km grid (Fig. 1) by the U.S. Bureau of Mines and were logged and described by the U.S. Geological Survey (Kehn, 1955). Partial chemical analyses were reported by the U.S. Geological Survey (Vine and Tourtelot, 1970; Brown, 1975) and Pennsylvania State University (Strahl, 1958). Core YB-15 encountered the Chattanooga Shale at a depth of 145.5-175.3 feet. Some cores were logged in great lithologic detail; this one was not. The Gasaway and Dowelltown Members and the units within them were identified at that time by T. M. Kehn (field description, 1953). The 21 cores were very

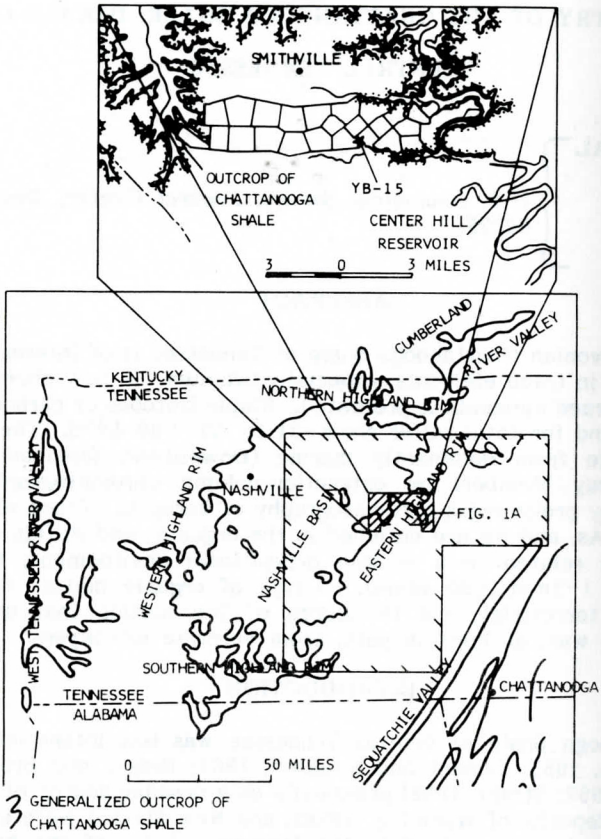


*Figure 1. Location map of Chattanooga Shale in central Tennessee and adjacent states showing outcrop. Figure 1a, (inset) shows location of 1953 coring grid and core YB-15 (from Kehn, 1951).*

similar in their stratigraphy (Fig. 2) and uranium content (the only parameters systematically determined) (Swanson and Kehn, 1955; Kehn, 1955). Subsequent work (Conant and Swanson, 1961; Swanson, 1960, 1961; Breger and Brown, 1962, 1963) established that uranium is closely related to organic content. From the stratigraphy, extensive uranium determinations, and limited work on organic contents it may be seen that the Chattanooga Shale in central Tennessee is relatively uniform. Therefore, core YB-15 is very similar to the other cores and is also representative of the Chattanooga Shale in central Tennessee. Reexamination of the core by Leventhal (Table 1) confirmed the earlier identifications of the stratigraphic units.

The 24 samples (Table 1) were 2- to 5-cm pieces from a 7- to 14-(or more) cm interval that had uniform physical appearance (color and lamination mode). By this sampling method, a compromise is made between sampling individual laminae (1 mm or less thick, which would be impossible to sample) and a channel or composite sample taken by the foot or stratigraphic unit. However, there is still variation, even on a several-inch scale, as evidenced by several adjacent samples analyzed for organic carbon (see Organic Geochemistry section).

Although the core was collected ~26 years ago, except for a slight oxidation of the sulfides at the surface to a white powdery material (especially in the upper unit of the Gassaway Member), the core is generally unfractured, unoxidized, and unaltered. A damp towel removes the white powder, revealing unweathered sulfide minerals and laminations.

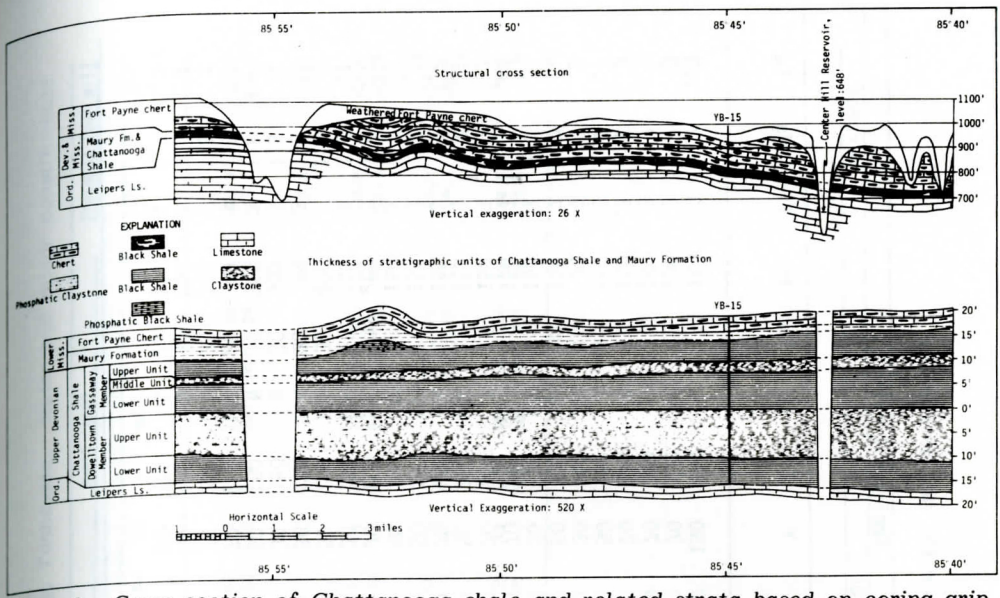


*Figure 2. Cross section of Chattanooga shale and related strata based on coring grip in DeKalb County, Tennessee; note core YB-15 on which this paper is based (from Kehn, 1955).*

*Table 1. Description of samples for DeKalb County Core YB-15 (top of Chattanooga Shale was 145 feet below surface).*

| Sample number | Depth below top of Chattanooga (ft) | (inches) | Comments (All units are shale) |
|---|---|---|---|
| | | | Upper unit, Gassaway Member |
| 1 | 0 | 2 | black finely laminated shale |
| 2 | 0 | 9 | black laminated shale with pyrite lens |
| 3 | 1 | 6 | black laminated shale |
| 4 | 2 | 10 | black laminated shale (thicker laminations than samples 1-3 |
| 4a | 3 | 2 | black laminated shale, thicker laminations (than 4), calcite in fracture, small pyrite |
| 5 | 4 | 3 | massive black |
| | 4 | 6 1/2 | Contact between upper and middle units, Gassaway Member |
| 6 | 5 | 5 | gray/dark-gray laminations |
| 7 | 5 | 9 | dark-gray laminations |
| | 6 | 11 1/2 | Contact between middle and lower Gassaway |
| 8 | 7 | 6 | black shale with pyrite, finely laminated |
| 8a | 9 | 6 | black shale with pyrite |
| 9 | 10 | 9 | massive black shale with pyrite |
| 10 | 12 | 9 | massive black shale with pyrite |
| 11 | 13 | 5 | massive black shale with pyrite, small pyrite nodule |
| | 14 | 10 | Contact between lower unit of Gassaway Member and upper unit of Dowelltown Member |
| 12 | 15 | 1 | gray shale |
| | 15 | 5-6 1/4 | Center Hill Ash Bed (1-1/4 inches thick) |
| 13 | 16 | 1 | gray shale, small pyrite |
| 14 | 19 | 0 | gray, 1/2-inch thick laminae |
| 15 | 20 | 6 | dark gray |
| 16 | 21 | 6 | gray, 1 to 2-inch thick laminae |
| 17 | 23 | 7 | gray |
| | 24 | 2 | Contact between upper and lower units, Dowelltown Member |
| 18 | 25 | 1 | black, finely laminated |
| 19 | 25 | 10 | black, irregular laminations |
| 20 | 27 | 2 | black, finely laminated |
| 21 | 28 | 6 | black, pyrite layer |
| 22 | 29 | 3 | black, laminations |
| | 29 | 8 | base of Chattanooga Shale |

*Table 2. Chemical analysis of Chattanooga Shale from DeKalb County, Tennessee (N, not detected).*

| | Quantitative | | | | Semi-quantitative | | | | | | | | | | | | | | | |
|---|---|---|---|---|---|---|---|---|---|---|---|---|---|---|---|---|---|---|---|---|
| | ppm | percent | | | parts per million | | | | | | | | | | | | | percent | | |
| | U | Org-C | S | $CO_3$-C | Co | Cr | Cu | La | Mo | Ni | Pb | V | Y | Zr | Ce | Ga | Mn | Ti | Mg | Ca |
| DK-1 | 105 | 14.32 | 9.42 | .01 | 300 | 30 | 150 | 100 | 70 | 700 | 70 | 300 | 150 | 150 | 150 | 15 | 150 | .3 | .7 | .3 |
| DK-2 | 97 | 14.97 | 7.70 | .01 | 70 | 30 | 150 | 70 | 200 | 300 | 70 | 150 | 70 | 150 | 100 | 15 | 100 | .3 | .7 | .3 |
| DK-3 | 116 | 14.97 | 7.37 | .01 | 70 | 30 | 150 | 70 | 150 | 150 | 30 | 150 | 70 | 150 | N | 15 | 150 | .3 | .7 | .3 |
| DK-4 | 92.6 | 13.11 | 7.06 | .03 | 70 | 30 | 150 | 70 | 150 | 150 | 20 | 150 | 70 | 200 | N | 15 | 150 | .3 | .7 | .3 |
| DK-4a | 83.7 | 12.12 | 6.71 | .14 | 70 | 30 | 150 | 30 | 150 | 150 | 20 | 150 | 50 | 150 | N | 15 | 150 | .3 | .7 | .7 |
| DK-5 | 78.8 | 12.10 | 4.65 | .03 | 70 | 70 | 150 | 70 | 150 | 150 | 15 | 150 | 30 | 150 | 100 | 15 | 70 | .3 | .7 | .5 |
| DK-6 | 45.3 | 1.81 | 1.38 | .01 | 30 | 70 | 70 | 70 | 30 | 100 | 20 | 200 | 50 | 300 | 100 | 30 | 150 | .7 | .7 | .15 |
| DK-7 | 37.5 | 4.08 | 2.41 | .01 | 30 | 70 | 150 | 70 | 30 | 150 | 15 | 200 | 30 | 150 | 100 | 15 | 150 | .7 | 1. | .7 |
| DK-8 | 75.4 | 14.2 | 8.45 | .01 | 50 | 30 | 150 | 50 | 150 | 150 | 30 | 150 | 70 | 200 | N | 15 | 150 | .3 | .7 | .3 |
| DK-8a | 64.1 | 13.51 | 4.73 | .01 | 50 | 50 | 200 | 50 | 70 | 150 | 30 | 150 | 70 | 200 | N | 15 | 150 | .3 | .7 | .3 |
| DK-9 | 63.8 | 10.25 | 3.31 | .01 | 50 | 70 | 150 | 70 | 100 | 150 | 30 | 200 | 50 | 150 | 100 | 15 | 150 | .3 | .7 | .15 |
| DK-10 | 74 | 10.86 | 4.34 | .13 | 50 | 50 | 150 | 70 | 70 | 150 | 30 | 150 | 70 | 150 | 100 | 15 | 150 | .3 | .7 | .7 |
| DK-11 | 80.4 | 17.29 | 4.31 | .03 | 30 | 70 | 200 | 70 | 150 | 150 | 30 | 200 | 50 | 150 | 100 | 15 | 150 | .3 | .7 | .15 |
| DK-12 | 37.2 | 1.32 | 1.00 | .21 | 15 | 70 | 100 | 70 | 7 | 70 | 20 | 150 | 50 | 150 | 100 | 30 | 150 | .3 | 1.5 | .5 |
| DK-13 | 17.5 | 2.07 | .86 | .23 | 15 | 70 | 150 | 70 | 15 | 100 | 30 | 150 | 70 | 200 | 100 | 30 | 200 | .7 | 1.5 | .7 |
| DK-14 | 9.18 | .65 | 1.50 | .52 | 15 | 70 | 150 | 70 | 7 | 70 | 15 | 150 | 30 | 150 | 100 | 20 | 150 | .3 | 1.5 | .7 |
| DK-15 | 16.5 | 5.36 | 1.68 | .14 | 20 | 100 | 150 | 70 | 30 | 150 | 20 | 300 | 50 | 200 | 100 | 30 | 200 | .7 | 1.5 | .3 |
| DK-16 | 10.9 | 6.76 | 1.47 | .14 | 15 | 70 | 150 | 70 | 7 | 70 | 20 | 150 | 30 | 150 | N | 30 | 150 | .3 | 1.5 | .3 |
| DK-17 | 10.5 | 2.32 | 1.29 | .44 | 15 | 70 | 150 | 30 | 7 | 70 | 20 | 150 | 30 | 150 | N | 30 | 300 | .3 | 1.5 | .7 |
| DK-18 | 31.7 | 9.83 | 1.89 | .37 | 15 | 50 | 300 | 30 | 30 | 150 | 20 | 150 | 50 | 150 | N | 15 | 300 | .3 | 1.5 | 1. |
| DK-19 | 43.1 | 8.53 | 3.15 | .42 | 30 | 70 | 150 | 70 | 70 | 150 | 30 | 200 | 70 | 150 | 100 | 20 | 300 | .3 | 1.5 | .7 |
| DK-20 | 43.4 | 6.71 | 2.54 | .07 | 15 | 150 | 300 | 70 | 30 | 300 | 30 | 700 | 70 | 200 | 150 | 20 | 150 | .7 | 1.5 | .3 |
| DK-21 | 41.1 | 9.91 | 4.50 | .29 | 30 | 70 | 150 | 70 | 70 | 300 | 30 | 500 | 50 | 150 | 100 | 30 | 200 | .3 | 1. | .7 |
| DK-22 | 46.1 | 13.13 | 3.86 | .17 | 30 | 70 | 200 | 50 | 70 | 300 | 30 | 300 | 50 | 70 | 100 | 20 | 300 | .3 | 1. | .7 |

*Na all 0.7 percent except DK-8 0.5 percent.

DK-1 3 ppm Ag

*Table 3. Chemical and isotopic analysis of Chattanooga Shale from DeKalb County, Tennessee. Major and minor constitutents.*

| | Semi-Quant XRF (percent) | | | | | | | | Quant (percent) | | Quant (ppm) | | | | | | | | Isotopes (per mil) | |
|---|---|---|---|---|---|---|---|---|---|---|---|---|---|---|---|---|---|---|---|---|
| Sample | $SiO_2$ | $Al_2O_3$ | FeO | $K_2O$ | $TiO_2$ | CaO | $Na_2O$* | MgO* | S | Organic matter | $CO_2$ | Mn | As | Cd | Hg | Mo | Zn | Cu | U | $\delta^{13}C$ | $\delta^{34}S$ |
| Upper Gasaway | | | | | | | | | | | | | | | | | | | | | |
| DK 2 | 49 | 10 | 10.8 | 3.6 | .7 | .5 | .9 | 1.2 | 7.7 | 19.5 | <.04 | 125 | 81 | 1 | 0.23 | 350 | 440 | 85 | 97 | -29.0 | -26.6 |
| 5 | 55 | 11 | 7.8 | 3.9 | .8 | .5 | .9 | 1.2 | 4.6 | 15.7 | .11 | 150 | 50 | 1 | 0.18 | 220 | 300 | 99 | 79 | -29.1 | -26.3 |
| Middle Gasaway | | | | | | | | | | | | | | | | | | | | | |
| 7 | 61 | 15 | 4.9 | 4.9 | .8 | .6 | .7 | 1.2 | 2.4 | 5.3 | <.04 | 190 | 32 | <1 | 0.14 | 62 | 160 | 72 | 38 | -29.0 | -24.3 |
| Lower Gasaway | | | | | | | | | | | | | | | | | | | | | |
| 9 | 57 | 13 | 5.8 | 4.5 | .8 | .8 | .9 | 1.2 | 3.3 | 13.3 | <.04 | 130 | 31 | 1 | 0.24 | 130 | 220 | 145 | 64 | -28.9 | -27.2 |
| 11 | 48 | 13 | 7.3 | 4.3 | .7 | .3 | .9 | 1.2 | 4.3 | 22.5 | .11 | 140 | 38 | 3 | 0.16 | 250 | 310 | 184 | 80 | -28.5 | -25.4 |
| Upper Dowelltown | | | | | | | | | | | | | | | | | | | | | |
| 14 | 60 | 17 | 4.4 | 4.9 | .9 | 1.5 | .9 | 2.5 | 1.5 | 0.9 | 1.9 | 360 | 14 | <1 | .09 | 6 | 125 | 76 | 9.2 | -28.0 | -26.0 |
| 16 | 60 | 17 | 4.5 | 5.0 | .9 | .8 | .9 | 2.5 | 1.5 | 8.8 | .5 | 305 | 12 | <1 | 0.10 | 6 | 115 | 95 | 11. | -29.1 | -21.2 |
| Lower Dowelltown | | | | | | | | | | | | | | | | | | | | | |
| 19 | 53 | 14 | 5.6 | 5.0 | .8 | 1.4 | .9 | 2.5 | 3.2 | 11.1 | 1.5 | 510 | 30 | <1 | 0.17 | 120 | 145 | 170 | 43 | -29.6 | -25.3 |
| 21 | 49 | 14 | 7.3 | 4.5 | .7 | 1.1 | .9 | 1.7 | 4.5 | 12.9 | 1.1 | 350 | 35 | 3 | 0.23 | 160 | 325 | 221 | 41 | -29.6 | -23.3 |

$P_2O_5$ <1.0% in all samples
*Emission spectroscopy
_____recalculated from original: organic C x 1.3; $CO_3$-C x 4; and $Fe_2O_3$ x 0.9

## ANALYTICAL METHODS AND RESULTS

Table 2 gives the results for samples analyzed by several analytical techniques; semiquantitative emission spectroscopy was used for most of the major and minor elements. Table 3 gives quantitative data for minor and trace elements, and semiquantitative data for major elements on 9 of the samples; isotopic data and organic geochemistry analyses will be discussed in a subsequent section. The analytical methods and their precision and accuracy are given in an earlier report (Leventhal and others, 1978). Total C and S were measured by high-temperature combustion, carbonate C by titration and organic C by difference. Uranium was measured by delayed neutron analysis. Semiquantitative determination of $SiO_2$, $Al_2O_3$, $Fe_2O_3$ (recalculated as FeO), $TiO_2$, and $K_2O$ were obtained by X-ray fluorescence on the ashed sample. Nickel, Cu, Zn, Co, and V were measured either by semiquantitative emission spectroscopy or by atomic-absorption spectrophotometry. Mercury and As were measured by flameless atomic-absorption spectrophotometry. Molybdenium was determined by emission spectroscopy or inductively-coupled-plasma spectroscopy. In general, based on splits and replicates, the results are precise to the following degree (in percent):

| | |
|---|---|
| ±2-5 | U, S, organic C |
| ±5-10 | Mn, Cu, Zn, carbonate C |
| | Mo, $Fe_2O_3$, As, Hg, Zn, $SiO_2$, $Al_2O_3$, CaO, $K_2O$, $TiO_2$ |
| ±33 | Semiquantitative emission spectroscopy results, Cd |

## DISCUSSION OF RESULTS

The significance of variations in amounts of the major elements are obscured in Table 3 because of substantial amounts of organic C, S, and, in some instances, carbonate. In order to make the major element results comparable, the organic matter (organic carbon X 1.3), sulfur, sulfide iron (S X 55/64) and carbonates (carbonate C X 44/12) are subtracted from the results, and the other major elements recalculated to 100 percent. The organic-, sulfide- and carbonate-free recalculated values are shown in Table 4. The upper unit of the Gassaway Member (samples 2 and 5) has higher $SiO_2$

*Table 4. Recalculated chemical composition of selected samples.*

| Member and Sample No. | (in percent) $SiO_2$ | $Al_2O_3$ | FeO | $K_2O$ | $TiO_2$ | CaO | $Na_2O$ | MgO |
|---|---|---|---|---|---|---|---|---|
| Upper unit, Gassaway | | | | | | | | |
| 2 | 70.0 | 14.3 | 5.8 | 5.1 | 1.0 | 0.71 | 1.3 | 1.7 |
| 5 | 71.4 | 14.3 | 4.9 | 5.1 | 1.0 | .65 | 1.2 | 1.6 |
| Middle unit, Gassaway | | | | | | | | |
| 7 | 70.1 | 17.2 | 3.2 | 5.6 | .92 | .69 | .8 | 1.4 |
| Lower unit, Gassaway | | | | | | | | |
| 9 | 70.3 | 16.0 | 3.6 | 5.6 | .99 | .99 | 1.1 | 1.5 |
| 11 | 66.7 | 18.1 | 4.9 | 6.0 | .97 | .42 | 1.3 | 1.7 |
| Upper unit, Dowelltown | | | | | | | | |
| 14 | 66.1 | 18.7 | 3.4 | 5.4 | .99 | 1.7 | 1.0 | 2.8 |
| 16 | 66.5 | 18.8 | 3.5 | 5.5 | 1.0 | .89 | 1.0 | 2.8 |
| Lower unit, Dowelltown | | | | | | | | |
| 19 | 65.9 | 17.4 | 3.5 | 6.2 | 1.0 | 1.7 | 1.1 | 3.1 |
| 21 | 65.1 | 18.6 | 4.5 | 6.0 | .93 | 1.5 | 1.2 | 2.3 |

and lower $Al_2O_3$ than the other units in the Gassaway; the Dowelltown Member has lower $SiO_2$ and higher $Al_2O_3$. These results may indicate there were several sources of quartz or amounts of different clays present (Hosterman and Whitlow, 1981), the Dowelltown being more clay-rich relative to the more quartz-rich upper unit of the Gassaway (Strahl and others, 1954, in Conant and Swanson, 1961, p. 46).

Figure 3 shows a Fe versus S plot (using quantitative data from the 9 samples on Table 3), which shows that increases in both elements are related, either because a constant fraction of the Fe (present in the seawater or sediment initially) was subjected to sulfidization, or because both the Fe and S were introduced together above the ~3 percent Fe present in clays as indicated by the intercept in Figure 3. The linear-least-squares treatment shows a correlation coefficient (r) of 0.98.

Figure 4 shows a down-hole plot of organic C, U, and S (all quantitative results)

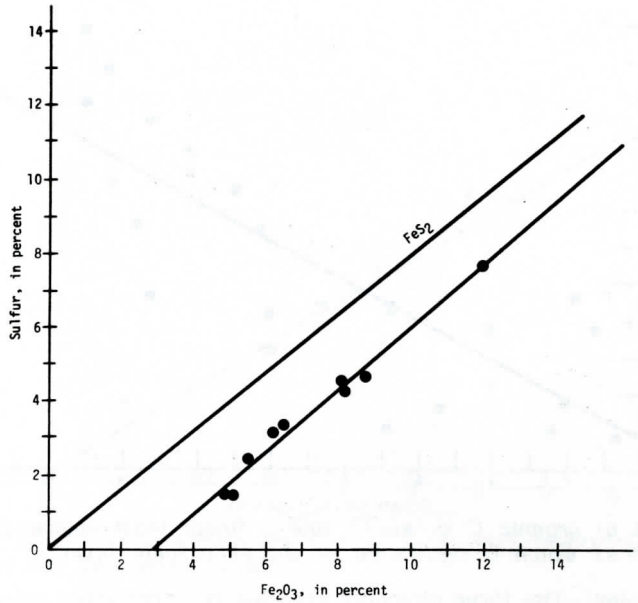


*Figure 3. Plot of S versus Fe (as $Fe_2O_3$) for 9 samples from the core YB-15, DeKalb County, Tennessee. Line through points is linear least-squares-fit; correlation coefficient, r, = 0.98. Line, $FeS_2$, represents pyrite stoichiometry.*

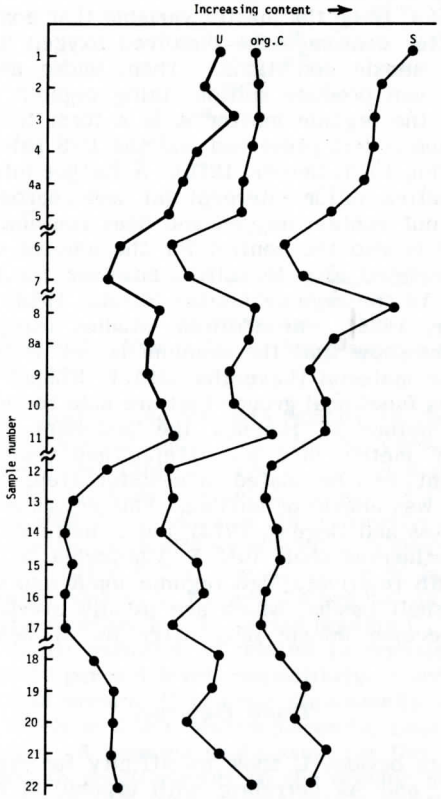


*Figure 4. Down-hole plot of U, organic C, and S for all 24 samples from core YB-15, DeKalb County, Tennessee. Increasing content to the right, axes not to scale.*

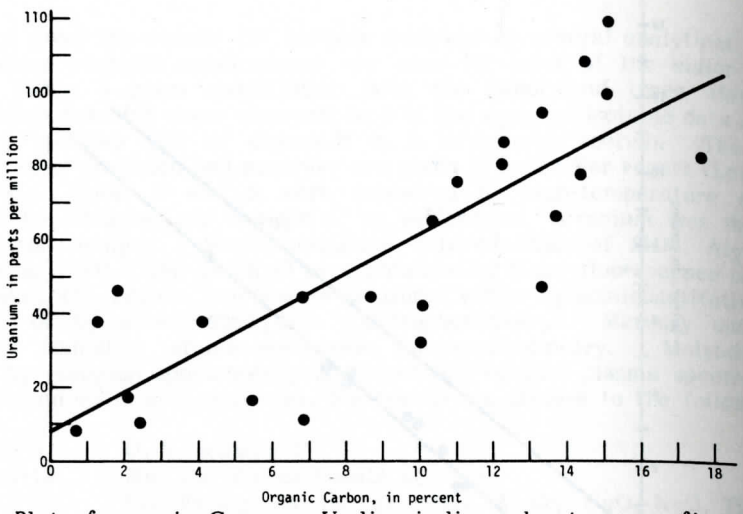


*Figure 5. Plot of organic C versus U; line is linear least-squares-fit; r, correlation coefficient, is 0.82 which is significant at the 99 percent level.*

for the 24 samples. The three elements are clearly interrelated as can be seen from the plot. Likewise, Figure 5 shows a plot of organic C and uranium. The linear-least-squares treatment shows statistical significance at the 99-percent level. The r (correlation coefficient) values are 0.82, 0.82, and 0.89 for organic C versus S, organic C versus U, and S versus U, respectively.

We interpret organic C to be the master variable that controls the other elements because the organic matter consumes the dissolved oxygen (by decay and biological activity) and establishes anoxic conditions. Then, under anaerobic conditions, the sulfate-reducing bacteria can produce sulfide, using organic matter as food source. However, only a part of the organic matter is in a form to be metabolized; thus, a relatively constant fraction is left preserved and the C-S relation is linear (Sweeney, 1972; Goldhaber and Kaplan, 1974; Berner, 1970). A further interpretation of the C and S results is that the positive sulfur intercept (at zero carbon) implies an overlying water column that does not contain oxygen and does contain $H_2S$ (Leventhal, 1979a).

The organic matter is also the control for the amount of U. In this particular core, U is statistically related also to sulfur; however for most black shales U is statistically related best to the organic matter (Strahl, 1958; Leventhal, 1978, 1979b; Leventhal and Goldhaber, 1978). In addition, studies using fission-track maps of polished-rock thin sections show that the uranium is not associated with sulfides and is associated with organic material (Leventhal and T. Knapp, unpublished data). The organic matter usually has functional groups that are able to ion-exchange or to chelate the uranium, probably before it reaches the sediment. Because of the low sedimentation rate of 10 meters in 5 m.y. (2mm/1000 years) (Conant and Swanson, 1961), high sulfide content, and laminated (non-bioturbated) sediments, it is believed that the overlying water was anoxic or euxinic. This environment is similar to that of the present Black Sea (Ross and Degens, 1974), but is quite different from the modern ocean basins in the continental shelf (off S. California or S.W. Africa) which are sometimes anoxic but with relatively high organic input and high sedimentation rate. In these modern ocean shelf basins, which are usually overlain by oxygen-containing water, the sediments become anoxic only after burial below the sediment-water interface.

## Trace Elements

Many trace elements besides U show an affinity for organic C and S in anoxic sediments: Mo, Zn, Hg, and As correlate with organic C and S. Presumably the oxygen-free depositional environment created by organic C and reduced S species and the low sedimentation rate are responsible for the enrichment in these metals.

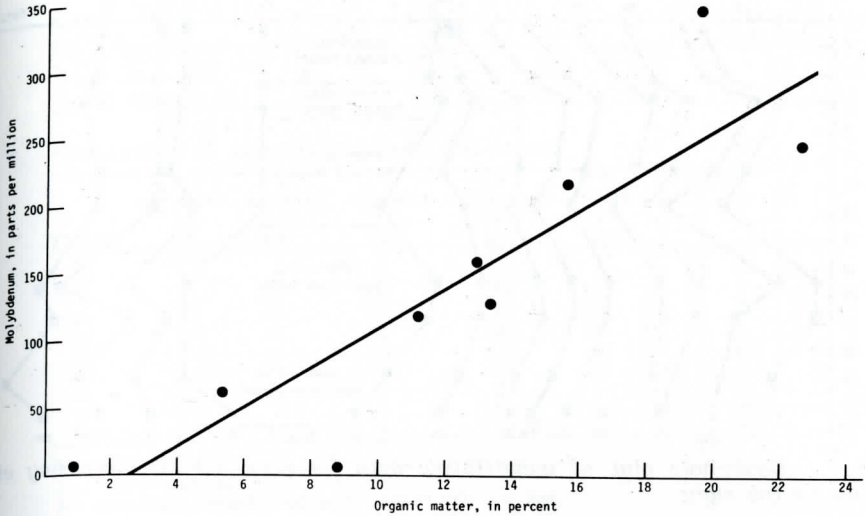


*Figure 6. Plot of organic C versus Mo; line is linear least-squares-fit; r = 0.90 which is significant at the 99 percent level.*

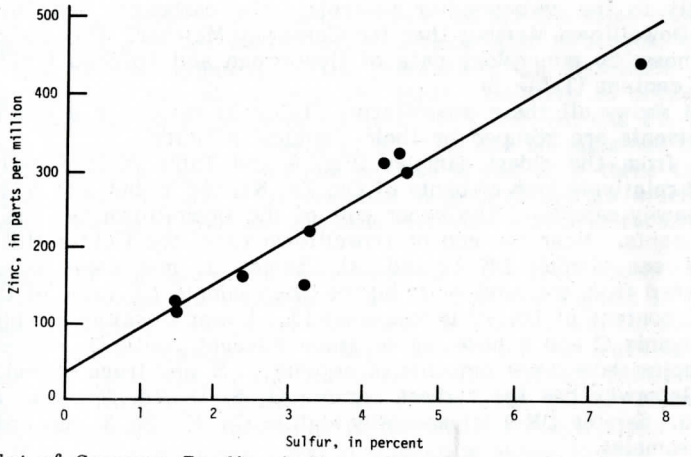


*Figure 7. Plot of S versus Zn; line is linear least-squares-fit of data, r = 0.96 which is significant at the 99 percent level.*

Figure 6 shows the quantitative Mo data relative to the data for organic C. The r values are 0.90 for Mo versus C and r = .95 for Mo versus S. Zinc is most related to S as shown on Figure 7 and Table 3. The r value is 0.80 for Zn versus organic C and 0.96 for Zn versus S. Mercury is related to organic C and S (Table 3), but the correlation (Hg versus C and S, r = .62 and .74, respectively) is not as high as for U or Mo. Arsenic is statistically more closely related to S than to organic C as indicated by the correlation coefficients r = 0.97 for As versus S, but only 0.69 for As versus organic C. Other elements such as V, Ni, and Cu are not as clearly related to organic C or S. For example, the r values for Ni (versus organic C, 0.44; S, 0.58) for Ni imply that only ~25 percent of its variation is related to organic C and S, but that it is significant at the 96 and 99 percent level, respectively. Correlation coefficients values for Cu and V versus S and organic C are not statistically significant.

Molybdenum and U show linear least-squares-fit lines that go near the origin, whereas Hg and Zn do not. A possible explanation for this difference is that the Mo and U are directly bound to specific sites on the organic matter, and, therefore, are proportional to its abundance. On the other hand, Hg and Zn only require reducing conditions, which obtain whenever $H_2S$ is present in the water column, and may or may

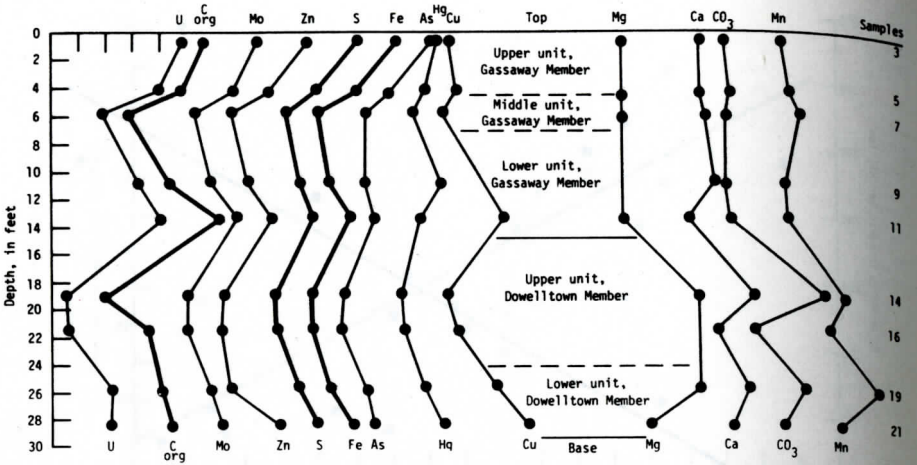


*Figure 8. Down-hole plot of quantitative data for core YB-15; increasing element contents to the right.*

not be related to the actual amount of sulfide in the sediment.

Manganese is somewhat related to carbonate (r = 0.66), which is an effect not related directly to the carbon-sulfur controls. The carbonate and Mn contents are higher in the Dowelltown Member than the Gassaway Member. This carbonate is partly dolomite as shown by mineralogy data of Hosterman and Loferski (1981) and also be increased Mg content (Table 2).

Figure 8 shows all these quantitative (Table 3) results in a down-hole plot, in which the elements are grouped by their chemical affinity.

Starting from the oldest samples (Fig. 8 and Table 3), the early Dowelltown sediments had relatively high amounts of Cu, Zn, Ni, and V, but less S, Fe, U, and Mo than the Gassaway samples. The upper unit of the Dowelltown has less organic C, S, and trace elements. Near the end of Dowelltown time, the Center Hill Ash Bed was deposited (between samples DK 12 and 13). Sample 12 may show the effects of this ash being leached from the land in its higher (than sample 13) value of U, even though the organic C content of DK 12 is less than 13. Lower Gasaway samples with higher amounts of organic C and S have higher trace element contents, whereas the middle Gassaway samples show lower amounts of organic C, S, and trace elements. The upper unit of the Gassaway has the highest organic C, S, U, Zn, Mo, and As, but lower amounts of Cu. Sample DK 1 is especially high in Co, Ni, Pb, V, Ag, and Zn compared to the other samples.

## Source of the Metals

In order to try to understand the overall source of the metals in the shale, the metal contents of sea water, ordinary shale, and the Center Hill Ash Bed and Black Sea were compared with the Chattanooga Shale (Table 6). Table 6 also gives the ratio, following recent work, of the concentrating elements in Chattanooga Shale relative to sea water (Holland, 1978 and 1979), ordinary shale (Brumsack, 1980), Black Sea sediments (Hirst, 1974), and the Center Hill Ash Bed. Relative to sea water, the shale is most enriched in Pb, Ni, Cu, Zn and V (in that order), and least enriched in Mo, As, Cd, Hg, and U. In comparison to ordinary shale the Chattanooga is most enriched in Mo, U, and Cd. Compared to our sample of Center Hill ash, the Chattanooga is most enriched in Ni and Mo. The Chattanooga Shale is similar to the recent Black Sea sediments in trace-metal element abundances.

These ratios may be interpreted in several ways. The high Pb enrichment relative to sea water is partly due to radioactive decay of U (in the shale since deposition) and presumably partly due to input of radiogenic Pb associated with U in rock being weathered. The Center Hill Ash Bed is unusually high in both U and Pb relative to most volcanic material (Turekian and Wedepohl, 1961). Relative to ordinary shales, the

Table 5. *Extract organic geochemistry of Chattanooga Shale samples.*

| Sample position | C org (percent) | Extractable Total bitumen (ppm) | s + a (ppm) | s/a | Bitumen/C (percent) |
|---|---|---|---|---|---|
| 1 inch above DK 3 | 14.6 | 2410 | 1590 | 0.48 | 1.7 |
| 1 inch above DK 9 | 18.0 | 4880 | 3280 | 0.66 | 2.7 |
| 1½ inch above DK 20 | 18.8 | 4710 | 3430 | 1.02 | 2.5 |

Table 6. *Comparison of element contents and ratios.*

| | 1 | 2 | 3 | 4 | 5 | Ratios | | | |
|---|---|---|---|---|---|---|---|---|---|
| | sea water | ordinary shale | ash bed | Chattanooga Shale | Black Sea | 4/1 | 4/2 | 4/3 | 4/5 |
| Element | ppb | ppm | ppm | ppm | ppm | | | | |
| Mo | 10 | 3 | 7 | 150 | 50 | 15 | 50 | 21 | 3 |
| U | 3 | 4 | 28 | 60 | 70* | 20 | 15 | 2 | 0.8 |
| V | 2 | 130 | 200 | 200 | 175 | 100 | 2 | 1 | 1.1 |
| Zn | 2 | 95 | 300 | 200 | 110 | 100 | 2 | 1 | 1.9 |
| Ni | .6 | 68 | 10 | 200 | 120 | 300 | 3 | 20 | 1.9 |
| Cu | .7 | 45 | 50 | 130 | 80 | 180 | 3 | 2.5 | 1.7 |
| Pb | .002 | 20 | 30 | 50 | 10 | 2500 | 2 | 1.5 | 5 |
| As | 3 | 13 | -- | 35 | -- | 10 | 3 | -- | -- |
| Cd | 0.1 | 0.1 | -- | 1 | -- | 10 | 10 | -- | -- |
| Hg | .02 | -- | -- | 0.15 | -- | 10 | -- | -- | -- |

1. Holland (1978)
2. Turekain and Wedepohl (1961)
3. Leventhal, unpublished data (Center Hill Ash Bed)
4. This paper
5. Hirst (1974) (sediments, cores 1432, 1462)

*Degens, and others, 1977.

Chattanooga is most enriched in Mo and U. These two are the same elements that are at highest concentration in sea water, and it is reasonable to suggest that either the high organic flux to the sediment or the presence of an $H_2S$-laden water column creates a sink for these two elements in the shale. Relative to ordinary shale, the Chattanooga is enriched by a factor of ~2 to 3 for V, Zn, Ni, Cu, Pb, and As; but it is also enriched in organic C by a factor of 3. This can be explained by three times less dilution by clastic material, and can be interpreted as a three times less than normal deposition rate. Mo and U are enriched by greater factors which could be due to U input from leaching of volcanic ash beds and more effective removal of Mo from sea water.

Some details of the source and abundance of the trace elements also may have changed with time because the amounts U, Mo, and As are highest in the upper unit of the Gassaway; Zn and Hg are rather uniformly distributed; and Cu and V are highest in the lower unit of the Dowelltown. A likely source for the trace elements is ash-fall tuffs that are prominent in the Devonian section (Roen, 1980), and which are represented by the Center Hill Ash Bed in the Chattanooga Shale. These ash units are commonly only several centimeters thick in the shale; however, they may have been much thicker (Dennison and Boucot, 1974) at a location closer to their source (on land), and it is the weathering (Zielinski, 1979) of the ash on land that would have contributed trace elements to the shale. Leventhal and Kepferle (1982) have discussed the ash as a source of metals and cite examples of increased metal values in shale stratigraphically above ash beds.

## STABLE ISOTOPES

The organic C and S isotope values for selected samples are given in Table 3 (in per mil notation) relative to the PDB and Canyon Diablo troilite standards, respectively. Although the range in carbon determinations is outside the precision of ±0.1 per mil, the determinations do not vary in a systematic way that can be clearly interpreted. However, samples 19 and 21 (-29.6 °/00), which are a more marine type of organic matter (based on the organic geochemistry, see next section), are lighter by about 0.5 per mil than samples 2 and 5 (-29.05 °/00) which are the most terrestrial (based on organic analysis). On the other hand, samples 9 and 11, which are intermediate between these groups, are approximately 0.3 per mil heavier (-28.7 °/00) than are samples 2 and 5. These values are lighter than modern marine and terrestrial

sediments, but are similar to ancient shales (Degens, 1969) probably due to different sizes of total carbon reservoirs at that time.

The S isotopes are also similar, but outside the analytical precision of +0.2 per mil. The relative constancy of the S isotope data indicates similar conditions during deposition relative to sulfate reduction, burial, and environment. Claypool and others (1980b) have shown that the S isotope difference between sulfides in these Appalachian basin sediments and worldwide ocean sulfate in Devonian times (Claypool and others, 1980a) is about 45 per mil. This isotope difference is similar to that (Sweeney and Kaplan, 1980) for the modern Black Sea, that has an $H_2S$-containing water column but one that is quite different from the normal modern marine environment in which the difference is about 25 per mil (Goldhaber and Kaplan, 1974). Thus, the S isotopic data for the Chattanooga Shale support the presence of a layer of $H_2S$-containing water above the sediments of the Chattanooga sea.

## Organic Chemistry

In addition to the samples mentioned, three samples were taken for detailed work on the organic material. These samples (Table 5) were taken adjacent to samples 3, 9, and 20 in the core.

The results are given in Table 5. The organic C contents are similar for these samples. However, the character of the organic carbon extract is quite different for the sample near 3 compared to that near 20. The bitumen is the total extract that includes (Table 5) the heptane-eluted saturated (s) hydrocarbons, the benzene-eluted aromatic (a) hydrocarbons, and the methanol-eluted polar (or NSO) fraction. The ratio of these, s/a, is also given.

Figure 9 shows the gas chromatograms of the alkane extracts (the s fraction) from samples near 3 and 20. The unresolved complex mixture ("hump") in these chromatograms is typical of Devonian shale of the Appalachian basin (Claypool, unpublished data).

Figure 10 shows results of pyrolysis gas chromatography (Leventhal, 1976) of samples 3 and 22. The n-alkanes are numbered, the other material is shown shaded.

## Discussion of Organic Geochemistry

These results--the extracts, amounts and ratios, the chromatogram of the extracts, and the pyrolysis-gas chromatography--indicate that the organic matter in sample 3 has a major component of terrestrial organic matter, and that sample 20 (and 22) has a major component of marine organic matter.

The organic-matter from the sample near sample 20 shows a larger amount of extractable bitumen and total hydrocarbons than does sample 3 indicating that the organic matter in the Dowelltown is more marine type. The higher ratio of saturated to aromatic hydrocarbons extract for the sample near 20 also suggests a dominantly marine origin. The chromatogram of the extract of sample 20 has a much larger component of n-alkanes (relative to the unresolved mixture) when compared to sample 3. Thus, this classical organic-extract geochemistry (Tissot and Welte, 1978; Hunt, 1979) indicates a major marine organic component for sample 20 and a major terrestrial organic component for sample 3.

Pyrolysis-gas chromatography of the insoluble organic material (kerogen) is also useful in typing organic matter (Leventhal, 1976). The results of sample 22 show pyrolysis products that are mainly n-alkanes and alkenes, whereas the results for sample 3 show mainly substituted aromatic molecules rather than n-alkanes (Leventhal, 1981). This difference between samples 3 and 22 also can be illustrated by examining adjacent alkane-alkene ($nC_{13}$, peak L) and non-n-alkane (naphthalene, peak M) in the pyrolysis products. From both the peak heights and areas, the relative amount of these two components can be seen.

## CONCLUSION

The Upper Devonian Chattanooga Shale of Tennessee was deposited at a slow rate (2mm/1000 yrs) under an anoxic water column. This type of deposition is evident from

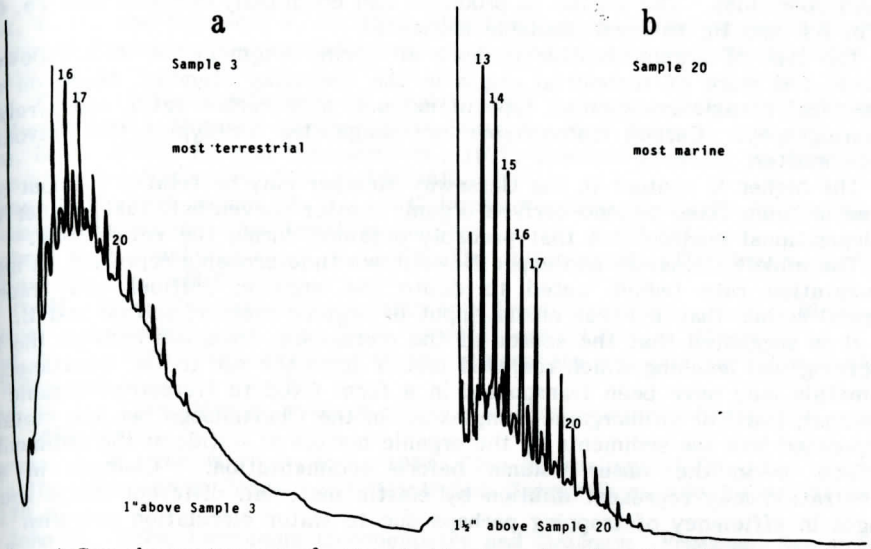


*Figure 9. a) Gas chromatogram of saturated hydrocarbon fraction of extract of sample near 3; note large hump relative to n-alkanes (number is number of C atoms). b) Gas chromatogram of saturated hydrocarbon fraction of extract of sample near 20; note large n-alkane peaks (number is number of carbon atoms) relative to hump.*

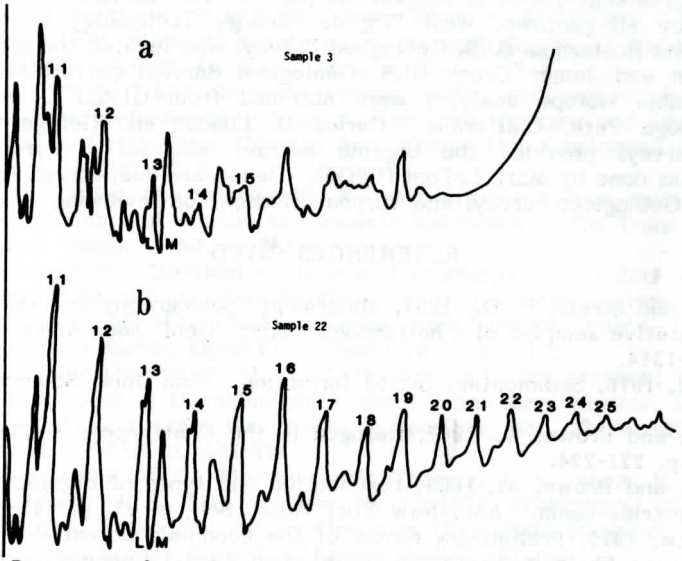


*Figure 10. a) Pyrogram of 750 step on sample 3; note lack of n-alkane-enes and peak L Y peak M for 750 step. b) Pyrogram of 750 step in sample 22; note n-alkanes are prominent and peak L Y peak M for 750 step.*

the finely laminated sediments that indicate the absence of bioturbation and the absence of oxygen. Based on the large amount of S, on C and S plots, and on S isotope measurements, the presence of an $H_2S$ layer was below the level of mixing by surface effects, such as wind and waves, and therefore, that the water body was certainly in excess of 30 meters and perhaps in excess of 100 meters deep. The lack of mixing may have been the result of density-stratification such as is true of the present Black Sea (Ross and Degens, 1974).

Organic carbon is the master variable in the trace-element enrichment, either by directly binding the element, as for U (and possibly for Mo) or by creating anoxic (and

euxinic) conditions. The sulfide so produced can chemically combine with Fe, Cu, Zn, Ni, Pb, As, and Hg to form insoluble sulfides.

The type of organic matter is more of marine origin in the (older) Dowelltown Member, and more of terrestrial origin in the Gassaway Member, based on organic geochemical parameters such as type of extract, hydrocarbon ratio, and pyrolysis-gas chromatography. Carbon isotopes are not diagnostic for typing this Devonian-age organic matter.

The higher U content in the Gassaway Member may be related to input of land-derived uranium fixed to land-derived organic matter (Leventhal, 1981) rather than to the depositional environment that probably obtained during the entire time.

The middle Gassaway and upper Dowelltown time probably represent an increased sedimentation rate (which acted to dilute the organic, sulfide, and trace-metal contents) rather than a lower annual input of organic matter, sulfide and U.

It is suggested that the source of the metals was from ash beds on the land by weathering and leaching which removed metals from the ash to the Chattanooga Sea. The metals may have been transported in a form fixed to terrestrial organic matter (Leventhal, 1981) or an inorganic complexes. In the Chattanooga Sea the metals were incorporated into the sediments by the organic matter or sulfide at the sediment-water interface or in the water column before sedimentation. Changes in element concentration may represent dilution by clastic material, different metal sources or changes in efficiency of trapping perhaps due to water circulation patterns.

## ACKNOWLEDGMENTS

Portions of this work were supported by U.S. Department of Energy under interagency agreement EX-76-C-01-2287 as part of the Eastern Gas Shales Project (coordinated by Morgantown, West Virginia, Energy Technology Center). We are indebted to John Hosterman (U.S. Geological Survey) who located the split of the core. Nancy Conklin and James Crock (U.S. Geological Survey) performed the inorganic analyses. Stable isotope analyses were obtained from Global Geochemistry Corporation, Canoga Park, California. Carlos M. Lubeck and George Claypool (U.S. Geological Survey) provided the organic extract analyses. Pyrolysis-gas chromatography was done by Mark LeFont (USGS). Thanks are due, Joseph Hatch and Terry Offield (U.S. Geological Survey) and Vernon Swanson for reviewing this paper.

## REFERENCES CITED

Bates, T. F., and Strahl, E. O., 1957, Mineralogy, petrography and radioactivity of representative samples of Chattanooga shale: Geol. Soc. Amer. Bull., v. 68, p. 1305-1314.

Berner, R. A., 1970, Sedimentary pyrite formation: Am. Jour. Science, v. 268, p. 1-23.

Breger, I. A., and Brown, A., 1962, Kerogen in the Chattanooga shale: Science, v. 137, p. 221-224.

Breger, I. A., and Brown, A., 1963, Distribution and types of organic matter in a barred marine basin: Ann. New York Acad. Sci., v. 25, p. 741-755.

Brown, Andrew, 1975, Preliminary report of the economic potential of the Chattanooga Shale in Tennessee, Data as of 1962: (Incomplete and unedited m.s.). U.S. Geological Survey Open-File 75-135.

Brumsack, H., 1980, Geochemistry of Cretaceous black shales from DSDP: Chem. Geol., v. 31, pl.-25.

Claypool, G. E., 1974, Anoxic diagenesis and bacterial methane generation [unpub. Ph.D. thesis]: UCLA, 276 p.

Claypool, G. E., Holser, W. T., Kaplan, I. R., Sakai, H., and Zak, I., 1980a, Age curves of sulfur and oxygen isotopes in marine sulfate: Chem. Geol., v. 28, p. 199-260.

Claypool, G. E., Leventhal, J. S., and Goldhaber, M. B., 1980b, Geochemical effect of early diagenesis of organic matter, sulfur and trace elements in Devonian black shales of the Appalachian Basin, USA; (abs.): AAPG Bull., v. 64, p. 692.

Conant, L. C., and Swanson, V. E., 1961, Chattanooga shale and related rocks of central Tennessee and nearby areas: U.S. Geological Survey Prof. Paper 357, 91 p.

Degens, E. T., 1969, Biochemistry of stable carbon isotopes: *in* G. Eglinton and M. Murphy (eds.), Organic Geochemistry, Springer, New York, p. 304-329.

Degens, E. T., Khoo, F., and Michaelis, W., 1977, Uranium anomaly in Black Sea sediments: Nature, v. 269, p. 566-569.

Dennison, J. M., and Boucot, A. J., 1974, Little War Gap at Clinch Mountain, eastern Tennessee: Southeastern Geology, v. 16, p. 79-101.

Goldhaber, M. B., and Kaplan, I. R., 1974, The sulfur cycle: The Sea, v. 5, Wiley, New York, p. 569-655.

Hirst, D. M., 1974, Geochemistry of sediments from Black Sea: *in* The Black Sea, Ross and Degens, eds., Am. Assn. Petrol. Geol., Tulsa, p. 430-55.

Holland, H. D., 1978, The chemistry of the atmosphere and oceans: New York, Wiley and Sons, p. 157-58.

Holland, H. D., 1979, Metals in black shales - a reassessment: Econ. Geol., v. 74, p. 1676-1680.

Hosterman, J. W., and Whitlow, S. I., 1981, Clay mineralogy of Devonian shales in the Appalachian Basin: U.S. Geological Survey Open-File Report 81-585, 170 p.

Hunt, John M., 1979, Petroleum Geochemistry and Geology: Freeman, San Francisco, p. 273-320.

Kehn, T. M., 1955, Uranium in the Chattanooga Shale Youngs Bend area, eastern Highland Rim, Tennessee: USAEC TEI-528A, 60 p.

Krumbein, W. C., and Garrels, R. M., 1952, Origin and classification of chemical sediments in terms of ph and Eh: Jour. Geol., v. 60, 1-33.

Leventhal, J. S., 1976, Stepwise pyrolysis-gas chromatography of kerogen in sedimentary rocks: Chem. Geol., v. 18, p. 5-12.

Leventhal, J. S., 1978, Trace elements, carbon, sulfur, and uranium in Devonian black shale cores from Perry County, Kentucky, Jackson and Lincoln Counties, West Virginia, Cattaraugus County, New York: U.S. Geological Survey Open-File Report 78-504, 32 p.

Leventhal, J. S., 1979a, The relationship between organic carbon and sulfide sulfur in recent and ancient marine and euxinic sediments: EOS Trans American Geophysical Union, v. 60, p. 286.

Leventhal, J. S., 1979b, Chemical analysis and geochemical associations in Devonian black shale core samples from Martin County, Kentucky, Carroll and Washington Counties, Ohio, Wise County, Virginia and Overton County, Tennessee: U.S. Geological Survey Open-File Report 79-1503, 51 p.

Leventhal, J. S., and Goldhaber, M. B., 1978, New data for uranium, thorium, carbon, and sulfur in Devonian black shale, from West Virginia, Kentucky and New York: First Eastern Gas Shales Symposium, Oct. 17-19, 1977, Morgantown, MERC/SP-77/5 p. 183-221.

Leventhal, J. S., Crock, J. G., Mountjoy, W., Thomas, J. A., Shaw, V. E., Briggs, P. H., Wahlbert, J. S., and Malcolm, M. J., 1978, Preliminary analytical results for a new U.S. Geological Survey Devonian Ohio shale standard, SDO-1: U.S. Geological Survey Open-File Report 78-447, 11 p.

Leventhal, J. S., 1981, Pyrolysis gas chromatography-mass spectrometry to characterize organic matter and its relationship to uranium content of Appalachian Devonian black shales: Geochim. Cosmoch. Acta, v. 45, p. 883-889.

Leventhal, J. S., and Kepferle, R. C., 1982, Geochemistry and geology of strategic metals in Devonian shales of the eastern interior basins of the United States: *in* Matthews, R. D. and others, eds. Synthetic fuels from oil shale II. Inst. of Gas Technology, Chicago, p. 73-96.

Matthews, R. D., and others, ed., 1982, Synthetic fuels from oil shale II: Symposium volume, October 1981. Institute of Gas Technology, Chicago, Illinois, 624 p.

Oliver, W. A., DeWitt, W., Dennison, J., Hoskins, K., and Huddle, J., 1969, Devonian of the Appalachian Basin, U.S.: *in* International Symposium in Devonian System: Alberta Society of Petroleum Geologists, Calgary, 1967, v. 1, p. 1001-1040.

Roen, J. B., 1980, Stratigraphy of previously unreported Devonian ash-fall localities in the Appalachian Basin; U.S. Geological Survey Open-File Report 80-505, 10 p.

Ross, D. A., and Degens, E. T., 1974, The Black Sea; Amer. Assoc. Petro. Geol., Memoir 20, Tulsa, p. 593.

Schott, G. L., and others, 1978, Proceedings First Eastern Gas Shales Symposium: October 1977, U.S. Dept. of Energy, Morgantown, WV, MERC/SP-77/5, 783 p.

Strahl, E. O., Camilli, E., and Short, N. M., 1956, Investigation of the mineralogy, petrography, and paleo-botany of uranium-bearing shales: USAEC NYO-6060, 70 p.

Strahl, E. O., 1958, Investigation of relationships between selected minerals, trace elements, and organic constituents in black shale [Ph.D. thesis]: Pennsylvania State University; also USAEC NYO-7908, 155 p.

Swanson, V. E., 1953, Uranium in the Chattanooga shale: Bull. Geol. Soc. Amer. (abstracts vol.), p. 1481.

Swanson, V. E., and Kehn, T. M., 1955, Results of 1952-53 sampling of Chattanooga shale in Tennessee and adjacent states: U.S. Geol. Survey TEI Report 366, 98 p.

Swanson, V. E., 1960, Oil yield and uranium content of black shales: U.S. Geol. Survey Prof. Paper 356-A, 43 p.

Sweeney, R. E., 1972, Pyritization during diagenesis of marine sediments [Ph.D. thesis]: UCLA, 184 p.

Sweeney, R. E., and Kaplan, I. R., 1980, Stable isotope composition of dissolved sulfate and hydrogen sulfide in the Black Sea: Marine Chemistry, 9, 145-152.

Tissot, B. P., and Welte, D. H., 1978, Petroleum formation and occurrence: Springer Verlag, Berlin, p. 99-109, 391-394.

Turekian, K., and Wedepohl, K., 1961, Distribution of elements in the earth's crust: Geol. Soc. Amer. Bull., v. 72, p. 175-192.

Vine, J. D., and Tourtelot, E. B., 1970, Geochemistry of black shale deposits: A summary report: Econ. Geol., v. 65, p. 253-272.

Zielinski, R. A., 1979, Uranium mobility during interaction of rhyolite obsidian felsite and perlite with alkaline carbonate solution: Chem. Geol., v. 27, p. 47-63.

# GEOCHEMICAL FACTORS RELATED TO FORMATION OF COALS IN THE NORTON FORMATION, SOUTHWESTERN VIRGINIA

Jack E. Nolde *Virginia Division of Mineral Resources, P. O. Box 3667, Charlottesville, Virginia 22903*

## ABSTRACT

The Norton Formation of Lower to Middle Pennsylvanian age in southwestern Virginia consists of cyclic deposits of coal, sandstone, siltstone and claystone. Correlation and R-mode factor analysis of 20 parameters on 63 coal samples from the formation identified five groups of geochemically associated parameters. These five groups represent elements or compounds 1) adsorbed on organic materials and hydrous iron oxides, 2) contained inherently within organic material, 3) contained in clay minerals, 4) representing various sulfur reactions, and 5) sorbed in clays.

## INTRODUCTION

The Norton Formation of Lower to Middle Pennsylvanian age underlies widespread areas of Buchanan, Dickenson, and Wise Counties in southwestern Virginia (Figure 1). It contains cyclic deposits of sandstone, siltstone, and claystone and eleven main interbedded coals (Figure 2). The chemical composition of selected coal samples from active mining areas were compiled (Henderson and others, 1981; Table 1). Sixty-three analyses, representing eleven coal beds were studied. The objective of the present study is to determine statistical interrelationships between basic inorganic and organic parameters commonly determined in routine coal analysis. An additional objective, is to use the data to gain a better understanding of the paleoenvironments of the Norton coals.

## METHODS AND MATERIALS

The parameters used for this study are 1) ash, 2) hydrogen (H), 3) carbon (C), 4) aluminum oxide ($Al_2O_3$), 5) calcium oxide (CaO), 6) iron oxide ($Fe_2O_3$), 7) magnesium oxide (MgO), 8) potassium oxide ($K_2O$), 9) silicon dioxide ($SiO_2$), 10) organic sulfur (OS), 11) pyritic sulfur (PS), 12) sulfate ($SO_4$), 13) total sulfur (TS), 14) cobalt (Co), 15) copper (Cu), 16) gallium (Ga), 17) germanium (Ge), 18) lead (Pb), 19) nickel (Ni), and 20) vanadium (V) (Table 1). These parameters were previously published by Henderson and others (1981). The first 13 parameters were recorded as weight percent and (14) through (20) were in parts per million.

R-mode factor analysis (Cattell, 1965; Harman, 1967) was used to find relationships among these parameters. In this procedure it is assumed that the original parameters are linear functions of a small number of underlying controlling factors. The analysis with varimax rotation of the axes was performed using the standard SPSS computer program available at the University of Virginia. Renton and Hidalgo (1975) and Wedge, Bhatia, and Rueff (1976) used factor analysis to determine if certain coal elements showed organic or inorganic affinity.

Proceeding with the matrix of observation (63 x 20), the correlation matrix (20 x 20) was computed. The principal function of this step is to standardize the data in order to reduce all means to zero and variances to unity. The correlation coefficients (Table 2) are significant at the five percent level if equal to or greater than 0.250 (Arkin and Colton, 1962).

To determine the underlying influences, the correlation matrix was resolved into the factor matrix which represents correlations of the original parameters and this matrix was rotated. The rotated factor matrix appears in Table 3. Only correlations with an absolute value greater than 0.25 were considered.

## RESULTS

Correlation coefficients for the Norton coals demonstrate the following geo-

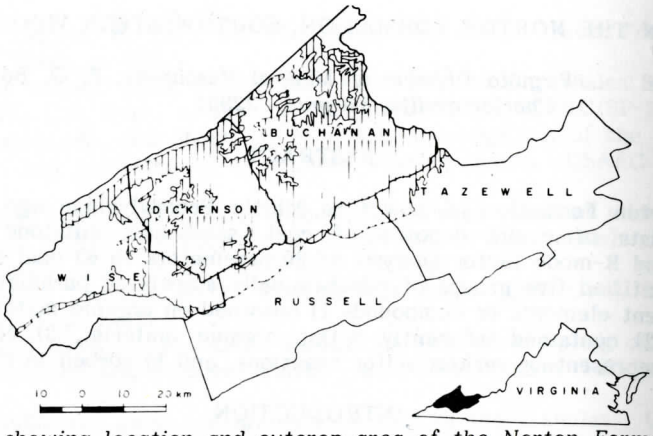


*Figure 1. Map showing location and outcrop area of the Norton Formation (hatched area), southwestern Virginia.*

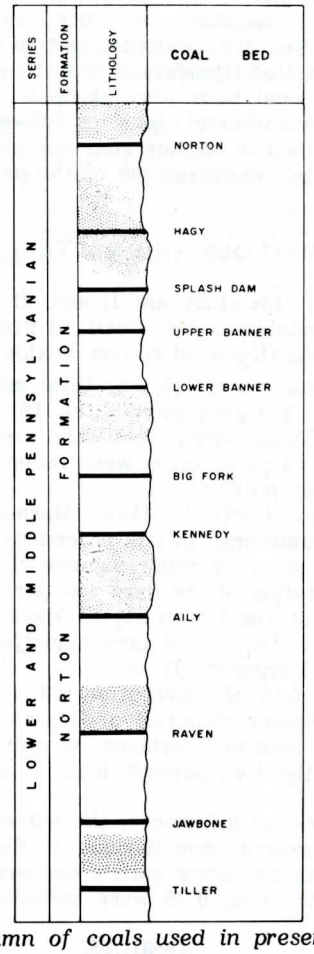


*Figure 2. Stratigraphic column of coals used in present study. Stippled areas are sandstone; blank areas siltstones and claystones.*

*Table 1. Means and standard deviations of major elements and trace elements in 63 Norton coals.*

| Parameter | Mean | Standard Deviation |
|---|---|---|
| 1. Ash | 15.2 | 10.7 |
| 2. $SiO_2$ | 48.4 | 7.9 |
| 3. $Al_2O_3$ | 24.4 | 3.7 |
| 4. CaO | 3.6 | 3.9 |
| 5. $Fe_2O_3$ | 8.9 | 6.4 |
| 6. $K_2O$ | 2.8 | 1.2 |
| 7. MgO | 1.2 | 0.4 |
| 8. Total Sulfur | 1.2 | 1.1 |
| 9. Organic Sulfur | 0.6 | 0.2 |
| 10. Pyritic Sulfur | 0.4 | 0.6 |
| 11. Sulfate | 0.03 | 0.06 |
| 12. C | 77.3 | 7.1 |
| 13. H | 4.9 | 0.5 |
| 14. Co | 64.1 | 45.8 |
| 15. Cu | 165.4 | 83.3 |
| 16. Ga | 42.2 | 13.9 |
| 17. Ge | 11.9 | 24.5 |
| 18. Pb | 63.0 | 37.7 |
| 19. Ni | 92.0 | 49.0 |
| 20. V | 150.4 | 42.4 |

Parameters: 1-13, weight percent
14-20, parts per million

*Table 2. Correlation coefficients greater than 0.25.*

| | Ash | $SiO_2$ | $Al_2O_3$ | CaO | MgO | $K_2O$ | $Fe_2O_3$ | TS | OS | PS | $SO_4$ | H | C | Co | Cu | Ga | Ge | Ni | Pb | V |
|---|---|---|---|---|---|---|---|---|---|---|---|---|---|---|---|---|---|---|---|---|
| Ash | 1 | | | | | | | | | | | | | | | | | | | |
| $SiO_2$ | .62 | 1 | | | | | | | | | | | | | | | | | | |
| $Al_2O_3$ | — | .31 | 1 | | | | | | | | | | | | | | | | | |
| CaO | — | -.49 | -.56 | 1 | | | | | | | | | | | | | | | | |
| MgO | — | — | — | — | 1 | | | | | | | | | | | | | | | |
| $K_2O$ | .45 | .41 | — | -.53 | .29 | 1 | | | | | | | | | | | | | | |
| $Fe_2O_3$ | -.39 | -.67 | .31 | — | — | — | 1 | | | | | | | | | | | | | |
| TS | — | — | — | — | — | — | — | 1 | | | | | | | | | | | | |
| OS | — | — | — | — | — | — | — | .33 | 1 | | | | | | | | | | | |
| PS | — | — | — | — | — | — | .33 | .53 | .46 | 1 | | | | | | | | | | |
| $SO_4$ | — | — | — | -.26 | — | .32 | — | — | — | .42 | 1 | | | | | | | | | |
| H | -.82 | -.52 | — | — | — | -.35 | .38 | — | .25 | — | — | 1 | | | | | | | | |
| C | -.86 | -.46 | — | — | — | -.31 | .32 | — | — | — | — | .74 | 1 | | | | | | | |
| Co | -.55 | -.57 | — | — | — | — | .55 | — | — | — | — | .33 | .51 | 1 | | | | | | |
| Cu | -.61 | -.57 | .37 | -.34 | — | — | .59 | — | .26 | — | — | .39 | .58 | .84 | 1 | | | | | |
| Ga | -.28 | — | — | — | — | — | .38 | — | — | — | — | .25 | .25 | .47 | .30 | 1 | | | | |
| Ge | -.26 | -.31 | — | — | — | — | .25 | — | — | — | — | — | — | — | .38 | .37 | 1 | | | |
| Ni | -.45 | -.38 | — | — | — | — | .50 | — | .25 | — | — | .38 | .38 | .75 | .58 | .52 | .41 | 1 | | |
| Pb | -.29 | — | .49 | — | — | — | — | — | — | — | — | — | .31 | .31 | — | .68 | — | .33 | 1 | |
| V | — | — | .39 | -.41 | — | .25 | — | — | — | — | .28 | — | — | — | — | .46 | — | .51 | — | 1 |

chemical associations:

1) Co and Cu are correlated at a high level (0.84),

2) The following elements have positive correlations with Ga: Ge, V, Ni, Pb, Co, and Cu,

3) $Al_2O_3$, $K_2O$, $SiO_2$, Ga, Pb, and V are positively correlated. These parameters are commonly found in silicates and are classified as lithophile. They occur in the coals

*Table 3. Varimax rotated factor matrix of loadings greater than 0.25.*

| PARAMETER | FACTOR | | | | | |
|---|---|---|---|---|---|---|
| | 1 | 2 | 3 | 4 | 5 | 6 |
| Ash | -.36 | -.89 | — | — | — | — |
| $SiO_2$ | -.58 | -.47 | .37 | — | — | — |
| $Al_2O_3$ | — | — | .80 | — | — | — |
| CaO | — | — | -.73 | — | — | — |
| MgO | — | — | — | — | .61 | — |
| $K_2O$ | — | -.41 | .41 | — | .60 | — |
| $Fe_2O_3$ | .64 | — | — | .30 | — | -.26 |
| TSulfur | — | — | — | .58 | — | — |
| OSulfur | — | — | — | .50 | — | .30 |
| PSulfur | — | — | — | .92 | — | — |
| Sulfate | — | — | — | .47 | .35 | — |
| Hydrogen | — | .85 | — | — | — | — |
| Carbon | .29 | .81 | — | — | — | — |
| Cobalt | .88 | .25 | — | — | — | — |
| Copper | .73 | .37 | — | — | — | — |
| Gallium | .54 | — | .54 | — | — | — |
| Germanium | .54 | — | — | — | — | — |
| Lead | — | — | .60 | — | -.43 | -.43 |
| Nickel | .75 | — | .26 | — | — | .27 |
| Vanadium | — | — | .41 | — | — | .74 |
| % of variance accounted for | 40.6 | 20.5 | 15.3 | 9.3 | 8.1 | 6.2 |

as constituents of clay minerals (illite and kaolinite) and of quartz,
4) The positive correlations of $Fe_2O_3$, H, C, Ge, Ni, Co, and Cu together with their negative correlations with $SiO_2$, $Al_2O_3$, $K_2O$, and ash, suggests that the $Fe_2O_3$ and associates are tied up as organic or organo-metallic complexes in the coal.

Five factors account for 94 percent of the data variation (Table 3). A sixth factor accounts for the remaining six percent and consists of V, Ni, and organic sulfur positively loaded and Pb and $Fe_2O_3$, negatively loaded.

Factor 1 accounts for 40.6 percent of the variability of the data (Table 3). The cluster is interpreted to represent elements with an affinity for organic matter O'Gorman and Walker (1972) show that Ge and Ga tend to have a strong organic affinity. The trace elements Co, Cu, Ga, Ge, and Ni have significant loadings for five of the seven elements, including Fe. The geological process represented by the cluster is probably cation adsorption on Fe-colloidal particles. Stumm and Morgan (1970) state that ion-exchange capacities of hydrous iron oxides are large; it is then expected that these oxides will modify the distribution of trace metals such as Co, Cu, and Ni which can be adsorbed on the hydrous iron oxides. The strong negative correlation of $SiO_2$ with the group suggests the lack of mineral constituents, except quartz.

The second factor accounts for 20.5 percent of the variation in the data. Carbon and hydrogen are at the positive end of this factor and $SiO_2$, $K_2O$ and ash are at the negative end. Cu and Co correlate moderately with the organic fraction, which has been found by other workers to be generally true in sedimentary environments. Co is common in organic materials and its presence in clastic sediments to any appreciable extent, probably indicates a nearby source from decaying organic matter, in this case plant matter. Co may or may not be present in fossil organic matter (Nicholls and Loring, 1962). It is inferred here that some of the Co released from the decay of plant materials was sorbed on surfaces of clay minerals as they were accumulating, and that some was adsorbed by organic material. The association of C and Cu seems to be similar to that between C and Co (LeRiche, 1959). The carbon of the Norton coals is derived almost entirely from plant matter. In a swamp environment the organic material is almost exclusively autochthonous detritus. The negative correlation of CaO probably indicates the formation of carbonate minerals.

The third factor accounts for 15.3 percent of the variability and comprises eight parameters, of which only CaO is negatively loaded, and $Al_2O_3$, $K_2O$, $SiO_2$, Ga, Pb, Ni, and V are positively loaded. The first three parameters together form aluminosilicates, that is, they form clay minerals. Gallium readily substitutes for aluminum in clay minerals. The lead content is probably the result of adsorption on the clay particles; illite is known to adsorb lead (Hirst, 1962). Ni and V show significant positive correlation with the group, but the reason for this relationship is not evident.

The fourth factor shows strong association among organic sulfur, sulfides, and sulfates and with moderate participation of $Fe_2O_3$ and represents the various reactions between the sulfur species. The highest correlation is between total sulfur and pyritic sulfur. One possible source of the sulfur is bacterial reduction of dissolved $SO_4$. Under reducing conditions $SO_4$ is converted to $HS^-$ or $H_2S$, either of which can react with iron to form iron monosulfides, which later are converted to pyrite. Because coal forms in reducing environments, most of the contained sulfur must have been in a reduced state. The sulfate in the system may well represent post depositional oxidation of pyrite. This factor represents the sulfur cycle.

Factor five is dominated by a strong association of MgO and $K_2O$ with a moderate contribution of $SO_4$ and an inverse relation to Pb. The association is considered to represent re-grading of clay minerals. Muds arriving at the site of deposition would contain degraded illite, chlorite, and kaolinite. In the depositional environment these clays would quickly adsorb available potassium and magnesium.

## PALEOENVIRONMENTAL MODEL

An idealized geochemical-paleoenvironmental model of a Norton coal swamp was constructed (Figure 3). The Norton coals and associated clastics were probably deposited in and adjacent to a delta distributary system. Most of the fine detritus brought to the site probably was in a reactive, degraded state. These particles underwent a series of reactions, mainly to replace alkali and alkaline-earths within clay minerals, when they interacted with the acidic waters of the delta swamps.

Along the lower delta plain, plant material accumulated in the reducing environment; when water occasionally wetted the area, the trace metals dissolved in it were adsorbed on colloidal-sized organic particles accumulating there. Organic reactions such as chelation would also tie trace elements to the coals, but this would have been a relatively minor process (Cook and Mayo, 1980; Nicholls and Loring, 1962). Figure 3 summarizes the dominant geochemical associations within the swamp. It does not, however, show the influence of the interactions on relative concentrations of the reactants throughout the lower delta plain.

At the time the Norton coals were being formed, the depositional environments were at times characterized by certain organic and inorganic reactions. The stability field of $FeS_2$, $FeSO_4$, and Fe-hydroxides in aqueous solutions at one atmosphere and 25° C are shown on an Eh-pH diagram of Figure 4. This diagram was constructed on selected sum dissolved sulfur species after the manner of Garrels and Christ (1965) and Berner (1971). We can use this diagram to estimate possible physio-chemical conditions during sediment deposition. The Eh-pH values deduced will be certainly lower than those of the depositing waters (Nicholls and Loring, 1962), but trends in the Eh of the sediments may reflect similar trends in the overlying waters. The pH of this water and of interstitial water in the sediment is unlikely to have been less than 4 or greater than 9.

The initial environment of deposition of the system (an ancient lower delta plain) was one in which inorganic detritus was unimportant and in which the inferred pH-Eh conditions were, pH 4.5-6.0 and Eh +0.2 to -0.1 mv (aerobic; see Figure 4). The trace metals Co, Cu, Ga, Ge, and Ni were most probably introduced to the area as ions or metal-organic complexes; Co, Ni, and Cu were adsorbed on negatively charged colloidal iron hydroxide particles. Decaying vegetation on the delta plain adsorbed Ge and Ga. Illite and kaolinite began to form from their degraded counterparts as K and Mg were adsorbed (Figure 3); some substitution of Ga, Pb, and V for Al also took place in these minerals. When the plain was no longer wetted, new ions were slowly added to the organic and inorganic detritus on the plain. At this time decay of the vegetation on the strath concentrated Co and Cu in the rotting masses. Following accumulation and

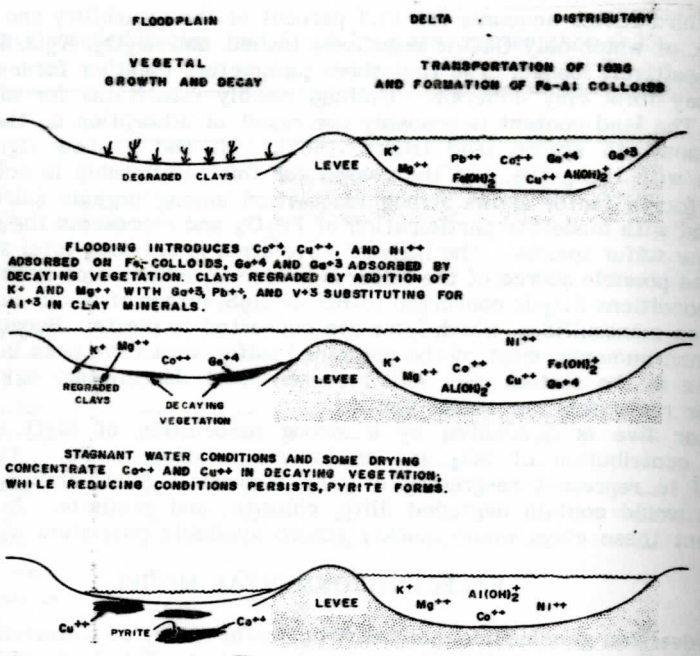


*Figure 3. Geochemical-paleoenvironmental model for the Norton Formation coals.*

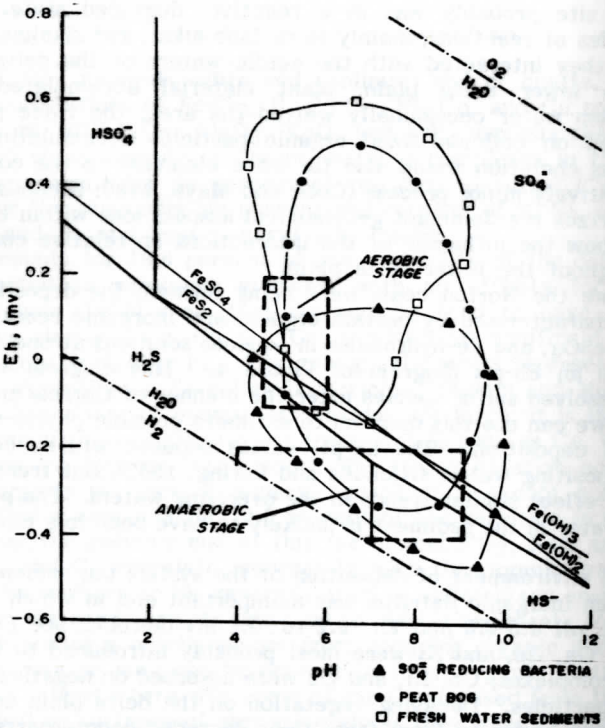


*Figure 4. Eh-pH stability diagram for iron hydroxides, iron sulfides, and sulfates at 25°C and one atmosphere pressure for (sum dissolved sulfur ionic species) = $10^{-3}$ m/l. Two stages of Norton coal environments indicated by bold dashed lines. Approximate limits for sulfate-reducing bacteria, peat bogs, and freshwater sediments were taken from Baas Becking, and others (1960).*

decay of vegetation, the environment of the substrate changed to one of reducing conditions. Thus, clay mineral formation halted and pyrite began to form in the organic material, with the inferred conditions being pH 4 to 9 and Eh -0.2 to -0.4 mv (anaerobic; see Figure 4). Subsequent flooding created new oxidizing conditions. The top of the most recently formed peat oxidized and caused certain trace elements to become mobile once again. These elements were then available for adsorption on the surfaces of the incoming clay and Fe-hydroxide colloids, thus beginning a new depositional cycle. Thus the general trend of change during the formation of the Norton coals was one of decreasing pH and possibly a slight increase in Eh.

## CONCLUSION

Correlation and R-mode factor analysis of parameters from routine coal analyses can successfully aid in paleoenvironmental interpretation. Five factors, accounting for 94 percent of the variability of the data, were extracted from a 20 x 20 correlation matrix. The geochemical significance of these factors in order of extraction (decreasing significance) are: 1) ions adsorbed on organic material and iron hydroxide colloids, 2) elements originally contained in organic matter, 3) contained in clay minerals, 4) various sulfur reactions, and 5) sorbed by clays.

According to this study, sorption was the most significant process by which trace elements were introduced in the coals and associated clastics of the Norton Formation from solution. The principal sorbents appear to be illite and organic material.

The major change in physio-chemical conditions of deposition was the variation in the Eh of the interstitial waters, with possible fluctuations in pH of the overlying waters. While the ashes of the Norton coals are relatively rich in certain trace metals, accumulation of these elements by coal-forming plants only appears feasible for Cu, Ni, and V.

## ACKNOWLEDGMENTS

The writer would like to thank Dr. Robert C. Milici and Dr. Sam O. Bird for their constructive criticism and review of the manuscript. The writer also acknowledges Mr. Oliver M. Fordham, Jr. for assistance in interpretation of the data. Special thanks goes to Drs. John Ferm, Bill Blackburn, and Paul Baker for valuable criticism which improved the manuscript. The author accepts sole responsibility for the contents of this paper.

## REFERENCES CITED

Arkin, H. and Colton, R, 1962, Tables for Statisticians: New York, College Outline Series, Barnes and Noble, Inc., 152p.

Baas Becking, L. G. M., Kaplan, I. R., and Moore, D., 1960, Limits of the natural environment in terms of pH and oxidation-reduction potentials: Jour. Geol., v. 68, pp. 243-284.

Berner, R. A., 1971, Principles of Chemical Sedimentology: New York, McGraw-Hill, 240p.

Cattell, R. B., 1965, Factor Analysis, an introduction to essentials: Biometrics, v. 21, pp. 190-215, 405-435.

Cook, P. J. and Mayo, W., 1980, Geochemistry of a tropical estuary and its catchment-Broad Sound, Queensland: Australian Bureau of Mineral Resources, Geology and Geophysics Bull. 182, 211p.

Garrels, R. M. and Christ, C. L., 1965, Solutions, Minerals, and Equilibria: New York, Harper and Row, 450p.

Harman, H. H., 1967, Modern Factor Analysis, 2nd ed: Chicago, Univ. Chicago Press, 474p.

Henderson, J. A., Jr., Oman, C. S., and Coleman, S. L., 1981, Analysis of coal samples collected 1975-1977: Virginia Division of Mineral Resources Publication 33, 135p.

Hirst, D. M., 1962, The geochemistry of modern sediments from the Gulf of Paria-(pt.) 2, The location and distribution of trace elements: Geochim. et. Cosmochim. acta, v. 26, pp. 1147-1187.

LeRiche, H. H., 1959, The distribution of certain trace elements in the Lower Lias of southern England: Geochim. et. Cosmochim. acta, v. 16, pp. 101-122.

Nicholls, G. D., and Loring, D. H., 1962, The geochemistry of some British carboniferous sediments: Geochim. et. Cosmochim. acta, v. 26, pp. 181-223.

O'Gorman, J. V. and Walker, P. L., Jr., 1972, Mineral matter and trace elements in U. S. coals: Office of Coal Research, Research and Development Rept. n. 61, 184p.

Renton, J. J. and Hidalgo, R. V., 1975, Some geochemical considerations of coal: West Virginia Geol. and Econ. Survey, Coal Geology Bull. n. 4, 38p.

Stumm, W. and Morgan, J. J., 1970, Aquatic Chemistry: New York, Wiley-Interscience.

Wedge, W. K., Bhatia, D. M. S., and Rueff, A. W., 1976, Chemical analysis of selected Missouri coals and some statistical implications: Missouri Geol. Survey, Rept. Inv. 60, 40p.

Zubovic, P., 1966, Minor element distribution in coal samples of the interior coal province, *in* Coal Science: Am. Chem. Soc., Adv. Chem. Series 55, pp. 232-247.

# BARRIER ISLAND DYNAMICS: THE EASTERN SHORE OF VIRGINIA

THOMAS E. RICE *Department of Geology, University of Massachusetts, Amherst, MA 01003*

STEPHEN P. LEATHERMAN *Department of Geography, University of Maryland, College Park, Maryland 20742*

## ABSTRACT

Analysis of historical shoreline records indicates that the twelve barrier islands on the Eastern Shore of Virginia are being continually reshaped in response to coastal processes. This barrier chain can be divided into three groups based on retreat rates and characteristics. Inlet offset growth and reversal are long-term events, resulting from the operation of known coastal processes. Geomorphic evidence and wave refraction analyses indicate that shoreline irregularity will diminish with time. Historical events and trends from 1852 to 1974 demonstrate that the geomorphic responses to tectonic movements, sediment supply, wave refraction effects, and underlying Pleistocene topography through known coastal processes can explain island behavior and observed trends in shoreline configuration. There is no basis for the prediction (or expectation) that any capes will develop within the next century along this shoreline in response to a theoretically trapped standing edge wave.

## INTRODUCTION

The Eastern Shore of Virginia barrier islands are essentially in a natural state, having largely escaped the ravages of human development. Most of the islands are owned by the Nature Conservancy and managed as the Virginia Coast Reserve. Wallops and Fisherman's Islands are owned and managed by the Federal government, while Wreck Island is owned by the State of Virginia (Fig. 1). The few private in-holdings have resulted in minimal human impact. These islands probably represent the largest natural and undisturbed barrier island system in the United States and provide an ideal laboratory for observing coastal processes that maintain and modify these dynamic landforms.

This microtidal barrier island chain may be divided conveniently into three groups of islands according to shoreline response (Fig. 2). Net shoreline changes during the past 122 years are schematically summarized to scale opposite each of the island silhouettes in Figure 1, and significant events affecting the geomorphology of the islands and inlets are also indicated, based on sequential shoreline change maps constructed from USCGS and other Federal government records (Rice and others, 1976).

The northern group of islands have experienced parallel beach retreat during historical times. This barrier sector has been sediment starved because of the updrift growth of Fishing Point spit at the southern end of Assateague Island (Fig. 3). This recurved sand spit has served as an effective sediment trap, elongating at the rate of 6.5 km per century (Field and Duane, 1976). The marked shoreline concavity or erosional arc of the nothern group of islands is a reflection of sediment supply deficiency, and this configuration has remained essentially unchanged for the past 122 years. A similar situation exists at the Ocean City Inlet area where sand trapping by the jetties has resulted in a concave-shaped erosional arc along the north end of Assateague Island, Maryland (Leatherman, 1979). These islands have retreated until their beaches now lie within 2.4 km of the mainland and their marshes extend to the mainland due to lagoonal narrowing through time (Figs. 2a and 3).

Retreat characteristics of the middle group of islands (Figs. 2b and c) can be described as "rotational instability." The term rotation does not mean actual physical rotation of the island, but is used here to describe changes in island shape and position due to erosion at one end and deposition at the other. This group of islands is characterized by offsets and stable inlets with large ebb-tidal deltas. Inlet offset reversals have been shown to be related to changing ebb-channel directions across large ebb-tidal deltas (Fig. 4). These changes have occurred during historical times at both ends of Hog Island (Fig. 1).

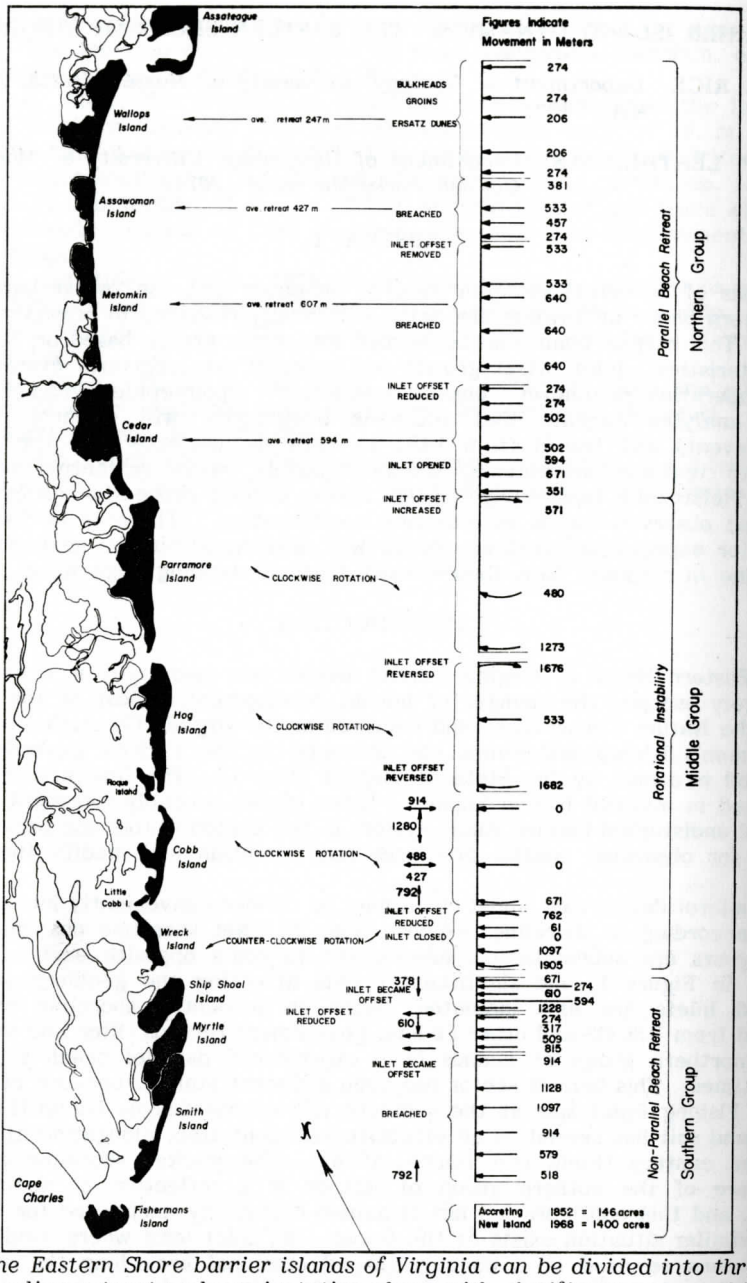


*Figure 1. The Eastern Shore barrier islands of Virginia can be divided into three groups. Rates of shoreline retreat and reorientation along with significant geomorphic changes are indicated.*

Islands in the southern group (Fig. 2d) have experienced varied amounts of shoreline change along each island. These islands have undergone shape alterations and have retreated toward the mainland except for Fishermans Island at the southern end of the littoral drift system. This island has accreted steadily since 1852, which has served to narrow and give definition to Smith Island Inlet. Retreat in this group of islands has been termed nonparallel because for each island there have been different responses due to variable causes (Rice and others, 1976). During historical times, however, the general trend for this island group has been a steady reduction in seaward

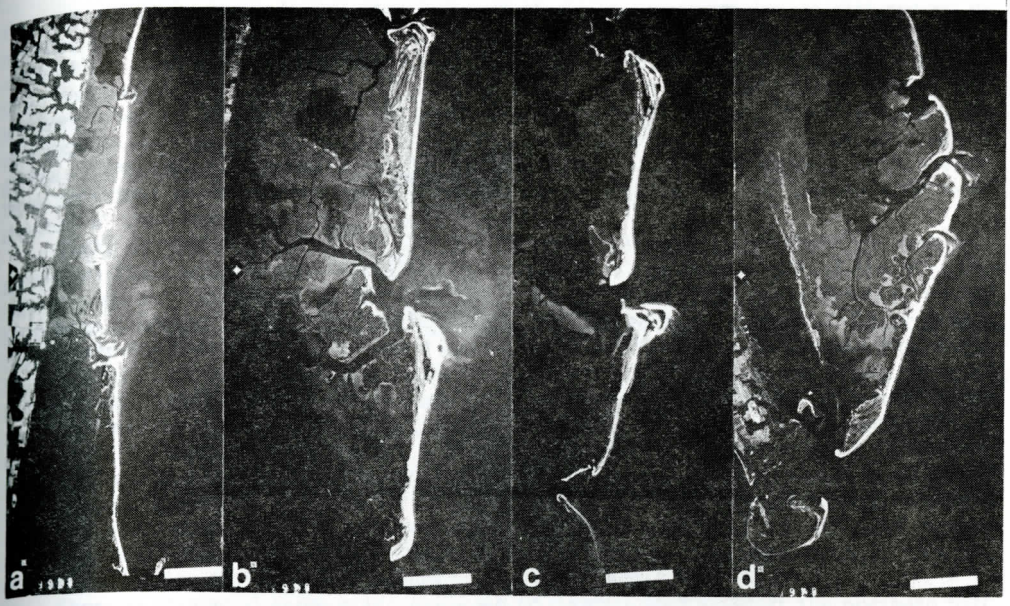


*Figure 2. Most of the Virginia barrier islands are shown on these reproductions from NASA false color IR imagery shot from 90,000 ft. (27.43 km) on 2 December 1972. North is at the top. A. The northern erosional arc in the system. From the south the islands are Cedar, Metomkin, Assawoman, and the southern tip of Wallops Island. B. & C. The mid-portion of the barrier island system where island offsets are prominent and rotational instability of the islands prevails. From the south, photo B shows Hog and Parramore Islands, and photo C shows Wreck, Cobbs, and Hog Islands. D. The convex southern part of the system where rapid island adjustments of shape, size, and orientation have all accompanied rapid retreat of this part of the system. Fisherman Island is the southern terminus of the system, with Smith, Myrtle, Ship-Shoal, and Wreck Islands lying to the north.*

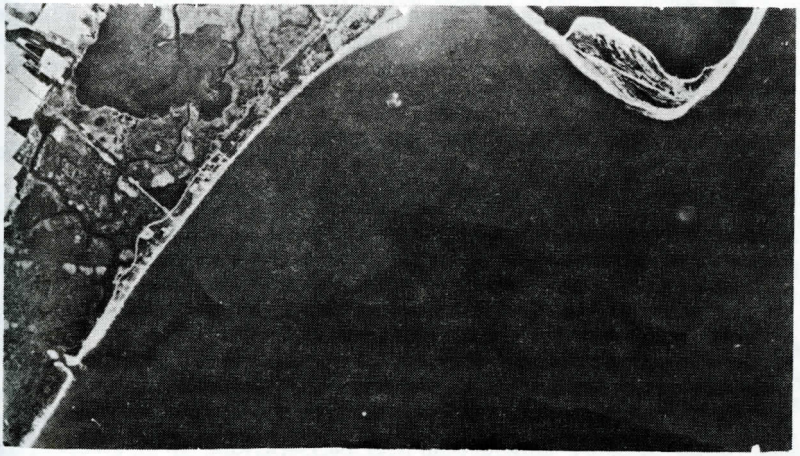

*Figure 3. The southern tip of Assateague Island is characterized by a hook-shaped feature (Fishing Point). Wallops Island, the most northern Virginia barrier, is shown just downdrift and offset landward of Assateague Island.*

convexity, and hence straightening of the shoreline.

Reasons for these shoreline retreat patterns along the Virginia barrier islands are generally understood. Tectonic movements (Heller and others, 1982), sediment supply

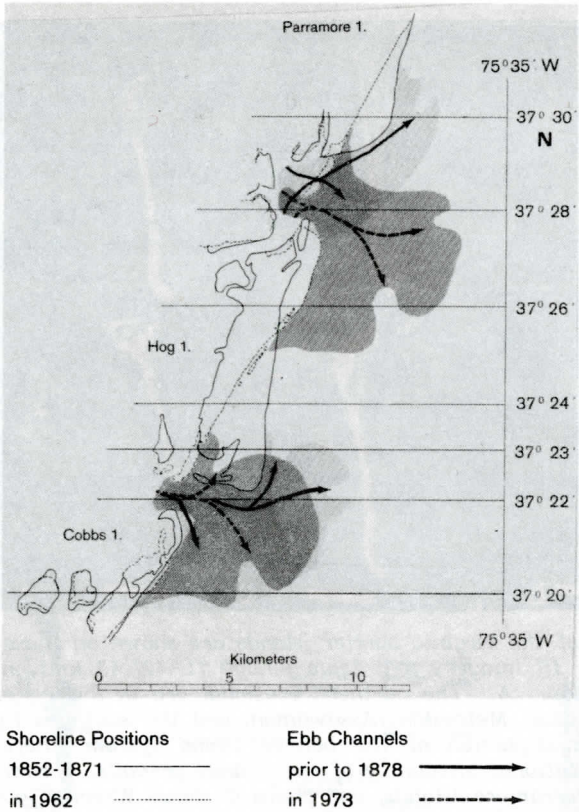


*Figure 4. Hog Island has undergone dramatic reorientations of the shoreline largely in response to the shifting position of the main ebb channel and associated ebb-tidal delta.*

(Rice and others, 1976), wave refraction effects (Goldsmith and others, 1975), and the underlying Pleistocene topography (Halsey 1979) have each been shown to play a role in this differential shoreline response. Time is also a factor; short-term island changes receive much attention, while longer-term responses (order of decades) often occur without notice. The role of these influencing factors becomes clearer when a long-term data base is examined.

## TECTONIC MOVEMENTS

Tectonic influences on the Eastern Shore, like changes in sea level, are part of the framework of conditions to which coastal processes shaping the islands must respond. There is evidence that tectonic movements have contributed to the present configuration of the island chain. Subsidence rates of 1.2 mm/yr at Fishermans Island and 2.0 mm/yr at the southern end of Assateague Island between 1944 and 1974 indicate the potential for tectonic movements to influence island development (Holdahl and Morrison, 1974). The time when the present cycle of subsidence first began and the consistency of the subsidence rates are discussed by Heller and others (1982). Subsidence has had the same effect as an eustatic rise in sea level; the islands have retreated landward and are drawn closer to the mainland because the mainland shoreline has retreated more slowly than the barriers (due to a steeper slope and protection from wave attack by marshes).

The Eastern Shore barrier islands have all (except Fishermans Island) been retreating at a relatively rapid rate. Differential subsidence from north to south indicates that relative sea level rise at the north end of the system is 0.8mm/yr greater than at the south end (Holdahl and Morrison, 1974). Therefore, the northern barriers should have been migrating landward at a more rapid rate than their southern counterparts. The northern group of islands are clearly closer to the mainland (Fig. 1)

than the islands in the other two groups, and this is not attributable to differences in offshore slope. However, the high retreat rates for all of the islands do not substantiate such a simple conclusion due to the focusing of wave orthogonals over the inner continental shelf on the southern island groups (Goldsmith and others, 1974). The northern group of islands is little affected by wave energy focusing. These islands have experienced less change in island orientation in comparison to the other two island groups. Diminished sediment supply, differential subsidence, and uniform wave attack have promoted steady beach retreat along the northern group of islands and have resulted in their close proximity to the mainland.

There is independent geomorphic evidence to support a pattern of tectonic movement that includes both upwarp and downwarp along the length of the Virginia barrier system. Southwest to northeast trending zones of apparently drowned marsh have been reported by Rice and others (1976) for the central portion of Cedar Island (Fig. 5) and for the Godwin Island-New Inlet area (Fig. 6) between Wreck and Ship Shoal Islands (Fig. 1). These zones are close to the major partitions of the island system. In both zones tidal creeks lead to flats or open water in the interior of marsh areas and terminate in birdfoot-like deltaic forms (Fig. 6b) -- a pattern that clearly differs from that of normal marsh creeks. These zones exhibit accreting mud flats with pioneering colonies of marsh grass (Fig. 6c), and newly-deposited sediment is soft and uncompacted to depths of at least three meters. Aerial photographs taken between 1949 and 1974 show that the appearance of the marsh and pattern of tidal creeks change quickly. Rapid deposition in these zones has been accompanied by rapid changes of ebb tide deltas and adjacent beaches.

There is also good geomorphic evidence to suggest that at least the northern half of Parramore Island has been undergoing uplift during the past 30 years (Fig. 7). Some tidal creeks in the marsh along the western edge of Parramore Island have undergone transition from the normal pattern of distributary channels to dendritic drainage systems. Headward erosion of those dendritic channels, after a century or more of normal marsh drainage (bifurcating channels with blunt termini), indicates rejuvenation, and in the past 30 years has extended these channels back into the main body of the island. The most striking example of this is a tidal creek that extended headward at the south end of Little Beach (an ancient beach ridge) until it tapped into two large swale ponds east of this beach ridge (Figs. 7b and c). While geomorphic evidence alone is insufficient to establish the existence of tectonic movements, it is sufficient to suggest that vertical movements beneath the barrier islands may have established a framework of conditions that have affected coastal processes along the Eastern Shore barrier system. It also appears to account for some of the differences in morphology among the three distinct groups of islands.

## SEDIMENT SUPPLY

Sediment supply is an important factor in the maintenance of barrier beaches and islands. Circumstances and events which alter or interrupt sediment supply have obvious effects on barriers. Generally, a sediment supply reduction produces beach erosion and retreat, while an excess supply will result in barrier accretion. Human intervention in the littoral drift system with engineering structures as well as natural events can initiate such responses by the barrier system.

Along the Eastern Shore the geomorphic response of each of the islands during the historical record (1852-1974) indicates an irregular, and often deficient, sediment supply along the length of the system. The southerly longshore transport of sediment on the Delmarva coast has been interrupted at Fishing Point (Fig. 3) at the southern end of Assateague Island since some time prior to 1852. Consequently, Wallops Island and the islands to the south have received insufficient sediment from the north for a very long time. As a result, Wallops Island and the other islands in the northern group have retreated in response to beach and shoreface erosion. The emplacement of bulwarks and groins by NASA during the 1950's aggravated the existing sediment deficiency, resulting in accelerated erosion along Assawoman and Metomkin Islands. This erosion along the northern group of islands puts sediment back into the longshore drift system so that islands to the south (central and southern groups) show fewer effects from a deficient sediment supply.

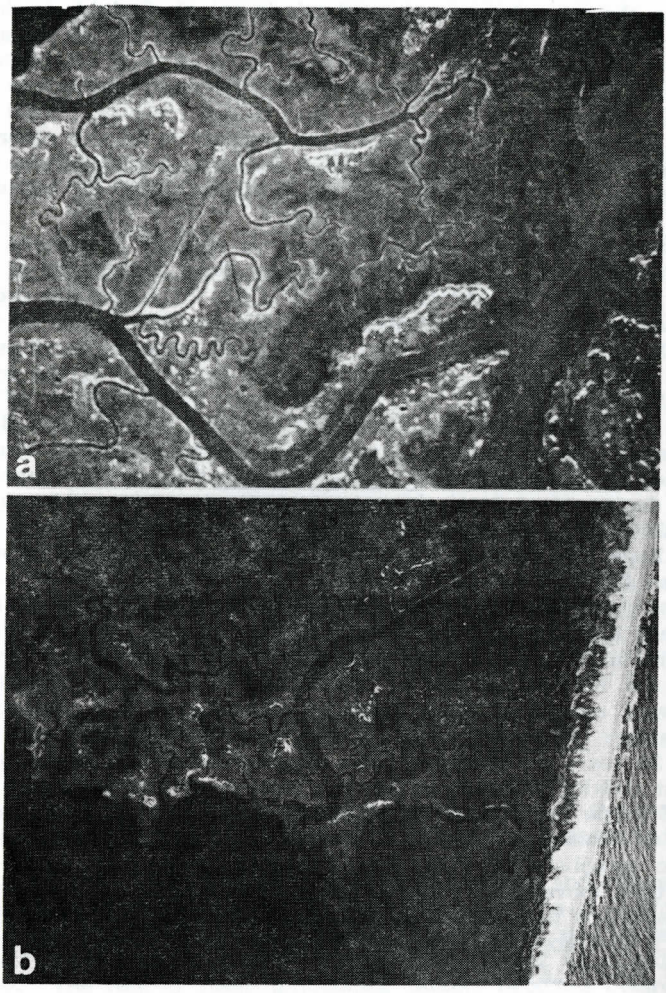


*Figure 5. Cedar Island Marsh: (a) southeast of Cedar Bay and (b) north of Burton Bay. North is toward the top. Dark grey areas are northeast trending zones of apparently drowned marsh. Light grey areas are normal marsh, and white patches are drift mats of cordgrass. Marsh canals and ponds are nearly black.*

Natural events, such as the opening of small ephemeral inlets, can temporarily reduce the supply of sediment downdrift of the opening and cause local and short-term erosion. Major island breaching is a low frequency, large magnitude event in terms of barrier island sedimentation. As long as the breach is open, there is relatively free circulation of water through the barrier between the sea and enclosed marshes and bays. This disrupts previously established patterns of tidal circulation and sediment transport, promoting deposition in the backbarrier environment (Morton and Donaldson, 1973). In addition, waves and tidal currents move large volumes of sediment through the breach to build the sediment platform required for healing the breach and rebuilding the island. During the many years that a breach is open, downdrift sediment supply is altered. The breached island retreats rapidly, and erosion of the adjacent shoreface mobilizes sediment which locally increases sediment supply to the breach in the island and to the littoral system.

Since the northern islands have been sand-starved for the longest period, changes are most dramatic in this shoreline sector. For example, Assawoman Island has been breached and healed during the past 30 years, leaving Gargathy Bay partially filled with

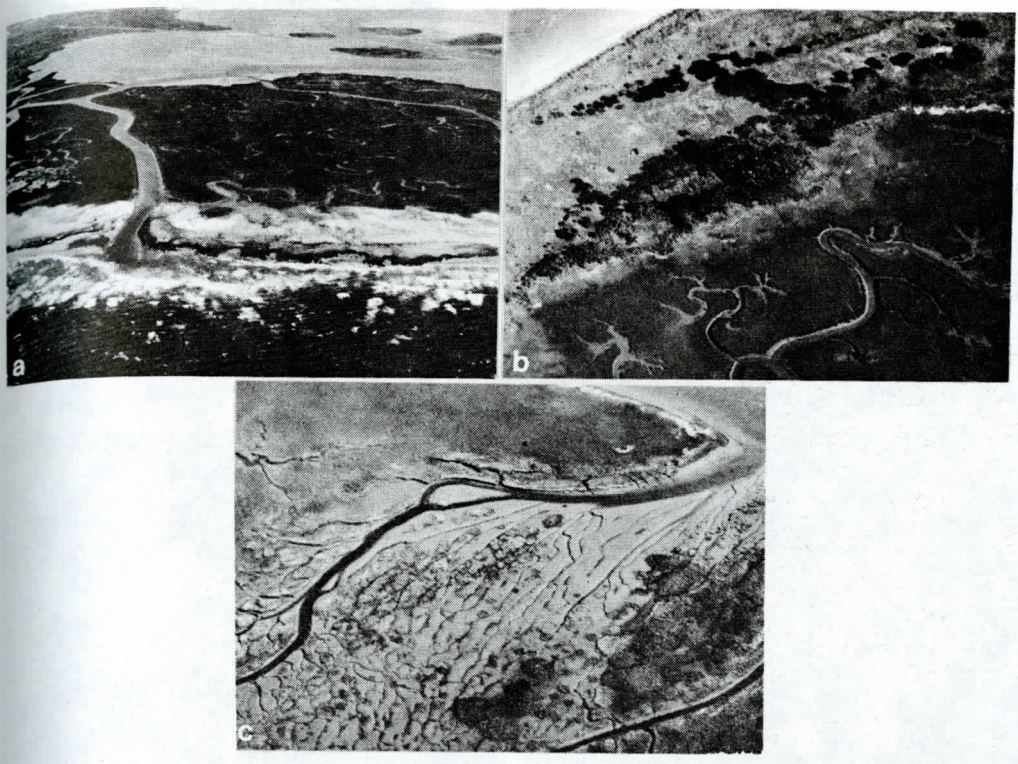


*Figure 6. Unusual marsh areas in the vicinity of New Inlet near the north end of the southern group of islands. (a) View southwest across Ship Shoal and Godwin Islands showing recently enlarged areas of open water within the marsh. Ship Shoal Island is experiencing very rapid rollover, and marsh canals and peat outcroppings extend seaward from the beach. (b) View southeast across Wreck Island. Marsh area is only sparsely vegetated, lacks peat, and is poorly consolidated to depths of at least three meters. (c) Former marsh area (historical) at southwest of Ship Shoal/Godwin Island characterized at present by rapid deposition of mud and pioneering colonies of marsh grass.*

sediment (Fig. 2a, top center). Metomkin Island began to breach in the late 1950's, and the inlet is still open (Figs. 2a and 8a). Large volumes of sediment have been moved into Metomkin Bay, and the northern part of the island has experienced rapid erosion. An ephemeral inlet developed across Cedar Island into Burton Bay in the late 1950's (Fig. 8b), resulting in the development of a very large flood tidal delta in the bay. Beach erosion on Cedar Island accelerated following the breaching of Metomkin Island, and it continued to erode rapidly until after the ephemeral inlet at Burton Bay closed in the early 1960's. Since that time the rate of retreat has slowed and finally reversed. These events have served to maintain the erosional arc of the northern group by altering the sediment supply within the group and by influencing the volume of sediment moving downdrift to the remaining islands in the system. Similar variations in sediment supply caused by local events have played a significant role in shaping the entire Eastern Shore barrier coastline.

## WAVE REFRACTION

Most of the energy required to drive coastal processes is derived from tides, waves, and wind. Differences in wave parameters (direction, height, and period) lead to variations in the rates at which coastal processes shape the barriers and affect the balance between accretion and erosion. Each wave is influenced by the bottom topography as it moves shoreward over the shallowing continental shelf. According to

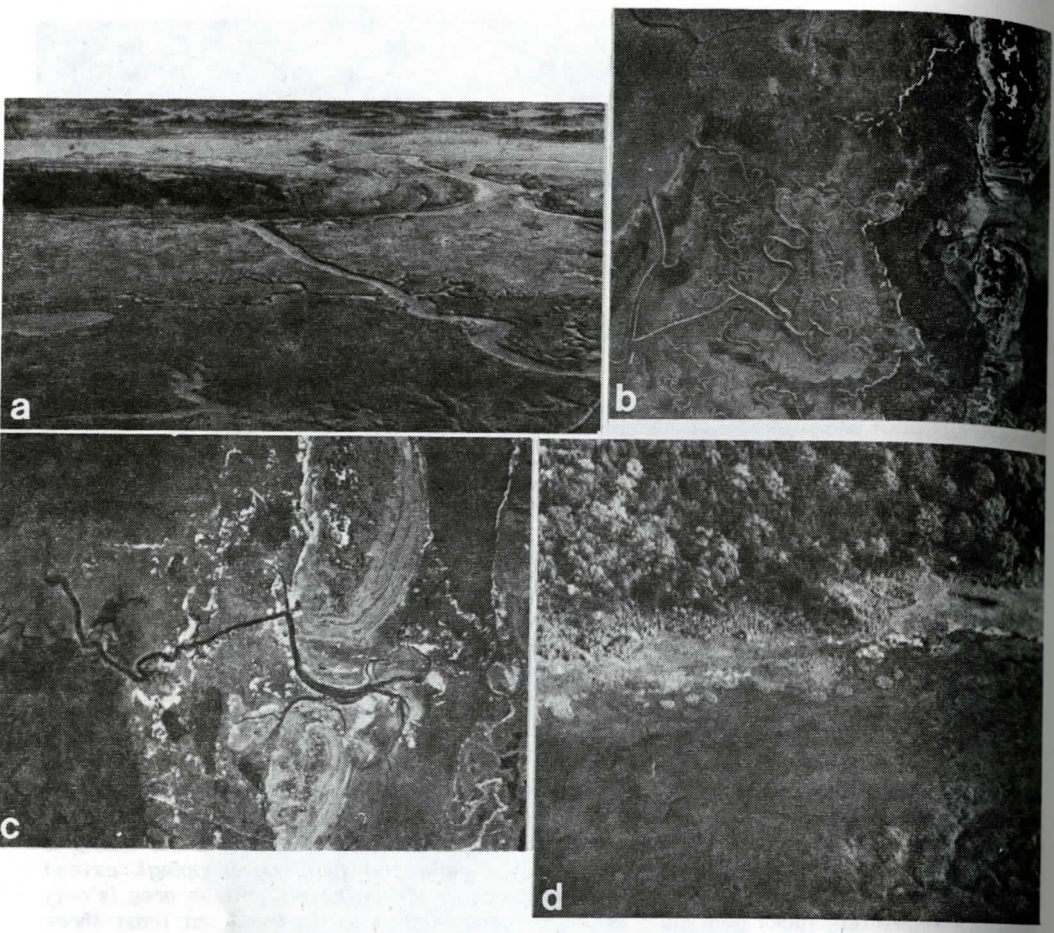


*Figure 7. Views of the Little Beach area of Parramore Island. (a) Little Beach (middle distance) is a breached ancient beach ridge near the western side of Parramore Island. Maximum relief is about 10 meters. The large canal draining through the breach from the interior of the island has formed since 1949. (b) Appearance of breach in Little Beach in 1949 (USDA photo). Dark shrub covered area west (left) of Little Beach is a sand apron that is generally between 1 and 2 meters above MHW. Discontinuous dark channels that curve into the breach from the marsh side are scour channels. The channels function only during storm surges and westerly wind set-ups on the bay, when water is driven over the sand apron and through the breach into a swale pond east of Little Beach. Light coloration in breach and swale pond is sand, carried through the scour channels and deposited as a fan extending from the breach into the swale pond. The surface of the swale pond is above MHW. (c) Appearance of breach in Little Beach in 1974. Growth of the sand fan at the breach has divided the swale pond into two ponds. The older scour channels are still present although they have been integrated into the drainage system leading from the swale ponds across the sand apron west of Little Beach. Small dendritic drainageways are shown along the western edge of the sand apron. (d) Dendritic drainage on sand apron west of southern part of Little Beach.*

the wave parameters, bottom topography focuses or disperses the waves as they approach the shoreline. With wave focusing, energy is concentrated, and shoreline adjustments are rapid and varied. In addition, nearshore wave refraction, such as around ebb-tidal deltas, causes further differential concentration of wave energy along the shoreline (Hayes and others, 1970; Goldsmith and others, 1975).

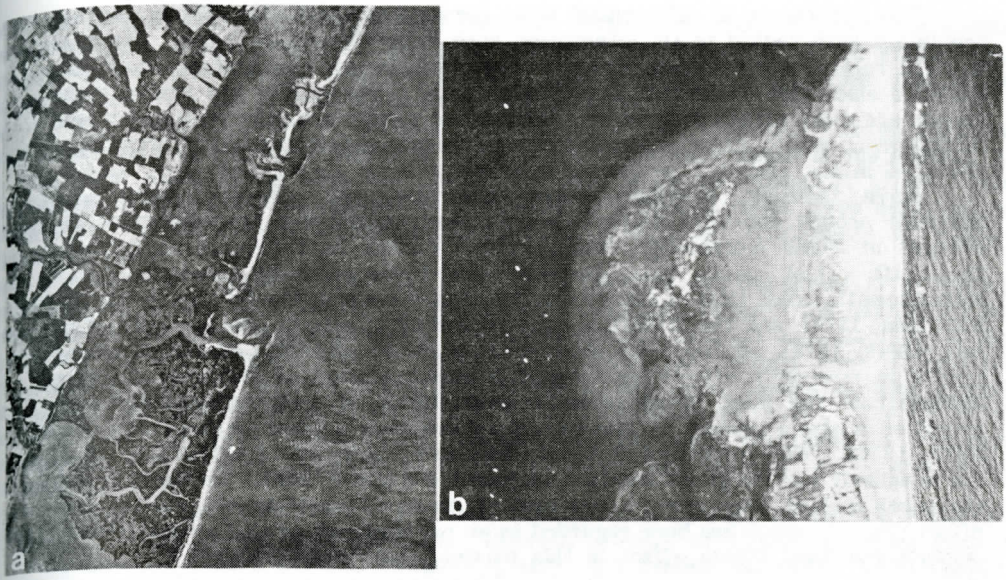


*Figure 8. Effects of localized coastal events. (a) Breach in the southern half of Metomkin Island at Metomkin Bay (1973 photo). Approximate bay side of former barrier beach is indicated by dark outcroppings of peat seaward of the present beach. Shifting multiple ephemeral inlets permit large volumes of sediment to be transferred into Metomkin Bay, interrupting the downdrift supply of sediment. (b) Sand delta built into Burton Bay behind Cedar Island while an ephemeral inlet was open briefly (5-6 years).*

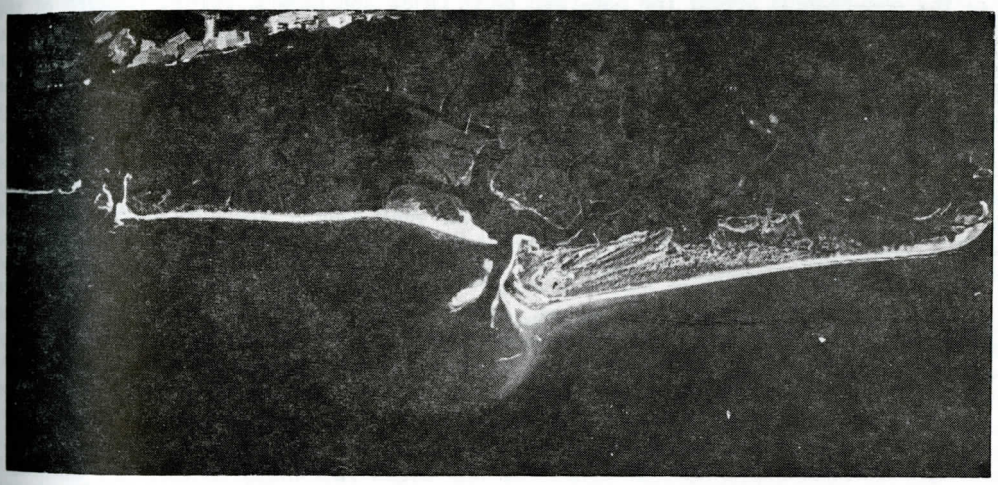

*Figure 9. Parramore Island, the crown jewel of The Nature Conservancy's Virginia Coast Reserve. The pronounced downdrift offset at Wachapreague Inlet has been remarkably stable since the mid-19th Century. The southern two thirds of the island has experienced beach retreat since an updrift offset of the south end of the island began to reverse in the late 19th Century. The forested (dark colored) beach ridges down the length of the island are ancient, whereas those near the inlet are historical in age. Little Beach is the breached ancient ridge at mid-island, and Italian Hill is the large ridge angled at the modern beach midway between Little Beach and the inlet. Photo reproduced from 1972 NASA false color image.*

The importance of differential wave focusing on the Eastern Shore was mentioned previously with regard to its interaction with differential subsidence. Wave climates and the role of bottom topography in wave focusing on the Eastern Shore have been reported elsewhere (Goldsmith and others, 1975). The middle and southern groups of islands are most affected by wave focusing; the results are clearly demonstrated in the middle group where major changes in ebb tidal delta shapes and island orientations have occurred in the past 125 years.

Wave focusing, nearshore wave refraction, and attendant bar-bypassing of sediment around ebb-tidal deltas at inlets have contributed to pronounced historical changes in island morphology, and downdrift offsets have become more pronounced. Downdrift offset inlets have been described along many coasts, including the Massachusetts coast (Hayes and others, 1970), the Copper River Delta in Alaska (Hayes and Kana, 1976), and the drumstick islands of South Carolina (Oertel, 1977; FitzGerald and others, 1978). It has been reported that wave refraction around ebb-tidal deltas results in downdrift offsets by creating a local reversal in transport direction, just downdrift of the inlet, which permits accumulation of inlet-bypassed sediment. The accretion is also a product of landward migrating bars welding to the beach (Hayes and Kana, 1976). With sufficient time and sediment supply an offset will be produced as the downdrift barrier grows seaward adjacent to a stable inlet. Wachapreague Inlet at the north end of Parramore Island exhibits those characteristics, and the Parramore offset (Fig. 9), which has been regarded as an evolving cape by Dolan and others (1979), displays the most stable offset in this barrier island chain (Fig. 2).

## INLET AND OFFSET STABILITY

Prominent offsets on the Eastern Shore have been interpreted as embryonic capes (Dolan and others, 1979), but offset reversals have been ignored. It is useful to examine the factors and conditions that effect these inlets and enter into the change and development of offsets. Offset reversals, such as those noted at both ends of Hog Island (Fig. 4), take place following abrupt major changes in the location and direction of the ebb-channel across the ebb-tidal delta (Rice and others, 1976). Growth of the terminal lobe of the ebb-tidal delta during one condition of island offset can lead to over-extension and inefficiency of the ebb-channel (FitzGerald and others, 1978). An over-extended ebb-channel can breach, permitting a new channel to be cut across the ebb tidal delta, and abandonment of the older channel. Major storm events accompanied by large storm surges provide conditions most favorable for breaching a new channel, and further entrenchment occurs as the storm surge exits through the inlet. These same conditions can also generate new ephemeral inlets along the barrier island chain. Following the establishment of a new ebb flow channel, the abandoned terminal lobe, which had been maintained by ebb-channel dynamics, falls under the direct influence of shoreface dynamics and the littoral drift system. In time, the abandoned lobe of sediment moves downdrift, re-establishing a normal shoreface profile (Oertel, 1977; FitzGerald and Hayes, 1980). The change in ebb-channel position initiates the growth of a new terminal lobe of the ebb-tidal delta. As the ebb-tidal delta morphology adjusts to the new channel position, nearshore wave refraction, longshore drift, and sediment bypassing around the ebb-tidal delta begin to rework the adjacent seaward beaches at the inlet (Fig. 4). A reversed offset may then develop. Adjustments in the modern reversed offsets of Hog and Cobb Islands began in the late 1800's, and have continued at a declining rate to the present (Rice and others, 1976).

It is also useful to examine the factors and conditions that enter into the change and development of offsets. Wave energy distributions along the islands, like tectonic influences, are part of the framework of conditions within which coastal processes operate. There has been a tendency for shoreline wave energy distribution to become more uniform along the Virginia barrier islands since 1852, resulting in diminished offset and greater inlet stability (Goldsmith and others, 1975). Profiles prepared from bathymetric data for the inner shelf were compared for 1852 and 1934. Their profiles (Goldsmith and others, 1975) showed that many of the subaqueous ridges on the inner shelf had heightened, and swales deepened during that time interval. The result was an alteration of the wave refraction patterns across the inner shelf. This produced less focusing of short period (erosional) wave energy, and shifted the focal areas for long

period (accretional) wave energy away from the north ends of the islands in the middle and southern groups (Goldsmith and others, 1975). Therefore, it can be argued that inlet offset development will continue to slow as barrier orientation approaches equilibrium with the present wave refraction pattern.

The downdrift offset of Parramore Island (Figs. 1 and 9) already existed when the first accurate hydrographic charts of the Eastern Shore were issued in the 1850's. In fact, older maps dating back into the 1660's show a similar downdrift offset. The persistence of that offset, without the formation of a cape, through three centuries of shoreline retreat attests to the stability of the inlet/offset relationship at Wachapreague Inlet.

Several investigators (that is, Kraft 1971; Morton and Donaldson 1973; Halsey 1979), have argued that buried late Pleistocene topography beneath the barrier islands influences inlet position and stability. However, detailed data are not complete for the Eastern Shore of Virginia. It is generally understood that valleys were entrenched across the continental shelf during low stands of sea level associated with glacial maxima, and then buried when sea level rose as the glaciers retreated. The thrust of the argument is that those buried valleys offer the least resistance to erosional processes, and thus the positions of inlets and major bay channels are controlled by exhumed valleys.

From the above discussion, it is clear that island.offsets do not develop uniformly through time or continue ad infinitum. Instead, reversal of offsets or offset growth rates, appears to be a normal, though long-term, phenomena associated with dynamic adjustments of ebb-channels, ebb-tidal deltas, and the two islands adjacent to the inlet. Similar reversals of island offsets have been reported in many other areas, for example, the vicinity of Chatham Inlet on Cape Cod (Goldsmith, 1972), the Massachusetts and New Hampshire barrier beaches (Hubbard, 1974), and the Georgia barrier islands (Oertel, 1977).

## FUTURE CAPE DEVELOPMENT

Dolan and others (1979) have suggested that future capes will develop along the Virginia barrier islands within the next 100 years. However, existing studies and current information refute this unproven hypothesis. Geomorphic evidence indicates that the shoreline was previously more irregular than is evidenced in historical records (since the late 1600's). Pronounced, truncated beach ridges meet the modern shoreline at marked angles. For example, Italian Hill, a heavily forested, high relief ridge on Parramore Island, joins the modern shoreline at an angle of 12° (Fig. 9). Past coastlines were clearly more irregular than the present configuration based on island restoration from ridge orientations and truncations (Rice and others, 1976). The historical trend toward a smoother, more regular coastline demonstrates that coastal processes along the Virginia barrier islands work toward reduced irregularities, rather than the evolution of cape features.

Hoyt and Henry (1971) postulated that true capes, such as Capes Hatteras, Lookout, and Fear in North Carolina, Cape Romain-Santee Point in South Carolina, and lesser capes at Tybee and Little St. Simons Islands in Georgia, correspond to the discharge areas of ancient and present day rivers. Capes did not develop under present conditions, but instead, originated as river deltas on the continental shelf several tens of thousands of years ago when sea level stood much lower than at present. Deltas became the loci of prominent capes and associated barrier island systems with the reworking of these deltaic sediments by waves and currents during the Holocene rise of sea level. The present coastal configuration of these well known capes can be attributed to the erosion and gradual landward retreat of formerly more extensive seaward projecting capes (Moslow and Heron, 1981). A modern example of barrier development in a deltaic setting has recently been described along the Louisiana coast (Penland and others, 1981).

From the prior discussion it is clearly unnecessary to draw upon edge wave theory to explain the evolution of the Virginia barrier islands or cape development, as suggested by Dolan and others (1979). In fact, edge waves have not been shown by any investigator (that is, Inman and others, 1976; Guza and Inman, 1975) to be the primary factor in shaping even moderate lengths (> 100m) of shoreline. Since the

Virginia barrier islands are located along the open mid-Atlantic coast, there are no effective headlands to trap a standing edge wave. Even if such waves were shown to exist, their low amplitude (order of centimeters) would result in little impact on the shoreline compared to the other, much higher wave energy input. By picking a certain wave period and mode, it is possible to match any spacing of edge waves with the scale of some feature (from 3 m beach cusps to 30 km capes), and hence the choice of edge wave modal number 3 by Dolan and others (1979) has no special meaning and lacks physical understanding of this phenomenon. In order to invoke edge waves to explain this kind of shoreline response, it is necessary to demonstrate why they exist and how they can persist through highly variable infragravity wave input (Leatherman and others, 1982).

## CONCLUSION

The present configuration of the barrier islands along the Eastern Shore of Virginia is the result of a regime of shoreline retreat responding to temporal and spatial variations in well understood and documented coastal processes. Alongshore variations in sediment supply, vertical tectonic movements, long-term changes in wave refraction over the continental shelf, and a possible influence of the late Pleistocene drainage systems, have resulted in differing shoreline responses and barrier groupings during the ubiquitous rise in sea level. More localized geomorphic responses can be related to meteorological events, local variations in sediment supply, and changes in inlet morphology and dynamics. Quantitative historical data and geomorphic evidence suggest that the Eastern Shore barriers will approach a smoother shoreline configuration in the future, rather than forming any cape-like features.

## ACKNOWLEDGMENTS

Critical views of various drafts of the manuscript by Drs. A.T. Williams, G. Oertel, R.T. Guza, J.M. Demarest, R.W.G. Carter, D.M. FitzGerald, and T.F. Moslow are much appreciated. A much shortened rendition of this article has been published in Science as a research note.

## REFERENCES CITED

DeAlteris, J. and Byrne, R., 1975, The Recent history of Wachapreague Inlet, Virginia: in Estuarine Research, L. E. Cronin, ed., Academic Press, New York, p. 167-181.

Dolan, R., Hayden, B., and Jones, C., 1979, Barrier island configuration: Science, v. 204, p. 401-403.

Field, M., and Duane, D., 1976, Post-Pleistocene history of the United States inner continental shelf: significance to origin of barrier islands: Geol. Soc. of Amer. Bull. v. 87, p. 691-702.

FitzGerald, D., Hubbard, K., and Nummendal, D., 1978, Shoreline changes associated with tidal inlets along the South Carolina coast: Proceedings of Coastal Zone 78, p. 1973-1994.

FitzGerald, D. M., and Hayes, M. O., 1980, Tidal inlet effects on barrier island management, Proceedings of Coastal Zone 80, ASCE, p. 2355-2379.

Goldsmith, V., 1972, Coastal processes of barrier island complex and adjacent ocean floor: Monomoy Island-Nauset Spit, Cape Cod, Massachusetts: Ph.D. Dissertation, University of Massachusetts - Amherst, 469 pp.

Goldsmith, V., Morris, W., Byrne, R., and Whitlock, C., 1974, Wave climate model of the mid-Atlantic continental shelf and shoreline (Virginia sea): Model development, shelf geomorphology and preliminary results, VIMS SRAMSOE No. 38, 146 pp.

Goldsmith, V., Byrne, R., Sallenger, A., and Drucker, D., 1975, The influence of waves on the origin and development of the offset coastal inlets of the southern Delmarva Peninsula, Virginia: *in* Estuarine Research, L. E. Cronin, ed., Academic Press, New York, p. 183-200.

Guza, R., and Inman, D., 1975, Edge waves and beach cusps: J. Geophys. Res., v. 80, p. 2997-3012.

Halsey, S., 1979, Nexus: New model of barrier island development: in Barrier Islands, S. P. Leatherman, ed., Academic Press, New York, p. 185-210.

Hayes, M., Goldsmith, V., and Hobbs, C., 1970, Offset coastal inlets: Proceedings of the 12th Coastal Engineering Conference, p. 1187-1200.

Hayes, M., and Kana, T., 1976, Terrigeneous clastic depositional environments: Tech. Report 11 CRD, Dept. of Geology, University of South Carolina, in two parts.

Heller, P. L., Wentworth, C. M., and Poag, C. W., 1982, Episodic post-rift subsidence of the United States Atlantic continental margin, Bull. Geol. Soc. Amer., v. 93, p. 379-390.

Holdahl, S., and Morrison, N., 1974, Regional investigations of vertical crustal movements in the U.S., using precise relevelings and mareography data: Tectonophysics, v. 23, p. 373-390.

Hoyt, J., and Henry, V., 1971, Origin of capes and shoals along the southeastern coast of the United States: Bull. Geol. Soc. Amer., v. 82, p. 59-66.

Hubbard, D., 1974, Tidal inlet morphology and hydrodynamics of Merrimack Inlet, Massachusetts: M.S. Thesis, University of South Carolina, 144 pp.

Inman, D., Nordstrom, C., and Flick, R., 1976, Currents in submarine canyons; an air-sea-land interaction: Annual Rev. Fluid Mech., v. 8, p. 275-310.

Kraft, J., 1971, Sedimentary facies patterns and geologic history of a Holocene marine transgression: Bull. Geol. Soc. Amer., v. 82, p. 2131-2158.

Leatherman, S. P., Rice, T. E., and Goldsmith, V., 1982, Virginia barrier island configuration: a reappraisal: Science, v. 215, p. 285-287.

Leatherman, S. P., 1979, Migration of Assateague Island, Maryland, by inlet and overwash processes, Geology, v. 7, p. 104-107.

Morton, R., and Donaldson, A., 1973, Sediment distribution and evolution of tidal deltas along a tide-dominated shoreline, Wachapreague, Virginia: Sed. Geol., v. 10, p. 285-299.

Moslow, T. F., and Heron, S. D., Jr., 1981, Holocene depositional history of a microtidal cuspate foreland cape: Cape Lookout, North Carolina, Mar. Geol., v. 41, p. 251-270.

Oertel, G., 1977, Geomorphic cycles in ebb deltas and related patterns of shore erosion and accretion: J. Sed. Petr., v. 47, p. 1121-1131.

Penland, S., Boyd, R., Nummendal, D., and Roberts, H., 1981, Deltaic barrier development on the Louisiana coast, Transactions Gulf Coast Association of Geological Societies, v. 31, p. 471-476.

Rice, T., Niedoroda, A., and Pratt, A., 1976, Coastal processes and geology, Virginia barrier islands, *in* Virginia Coast Reserve Study: Ecosystem Description, The Nature Conservancy, Arlington, VA., p. 109-382.

# THE SIGNIFICANCE OF ABUNDANT K-FELDSPAR IN POTASSIUM-RICH, CAMBRIAN SHALES OF THE APPALACHIAN BASIN

Vishnu Ranganathan Department of Geology, University of Tulsa, Tulsa, OK 74104

## ABSTRACT

Cambrian shales from the Rome, Rogersville, and Nolichucky formations in the southern Appalachian Basin have anomalously high $K_2O$ contents (9% mean) in comparison with the $K_2O$ content for Paleozoic shales in North America (3.6% mean). Much of the increased $K_2O$ is due to detrital K-feldspar which averages 14 percent in Cambrian shales and only 1 percent in post-Cambrian shales. Detrital K-feldspar was probably provided by the Canadian Shield. After Cambrian time, the Taconic uplift, an eastern source area, provided detritus sparse in K-feldspar but slightly richer in plagioclase.

A total of 135 Phanerozoic shales from the Appalachian Basin and from outside were analyzed for feldspar content by semi-quantitative x-ray diffraction. Fifteen Cambrian shales rich in K-feldspar (20% mean) have anomalously high $K_2O$ contents, 9.1 percent in the 0.005-0.140 mm. fraction and 9.0 percent in the $<0.005$ mm. fraction. Much of the K-feldspar is detrital and luminesces blue under cathode-rays. The normative contribution of K-feldspar is 3.4% $K_2O$ to the bulk rock. It is not known how much $K_2O$ is due to illite. Nine Phanerozoic shales without K-feldspar have only 2.1 percent $K_2O$ in the 0.005-0.140 mm. fraction and 4.1% $K_2O$ in the $<0.005$ mm. fraction. Previous studies have shown that since the Cambrian there is a worldwide decrease of $K_2O$ with geologic age in shales. Further work is needed to determine the extent to which K-feldspar abundance is responsible for this trend.

## INTRODUCTION

The $K_2O$ content of argillaceous rocks decreases through time from the Cambrian to the present. This phenomenon appears to be worldwide. On the North American platform it is shown from chemical analyses of argillaceous rocks of Paleozoic, Mesozoic, and Cenozoic ages (Nanz, 1953; and White, 1959). On the Russian platform it is shown from analyses of argillaceous rocks by Ronov and Migdosov (1971, pp. 149-160), and a similar trend is seen from analyses of argillaceous rocks from the Australian platform (Van Moort, 1972). In general, $K_2O$ decreases from about 4-5% in Cambrian shales to about 2-3% in Mesozoic and Cenozoic shales.

Vinogradov and others (1956a) suggested that the higher potassium content of ancient shales is a consequence of more intensive formation of K-micas and slightly altered K-feldspars on the ancient continents. According to these authors, the exposed area of such rocks was considerably larger in the pre-Devonian than it is today and chemical weathering was milder. Alternatively, Mackenzie (1975, p. 319) suggested that the increased $K_2O$ is due to addition of $K_2O$ with deep burial. Conway (1945) proposed that the increased $K_2O$ in older shale is due to the abundance of syngenetic clay minerals bearing $K^+$. He suggested that $K^+$ concentration in seawater reached a maximum in the late pre-Cambrian and preferential adsorption of $K^+$ by clay minerals reached a peak at that time.

The purpose of this study is to show the important contribution of detrital K-feldspar to the high $K_2O$ content of Cambrian shales within the Appalachian Basin. A good representation of samples worldwide from various tectonic settings and source areas is needed to determine the extent to which K-feldspar is responsible for the worldwide trend of $K_2O$ decreasing with age.

## LOCATION OF SAMPLES

Feldspar content of 135 Phanerozoic shales was determined by x-ray diffraction; 34 Cambrian shales and 35 Ordovician-Devonian shales were from the Appalachian Basin in southwestern Virginia; 66 shales ranging in age from Ordovician-Holocene were

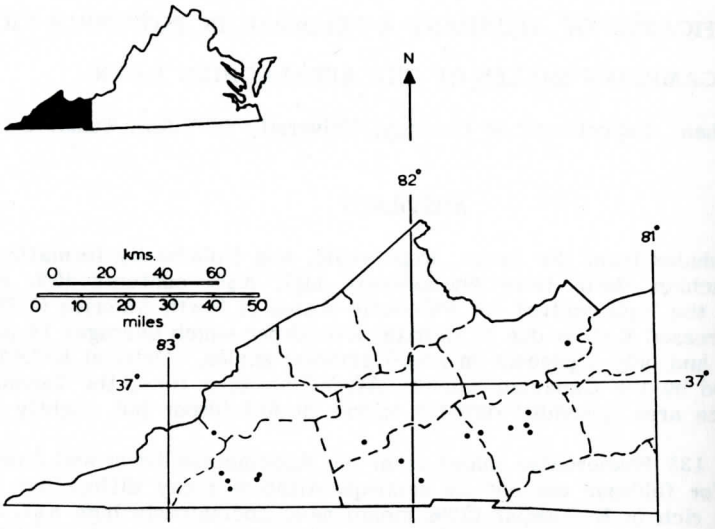


*Figure 1. Outcrop locations of Lower Paleozoic shales analyzed from the Appalachian Basin in southwestern Virginia.*

from areas outside the Appalachian Basin and were obtained from a collection at the University of Cincinnati Geology Department. Most of these were North American although a few were South American and European. In the Appalachian Basin, outcrops from previously measured sections were sampled (Fig. 1). Samples analyzed in this study were fresh and sparse in carbonates.

The Cambrian shales with abundant K-feldspar are characterized by features of shallow water origin. Parts of the Rome formation have ripple marks, red beds, and mud cracks suggesting deposition in the intertidal zone. Abundant scolithus burrows in many of the Lower Cambrian orthoquartzites interbedded with the shales suggest deposition in subtidal conditions. Glauconite is abundant both in the Rome and in the Nolichucky shales. Nolichucky shales are interbedded with carbonate mudstones and packstones containing rip-up clasts, discoid-oval pebbles, and chunks of micrite. Bottom surfaces sometimes have load casts. Trilobites and brachipods are common in the interbedded carbonates. Deposition occurred in very shallow water from a few meters to a few tens of meters deep (Markello and Tillman, 1979, p. 50). According to these authors, Nolichucky shales were deposited behind a shallow-water carbonate barrier, within an embayment on the carbonate shelf.

## ANALYTICAL METHODS

Feldspar abundances were determined by x-ray powder diffraction (XRD) from calibration curves. The accuracy of the determinations is ±10% of the amount present. The calibration curves were obtained by plotting the 3.24 A peak height of standard microcline and the 3.19 A peak height of a standard plagioclase versus concentration. The standard feldspars were mixed in a matrix of a non-feldspathic Devonian black shale to standardize matrix effects. Calibration curves are shown for K-feldspar in Figure 2 and for plagioclase in Figure 3. Although the best-fit curves do not pass through the origin, they were forced to pass through the origin because precision was low when K-feldspar content was less than 5% and when plagioclase was less than 2%. The mixtures were homogenized in plastic vials by tumbling in a Spex Mixer. Disoriented mounts were prepared on styrofoam mounts by a method modified after Thompson, Duthie, and Wilson (1972): 0.33 g of the sieved, < 0.140 mm. powder is mixed with about 1 ml. of ethanol; the mixture is homogenized and poured little by little onto styrofoam squares 1" x 1" x 1/4". Ethanol permeates through the pores and evaporates rapidly leaving disoriented mounts.

In order to study variations in mineralogy and chemistry with grain size, 15 Cambrian shales rich in K-feldspar and 9 Phanerozoic shales rich in plagioclase as

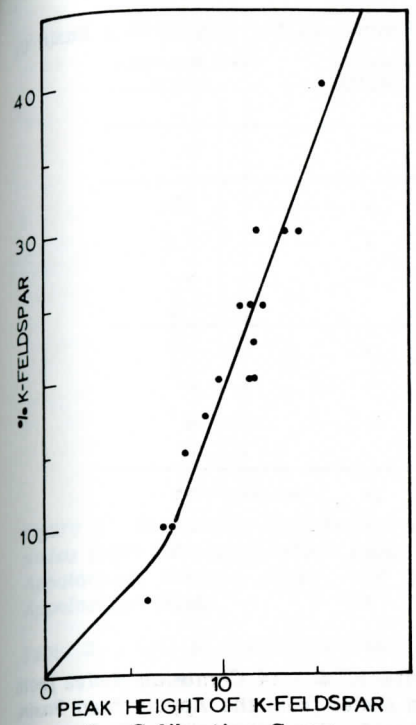


*Figure 2. Calibration Curve for K-feldspar.*

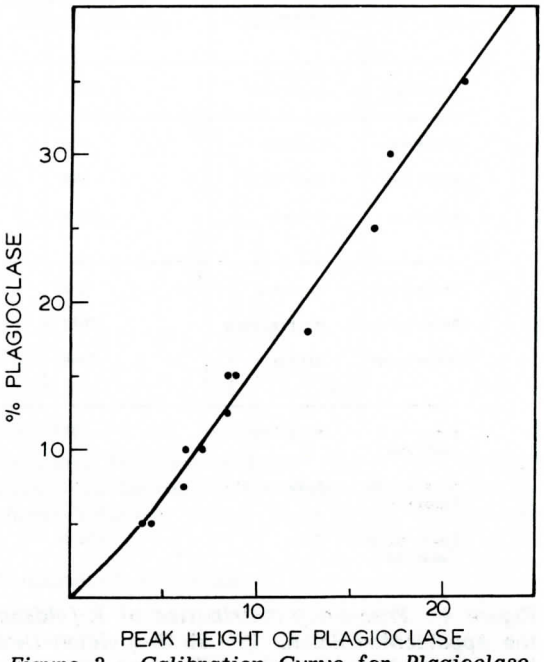


*Figure 3. Calibration Curve for Plagioclase.*

determined from bulk XRD were selected for grain size separations. The shales were ground in a Spex Mixer for about 15 minutes and sieved through an ASTM sieve No. 110 with an opening size of 0.140 mm. The < 0.140 mm. fraction was repeatedly treated with 30% $H_2O_2$ solution until organics were oxidized and then dispersed in distilled water in an ultrasonic disaggregator for 10 minutes. Grain size separations into <0.005 mm. and 0.005-0.140 mm. fractions were made by sedimentation following a method by Jackson (1969, p. 110-141). The 0.005 mm. break was chosen because it was believed that the best separation of clay minerals and non-clay minerals would be observed here. For a few shales, the 0.005-0.140 mm. fraction was separated into two fractions, 0.005-0.050 mm. and 0.050-0.140 mm. Each grain size fraction was collected on an evaporating dish, dried at 110°C in an oven, and weighed. For 17 of these shales, <0.002 mm. fractions were also obtained to study the clay mineralogy. Oriented mounts were made for all the fractionated shales by the smear method (Gibbs, 1965) and x-ray diffractograms were obtained. The 3.24 A peak height for K-feldspar, the 3.19 A peak height for plagioclase feldspar, and the 10.2 A peak height for illite and micas were measured. A General Electric powder diffractometer model SRD-6, with a Cu target, was used. Silt fractions of shales rich in K-feldspar were examined with a cathodoluminoscope. For 15 fractionated shales rich in K-feldspar, and 9 fractionated shales rich in plagioclase, chemical analyses of major elements were done by Atomic Absorption, following the method of Medlin and others (1969).

## RESULTS

Cambrian shales from the Appalachian Basin are exceptionally rich in K-feldspars. K-feldspar content averages 14% in shales from the Rome, Rogersville and Nolichucky formations (Table 1 and Figure 4). Post-Cambrian shales, in contrast, have an average of only 0.3-1.2% K-feldspar. The plagioclase content of shales increases slightly after the Cambrian. Cambrian shales have an average of 1.8% plagioclase, whereas post-Cambrian shales have an average of 3.7% plagioclase in the Appalachian Basin and 7.3% plagioclase in areas outside the Appalachian Basin (Table 2 and Figure 5).

*Table 1. K-Feldspar contents of Lower Paleozoic shales in the Appalachian Basin in Southwestern Virginia.*

| Age | Formation | Maximum Thickness in Area Sampled | Number of Samples | Mean K-feldspar Content |
|---|---|---|---|---|
| Devonian | Chemung-Braillier | = 3500' | 5 | 0 |
| Silurian | Clinton | 150' | 9 | 0.5% |
| Silurian | Rose Hill | 288' | 4 | 1.6% |
| Silurian | Sevier | 1500' | 5 | 0 |
| Ordovician | Juniata | 400' | 3 | 0 |
| Ordovician | Martinsburg | 1617' | 6 | 0 |
| Ordovician | Athens | 1566' | 3 | 0 |
| Upper Cambrian | Nolichucky | 725' | 24 | 11% |
| Middle Cambrian | Rogersville | 60' | 2 | 31% |
| Lower-Middle Cambrian | Rome | >1010' | 8 | 17.6% |

*Figure 4. Frequency distribution of K-feldspar content. I. - 34 Cambrian shales from the Appalachian Basin. II. - 35 Ordovician-Devonian shales from the Appalachian Basin. III. - 66 Ordovician-Holocene shales from areas outside the Appalachian Basin.*

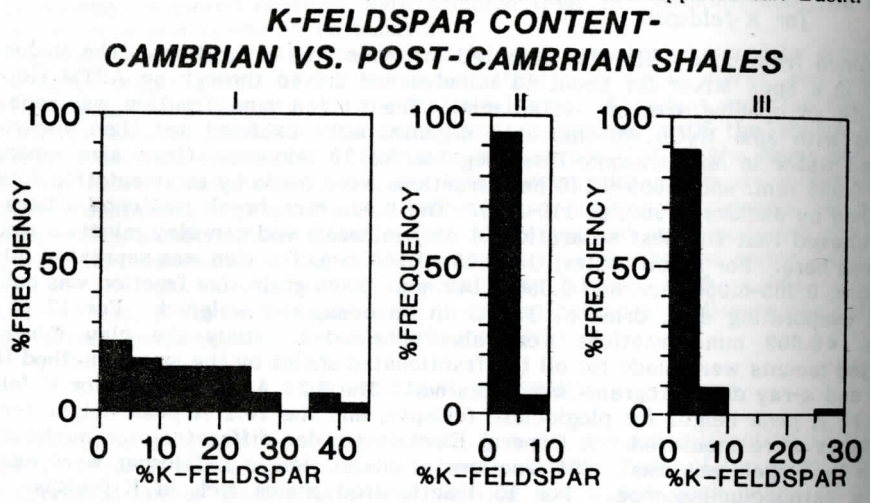


*Table 2. Plagioclase Content of Shales (Bulk Analyses).*

| Sample Set | Number of Samples | Number of Samples with Detectable Plagioclase | Mean % Plagioclase |
|---|---|---|---|
| All Cambrian shales from the Appalachian Basin | 34 | 9 | 1.8 |
| All Ordovician-Devonian shales from the Appalachian Basin | 35 | 22 | 3.7 |
| All Ordovician-Holocene shales from outside the Appalachian Basin | 66 | 43 | 7.3 |

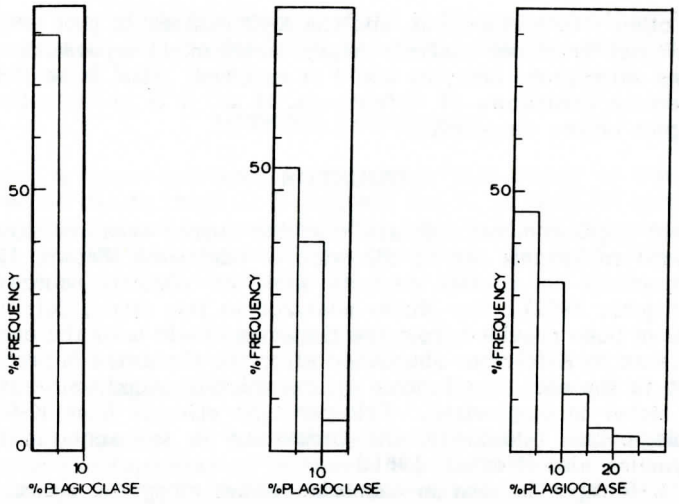


*Figure 5. Frequency distribution of plagioclase feldspar content. Left - 34 Cambrian shales from the Appalachian Basin. Middle - 35 Ordovician-Devonian shales from the Appalachian Basin. Right - 66 Ordovician-Holocene shales from areas outside the Appalachian Basin.*

*Table 3. $K_2O$ in Cambrian Shales with abundant K-feldspar.*

| Age | Formation | Sample No. | % $K_2O$ <0.005 mm. | % $K_2O$ 0.005-0.140 mm. |
|---|---|---|---|---|
| Upper Cambrian | Nolichucky | ClQ-3-1 | 8.6 | 7.2 |
| " " | " | ClQ-3-4 | 7.1 | 8.7 |
| " " | " | DQ-1-2 | 8.3 | 8.1 |
| " " | " | DQ-1-3 | 8.4 | 8.1 |
| " " | " | DQ-1-4 | 7.9 | 7.1 |
| " " | " | Hans-1-1 | 9.5 | 8.8 |
| " " | " | Hans-1-2 | 10.7 | 11.1 |
| " " | " | Hans-1-3 | 9.9 | 11.7 |
| " " | " | Wyn-1-3 | 7.9 | 10.8 |
| Lower-Middle Cambrian | Rome | DQ-3-1 | 10.4 | 9.7 |
| " " | " | DQ-3-2 | 10.0 | 9.3 |
| " " | " | DQ-3-5 | 10.1 | 9.6 |
| " " | " | DQ-3-7 | 9.2 | 10 |
| " " | " | DQ-4-1 | 9.0 | 7.4 |
| " " | Forteau | Forteau | 8.6 | 8.3 |
| | | Mean | 9.0 | 9.1 |
| | | S.D. | 1.1 | 1.4 |

Shales rich in K-feldspar were separated according to grain size and silt and sand fractions < 0.050 mm. were examined under a cathodoluminoscope. Most of the silt grains exhibit bright blue cathodoluminescence, a characteristic of detrital K-feldspars only: authigenic K-feldspars do not luminesce (Odom, 1975; Kastner, 1974). Because high power objectives cannot be used with a cathodoluminoscope, it is not possible to determine the nature of K-feldspars which are finer than silt size.

The average $K_2O$ content of 15 Cambrian shales chemically analyzed is 9.0% (mean) in the 0.005-0.140 mm. fraction and 9.1% (mean) in the < 0.005 mm. fraction (Table 3).

The change in $K_2O$ content between the 0.005 mm. - 0.140 mm. fraction and the < 0.005 mm. fraction is imperceptible. K-feldspar averages 20% by weight in this set of shales. Pure K-feldspar has 16.9% $K_2O$. Thus K-feldspar should contribute 3.4% $K_2O$ to the bulk rock. Though this is significant, the remaining 5.6% $K_2O$ is unaccounted for. Pure illites with up to 11% $K_2O$ have been reported by Weaver and Pollard (1973, p. 8). The occurrence of a very potassic illite in abundance (50% or more) is required to account for the remaining 5.6% $K_2O$ and this is possible. Data collected in this study are insufficient to determine conclusively what the relative contributions of K-feldspar and illite are to $K_2O$ content. The abundance of K-

feldspar, illite, other minerals present, and the $K_2O$ content of pure illite need to be known. Because wet chemical analyses require mechanical separation of pure illite from other phases microprobe analyses would be required. Also, some of the illite may be due to diagenetic breakdown of K-feldspars. If so, it is possible that K-feldspar content was higher before diagenesis.

## DISCUSSION

Paleocurrent measurements indicate that the source area for Lower Cambrian rocks in southwestern Virginia lay to the west or northwest (Brown, 1980); whereas paleocurrent directions in alluvial deposits show an easterly source area in the Ordovician (Pettijohn, 1962). For shales analyzed in this study, detritus rich in K-feldspar must have been provided from the Canadian Shield until the end of Cambrian time. The decrease in K-feldspar abundance after the Cambrian is probably due to a new source area to the east, the Taconic uplift, which provided source rocks sparse in K-feldspar but richer in plagioclase. Feldspar type changes from K-feldspar in the Cambrian to plagioclase feldspar in the Ordovician in sediments in the Ouachita-Marathon geosyncline also (Weaver, 1961.)

Abundant K-feldspar is seen in Cambrian shales along the entire length of the Appalachian Basin. Lower Cambrian shales with 6-9% $K_2O$ and abundant K-feldspar are found in East-Central Greenland and Newfoundland (Swett and Smit, 1972). Shales with 8-12% $K_2O$ and abundant K-feldspar occur in the Lower Cambrian of Scotland (Bowie, and others, 1966). Lower Cambrian shales with 8.6% $K_2O$ and abundant K-feldspar occur in Georgia (Shearer, 1918). Insoluble residues in Lower Ordovician carbonate rocks in New York have 40% K-feldspar (Buyce and Friedman, 1975). Arkosic arenites with abundant K-feldspar, up to 50%, occur in the Cambrian of Wisconsin (Odom, 1975; Stablein and Dapples, 1977; Berg, 1952).

K-feldspar abundance decreases very abruptly after the Cambrian along the entire length of the Appalachian Basin. The Cartersville Formation in Georgia, a stratigraphic equivalent of the Rome, has an average of 30.8% normative K-feldspar, whereas the overlying Connasauga slate of Middle Cambrian age and the Rickmart slate of Upper Ordovician age have 0% normative K-feldspar (Shearer, 1918, p. 24). In this study, K-feldspar is abundant in shales from the Lower Cambrian Rome, the Middle Cambrian Rogersville, and the Upper Cambrian Nolichucky formations, but decreases abruptly after the Cambrian (Table 2). In Cambro-Ordovician carbonates in New York State, K-feldspar decreases in abundance very abruptly after the Middle Ordovician (Buyce and Friedman, 1975).

From thin-section analyses, Odom (1975) found that 85% of the K-feldspar was detrital and 15% authigenic in Cambrian Arkosic arenites of Wisconsin. Similar observations have been made in the Cambrian Mt. Simon sandstone (Metarko, 1980) and in the Rome Sandstones (Webb, 1980). According to Bowie, and others (1966), sand sized K-feldspars in potassic Lower Cambrian shales of Scotland have euhedral overgrowths of authigenic K-feldspar and are low in $Na_2O$ content (a characteristic of authigenic K-feldspars). The ratio of detrital to authigenic K-feldspar is 40:60 in Cambro-Ordovician carbonates of New York according to Buyce and Friedman (1975). This estimate was obtained from thin-section using a cathodoluminoscope. Swett and Smit (1975) feel that most of the K-feldspar in Lower Cambrian potassic shales of Newfoundland and East Greenland is authigenic, but do not present any modal analyses to prove this. It is possible that some authigenic K-feldspar exists in the $< 0.005$ mm. fraction of Cambrian shales analyzed in this study. The abundance of authigenic K-feldspar in the $< 0.005$ mm. fraction would be hard to determine quantitatively, so the ratio of detrital K-feldspar to authigenic K-feldspar remains unresolved. However, most of the shales are silty, less than 50% by weight of shales is $< 0.005$ mm. size and K-feldspar concentration in this fraction is less than half of that in the $> 0.005$ mm. fraction. Therefore, it seems likely that at least half the K-feldspar in these shales is detrital.

This study shows that the $K_2O$ content of Cambrian shales in the Appalachian Basin is high (9.0% mean) in comparison with the $K_2O$ content of Paleozoic shales in North America (3.6% mean), and that about 38% of the $K_2O$ is due to K-feldspar. Cathodoluminescence studies of silt in the shales and petrographic studies of associated

sandstone suggest that much, but not all, of the K-feldspar is detrital. Data collected in this study are insufficient to determine accurately what the contribution if illite is towards the increased $K_2O$.

## ACKNOWLEDGEMENTS

This paper is based on work I did for an M.S. thesis at the University of Cincinnati. I would like to thank J. B. Maynard and W. D. Huff for serving as advisors on my thesis committee and for reviewing initial drafts of this manuscript. Field work done to collect samples was supported by a grant from the H. N. Fisk Laboratory of Sedimentology, University of Cincinnati.

## REFERENCES CITED

Berg, R. R., 1952, Feldspathized sandstone. Jour. Sed. Petrology, v. 22, pp. 221-223.

Bowie, S. H. U., J. Dawson, M. J. Gallagher, and D. Ostle, 1966, Potassium rich sediments in the Cambrian of northwest Scotland. Trans. Institution of Mining and Metallurgy, v. 75, B125-B145, and Discussion, v. 76, B60-B-69.

Brown, William Randall, 1970, Investigations of the sedimentary record on the Piedmont and Blue Ridge of Virginia, Chapter 23 *in* Studies of Appalachian Geology: Central and southern. Wiley Interscience, New York, 460 pp.

Buyce, M. Raymond, and Gerald M. Friedman, 1975, Significance of authigenic K-feldspar in Cambrian-Ordovician carbonate rocks of the Proto-Atlantic Shelf in North America. Jour. Sed. Petrology, v. 45, no. 4, December, pp. 808-821.

Gibbs, R. J., 1965, Error due to segregation in quantitative clay mineral x-ray diffraction mounting techniques. Am. Min., v. 50, pp. 791-751.

Jackson, M. L., 1969, Soil Chemical Analysis - Advanced Course, 2nd edition, published by the author. Madison, Wisconsin, 895 pp.

Kastner, Miriam, 1974, The contribution of authigenic feldspars to the geochemical balance of alkali metals. Geochim. Cosmochim. Acta, v. 38, pp. 650-653.

Mackenzie, Fred T., 1975, Sedimentary cycling and the evolution of seawater, Chapter in Chemical Oceanography, v. I, eds. J. P. Riley and G. Skirrew. Academic Press, New York, 606 pp.

Markello, J. R., C. G. Tillman, and J. F. Read, 1979, Lithofacies and biostratigraphy of Cambrian and Ordovician platform and facies carbonates and clastics, southwestern Virginia. Field Trip no. 2 *in* Guides to Field Trips 1-3 for Southeastern Section Meeting of the Geological Society of America, Blacksburg, Virginia. Virginia Polytechnic and State University, 143 pp.

Medlin, J. H., N. H. Suhr, and J. B. Bodkin, 1969, Atomic absorption analysis of silicates employing $LiBo_2$ fusion. Atomic absorption Newsletter, v. 8, no. 2, pp. 25-29.

Metarko, Thomas, 1980, Porosity, water chemistry, cement and grain fabric with depth in the Upper Cambrian Mt. Simon and Lamotte sandstones of the Illinois Basin, 89 pp. M.S. thesis, University of Cincinnati.

Nanz, R. H., Jr., 1953, Chemical composition of Precambrian slates with notes on the geochemical evolution of lutites. Jour. Geology, v. 61, pp. 51-64.

Odom, I. Edgar, 1975, Feldspar-grain size relations in Cambrian arenites, Upper Mississippi Valley. Jour. Sed. Petrology, v. 45, pp. 636-651.

Pettijohn, F. J., 1962, Paleocurrents and paleography. Am. Assoc. Petroleum Geol. Bull., v. 46, pp. 1468-1493.

Ronov, A. B., and A. A. Migdisov, 1971, Geochemical history of the crystalline basement and the sedimentary cover of the Russian and North American platforms. Sedimentology, v. 16, pp. 127-185.

Shearer, H. K., 1918, The slate deposits of Georgia. Bull. Geol. Surv. Georgia, no. 34, 192 pp.

Stablein, N. K., III, and E. C. Dapples, 1977, Feldspars of the Tunnel City Group (Cambrian) western Wisconsin. Jour. Sed. Petrology, v. 47, no. 4, pp. 1512-1538.

Swett, K., and David E. Smith, 1972, Paleogeography and depositional environments of the Cambro-Ordovician shallow marine facies of the North Atlantic. Geol. Soc. America Bull., v. 83, no. 11, pp. 3228-3248.

Thomson, A. P., D. M. L. Duthie, and M. J. Wilson, 1972, Randomly oriented powders for quantitative x-ray determination of clay minerals. Clay Minerals, v. 9, pp. 345-348.

Van Moort, J. E., 1972, the $K_2O$, CaO, MgO and $CO_2$ contents of shales and related rocks and their importance for sedimentary evolution since the Proterozoic. Internal, Geol. Cong., 24th Session, Sec. 10, pp. 427-439.

Vinogradov, A. P., and A. B. Ronov, 1956 ., Evolution of the chemical composition of clays of the Russian platform. Geokhim., 2, pp. 3-18 (in Russian). English trans. in Geochemistry 2, 1960, pp. 123-139.

Weaver, Charles E., 1961, Clay minerals of the Ouachita structural belt and adjacent foreland. University of Texas, Publ. no. E120, pp. 147-162.

Weaver, Charles E., and Lin D. Pollard, 1973, The chemistry of clay minerals. Developments in sedimentology, v. 15. Elsevier Scientific Publishing Company. 213 pp.

Webb, E. J., 1980, Cambrian sedimentation and structural evolution of the Rome trough in Kentucky. 98 pp. PhD. thesis, University of Cincinnati.

White, W. A., 1959, Chemical composition and spectrochemical analyses of the Illinois clay material. Illinois State Geol. Surv. Circ. 282, 55 pp.

# THE CLINGMAN LINEAMENT, OTHER AEROMAGNETIC FEATURES, AND MAJOR LITHOTECTONIC UNITS IN PART OF THE SOUTHERN APPALACHIAN MOUNTAINS

A. E. Nelson *U. S. Geological Survey, Reston, VA, 22092*

Isidore Zeitz *Phoenix Corporation, McLean, VA, 22092*

## ABSTRACT

Some aeromagnetic anomalies and gradient trends in the southern Appalachians reflect deeply buried source rocks, whereas others apparently are related to the surface rocks. Parts of four lithotectonic units form the southern Appalachians in the Greenville and Knoxville 2 degree quadrangles. From northwest to southeast they are the Valley and Ridge, the Great Smoky thrust sheet, the Hayesville thrust sheet, and the Helen-Coweeta terrane, which separates the Hayesville thrust sheet into two parts. Magnetic anomalies over the Valley and Ridge and the western part of the Great Smoky thrust sheet generally have large wavelengths that reflect deeply buried magnetic source rocks in the Proterozoic Y(?) basement. Short wavelength anomalies in the eastern part of the Great Smoky thrust sheet, the Hayesville thrust sheet, and the Helen-Coweeta terrane appear to be superposed on broad wavelength anomalies. The short wavelength anomalies are believed to represent magnetic source rocks at or near the surface. Some zones of sheared rocks in the Helen-Coweeta terrane correspond closely to narrow northeast-trending magnetic lineaments.

A northeast-trending aeromagnetic lineament—the Clingman lineament—crosses parts of the Valley and Ridge and the Great Smoky thrust sheet and separates an area to the northwest, in which many of the broad wavelength anomalies trend N.15°E, from an area to the southeast in which the broad wavelength anomalies trend N.45-50°E and the overall magnetic intensities are higher. The broad wavelength anomalies and associated magnetic gradients are believed to reflect structural trends or trends of magnetic rock units in the basement. They do not appear to represent magnetic units in either the Valley and Ridge or the western part of the Great Smoky thrust sheet, both of which consist of rocks that are non- or only weakly magnetic. The Clingman lineament probably reflects a structural discontinuity, probably a fault, in the deeply buried Proterozoic Y(?) basement.

## INTRODUCTION

This report, which is based upon reconnaissance and some detailed geologic mapping in the Knoxville and Greenville quadrangles discusses the relationship between the geology and the aeromagnetic patterns in four tectonic-lithostratigraphic units, that form parts of the Valley and Ridge and Blue Ridge provinces (fig. 1). From northwest to southeast these are the undivided rocks of the Valley and Ridge, the Great Smoky thrust sheet, the Hayesville thrust sheet, and the Helen-Coweeta terrane (fig. 1).

Aeromagnetic and geologic maps covering parts of the Greenville and Knoxville quadrangles and adjacent parts of the southern Appalachians (figs. 1, 2 and 3) show that some areas are characterized by broad wavelength magnetic anomalies, whereas in other areas short wavelength anomalies predominate. The area shown in figure 3 and the ground underlain by the Valley and Ridge and the northwest part of the Great Smoky thrust sheet (fig. 2) have broad wavelength magnetic anomalies that probably represent the magnetic expression of deeply buried magnetic source rocks. In contrast the terrane underlain by the Hayesville sheet, Helen-Coweeta terrane, and the southeastern part of the Great Smoky sheet commonly have short wavelength anomalies that represent magnetic source rocks at or near the surface.

The rocks underlying the study area are allochthonous. Numerous southeast-

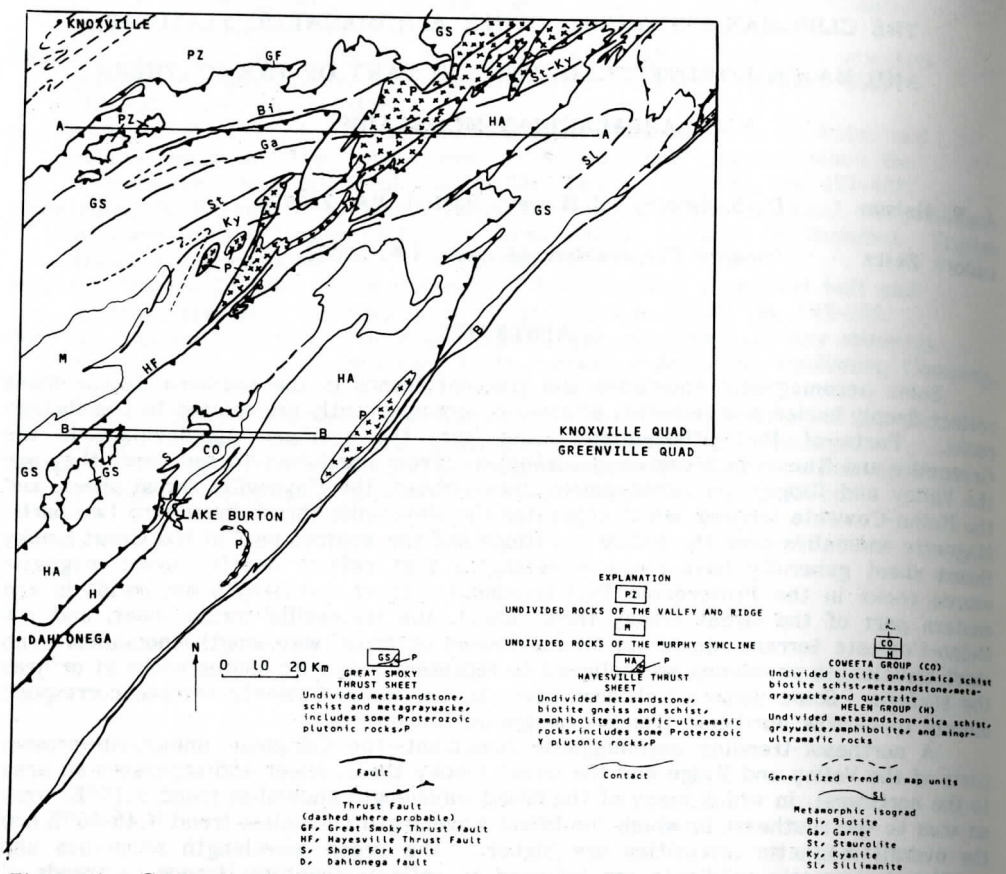


*Figure 1. Generalized geologic map of the study area in parts of the Knoxville and Greenville quadrangles, cross sections shown on figure 4.*

dipping thrust faults with westerly directed tectonic transport displace the folded rocks of the Valley and Ridge and those of the immediately adjacent western Blue Ridge province (Rodgers, 1953; King, 1964; Hadley and Goldsmith, 1963). One of these thrusts, the Great Smoky thrust fault, emplaces the western part of the Blue Ridge over the Valley and Ridge. Thrust faults also deform the Blue Ridge rocks farther east (Hadley and Goldsmith, 1963; Hadley and Nelson, 1971; Hatcher, 1971a and 1972). One of these eastern thrusts, the Hayesville fault (Hatcher, 1976, 1978; Wooten, 1979; Shellebarger, 1980) divides the Blue Ridge of the study area into two distinct terranes--the Great Smoky thrust sheet with its nonvolcanic rock assemblage deposited on Greenville basement to the northwest, and the Hayesville thrust sheet with its mafic volcanic units and associated metasedimentary rocks, granitic plutons, and mafic and ultramafic rocks to the east and southeast. The Hayesville thrust sheet is emplaced over the Great Smoky thrust sheet along the Hayesville fault, as indicated by the Brasstown Bald and Shooting Creek windows (fig. 1).

The unmetamorphosed rocks of the Valley and Ridge have been folded, and the Blue Ridge rocks are polydeformed and metamorphosed, except along the frontal edge. The metamorphic grade ranges from subchlorite and chlorite in the northwest to kyanite and sillimanite farther southeast (fig. 1).

## VALLEY AND RIDGE AND GREAT SMOKY THRUST SHEET

### General Geology

Sedimentary rocks underlying the Valley and Ridge range in age from Cambrian

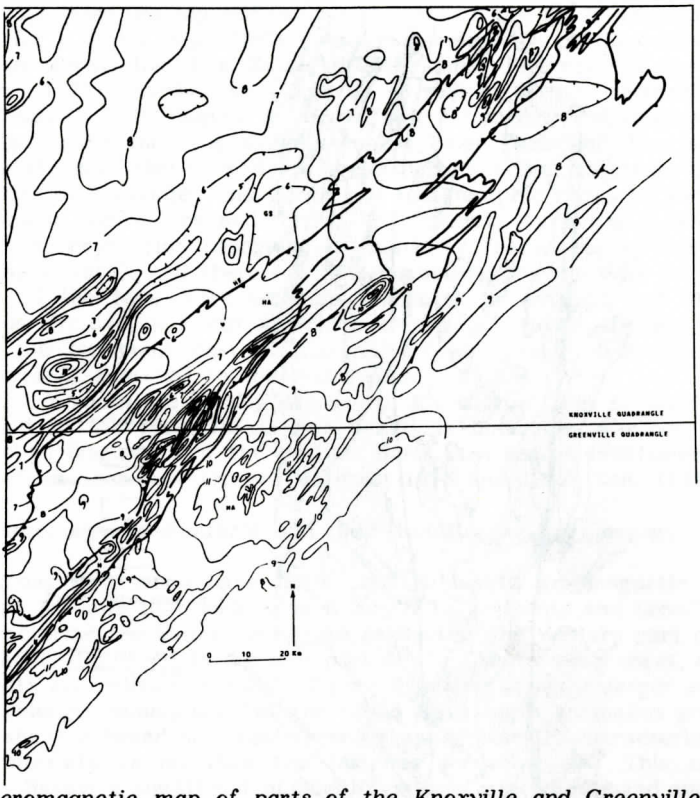


*Figure 2. Aeromagnetic map of parts of the Knoxville and Greenville quadrangles showing the distribution of some lithotectonic units, letter symbols same as on figure 1. Contour interval is one hundred gammas.*

to Pennsylvanian and consist of interlayered shale, siltstone, sandstone, quartz sandstone, arkose, conglomerate, limestone and dolomite, (fig. 1). These rocks, which generally strike northeast, are folded about northeast-trending fold axes.

Rock assemblages of the Ocoee Supergroup, the Chilhowee Group, and the Murphy syncline form the Great Smoky thrust sheet (fig. 1), exclusive of the basement rocks. Metamorphosed Proterozoic Z conglomerate, sandstone, quartzite, graywacke, siltstone, shale, and some dark carbonate rock make up most of the Ocoee Supergroup (Higgins and Zietz, 1975), they also form most of the Great Smoky thrust sheet. Metasandstone, ferruginous schist, mica schist, carbonaceous metasandstone and marble of Cambrian age form the rocks in the Murphy syncline, located in the east central part of the Great Smoky thrust sheet. Cambrian and Cambrian(?) shale, siltstone, sandstone and quartzite rock units form the Chilhowee Group (King, 1964; Neuman and Nelson, 1965) that is exposed in the western part of the Great Smoky thrust sheet. The Chilhowee rocks lie unconformably upon late Precambrian rocks of the Ocoee Supergroup.

Although some rocks of the Great Smoky thrust sheet have been metamorphosed to sillimanite grade and polydeformed, original bedding is locally preserved even at high grade. The major folds are commonly overturned to the northwest.

Exposed Proterozoic Y plutonic rocks and variably layered paragneisses form the basement rocks in the eastern part of the Great Smoky thrust sheet (fig. 1; Hadley and Nelson, 1971). The plutonic rocks include biotite augen gneiss, gneissic granite, calc-alkaline migmatite, and undifferentiated metagabbro or metadiorite. The paragneisses include biotite gneiss and schist, hornblende gneiss, amphibolite, biotite augen gneiss lenses, minor muscovite schist, and rare marble in addition to migmatite gneiss. Where the basement rocks have been dated in the Blue Ridge province, the ages range from 1,000 to 1,300 m.y., ages typical of the Greenville Province of eastern Canada and elsewhere in the Appalachian orogen (Rankin, 1975, p. 304).

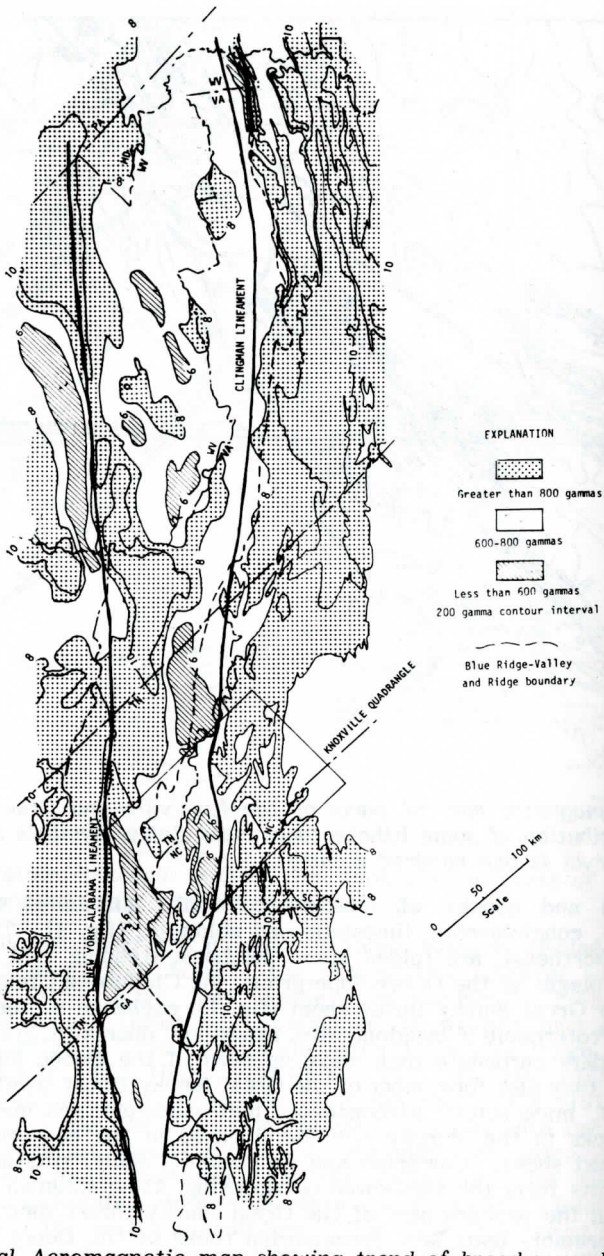


*Figure 3. Regional Aeromagnetic map showing trend of broad wave length anomalies. Between the New York-Alabama lineament and close to the Clingman lineament the anomalies commonly trend north-northeast whereas southeast of the Clingman lineament they trend northeast.*

King and Zietz (1978), Bass (1960), and Lidiak and others (1960) suggest that Proterozoic Y rocks form the basement west of the New York-Alabama lineament (King and Zietz, 1978; fig. 3). East of the New York-Alabama lineament (fig. 3) Proterozoic Y rocks are also believed to continue as the North American craton beneath the thick cover of the Valley and Ridge and Blue Ridge rock assemblages. From the New York-Alabama lineament (King and Zietz, 1978) southeastward for about 80 km (fig. 1), Proterozoic Y basement is not exposed at the surface. Within this area

the rocks covering basement are estimated to be at least 5 km thick based upon stratigraphic projections (Hadley and Goldsmith, 1963; King, 1964; Neuman and Nelson, 1965). Except for a 60 km gap, COCORP seismic reflection profiles extend from the Valley and Ridge across the Blue Ridge into the Inner Piedmont in the report area (Cook and others, 1979). Farther northeast, in the vicinity of the Grandfather Mountain area, discontinuous U. S. Geological Survey seismic reflection profiles extend from the Valley and Ridge across the Blue Ridge into the Inner Piedmont (Harris and others, 1981). Interpretations of these profiles suggest that crystalline basement is overlain by sedimentary rocks of the Valley and Ridge and metamorphic rocks of the Blue Ridge along a detachment zone (Cook and others, 1979; Harris and Bayer, 1979; Harris and others 1981). The crystalline basement is relatively featureless in seismic profiles (Harris and others, 1981), and there are not compelling seismic data to suggest that basement east of the New York-Alabama lineament is anything but the eastward extension of the Grenvillian North American craton. However, the possibility exists that parts of the basement east of the New York-Alabama lineament represents Precambrian terranes accreted to the craton (Zen, 1981).

Proterozoic Y rocks are locally exposed in the eastern part of the Great Smoky thrust sheet and in the Hayesville sheet but it is uncertain whether those rocks represent detached fragments of the cration, parts of a parauthochthonous craton, or possibly parts of an accreted terrane (Hatcher, 1978 and 1982; Zen, 1981).

## Aeromagnetic Features and their Relation to the Geology

Two aeromagnetic maps have been used to relate aeromagnetic features to geology. Figure 2 shows that wide spaced magnetic gradients and broad wavelength anomalies characterize the Valley and Ridge as well as the western part of the Great Smoky thrust sheet. However, in the east part of the Great Smoky sheet, close spaced short wave length anomalies dominate. Figure 3, which covers a larger area contains some short wavelength anomalies, but the broad wavelength anomalies predominate.

Figure 3 shows a broad northeast-trending zone generally characterized by lower aeromagnetic intensity values than the terranes bordering it. This zone is also distinguished by having a significant number of magnetic gradients and anomalies that trend N15°E, together with some that trend N45°E. This contrasts with the terrane to the southeast where the gradients and anomalies mostly trend N45°E. Within the Knoxville-Greenville area this lower intensity magnetic zone is about 95 km wide and farther to the northeast in the Maryland-West Virginia area it is about 140 km wide. The New York-Alabama lineament (King and Zietz, 1978) defines the northwest border of the zone. Another aeromagnetic lineament, herein called the Clingman lineament, marks its southeastern boundary. The Clingman lineament can be seen on regional aeromagnetic maps (King and Zietz, 1978; Zietz and Gilbert, 1980, and Zietz and others 1982), but it is somewhat obscured by the short wavelength anomalies (fig. 2). Northeast from near the central part of the Knoxville quadrangle the Clingman lineament parallels steep gravity gradients (Keller, 1979), between -70 and -80 mgal, that form the west side of a regional gravity low over a large part of the Blue Ridge and Inner Piedmont in North Carolina, Tennessee, and Virginia.

Figure 3 also shows the boundary between metamorphosed rocks of the Blue Ridge to the southeast and the generally unmetamorphosed rocks of the Valley and Ridge to the northwest. Most of the Blue Ridge rocks were emplaced over the Valley and Ridge rocks along a family of east-dipping thrust faults with a westerly-directed tectonic transport. In places the Blue Ridge Valley and Ridge boundary appears to follow the Clingman lineament. This might imply that the broad band of higher magnetic intensity values of the terrane east of the lineament is due to the Blue Ridge rocks; however, elsewhere, especially in the vicinity of the Knoxville quadrangle (fig. 3), the Blue Ridge Valley and Ridge boundary diverges considerably from the lineament at several places. This suggests that the broad band of higher magnetic values southeast of the Clingman lineament probably does not reflect the surface rocks of the Blue Ridge.

In the Knoxville quadrangle (fig. 2) the surface rocks of the Valley and Ridge and the western part of the Great Smoky thrust sheet have strike trends that cross the N15°E trending aeromagnetic gradients. The Proterozoic Z rocks, which form most of the western Great Smoky thrust sheet, are locally folded about northeast-trending fold

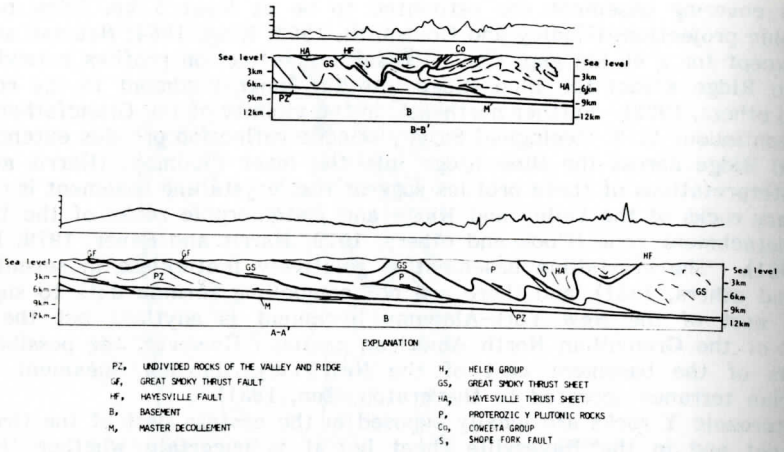


*Figure 4. Cross sections of lines A-A' and B-B' of figure 1 and corresponding magnetic profiles with scale of 100 gammas (LKB Resources, 1979). Position of master decollement extrapolated from COCORP seismic line (Cook and others, 1979) and U. S. Geological Survey seismic line (Harris and others, 1981).*

axes, and the lithologic units have variable strike trends, some of which are at a high angle to the aeromagnetic gradient trends (Hadley and Nelson, 1971; figs. 1 and 2). Except around some minor folds, the Paleozoic rocks that underlie the Valley and Ridge province strike uniformly N45-50°E (Hadley and Nelson, 1971) in contrast to the more northerly-trending magnetic gradients. The surface rocks in both the Valley and Ridge and the western part of the Great Smoky sheet do not have any appreciable effect on the aeromagnetic patterns and they are believed to be non- or only slightly magnetic. Therefore the broad wavelength anomalies in these areas probably correspond to magentic fields associated with the deeper buried basement.

East-west magnetic profiles (LKB Resources, Inc., 1979; fig. 1 and fig. 4) were drawn across the Valley and Ridge and the Great Smoky thrust sheet in the Knoxville quadrangle. These profiles show that rock units of the Valley and Ridge and the Proterozoic Z rock units of the Great Smoky thrust sheet are not strongly magnetic. In contrast, the Proterozoic Y rocks of the Great Smoky thrust sheet and the rock units of the Hayesville thrust sheet are both moderately magnetic. The profiles do not show any changes across those areas where rocks of the Valley and Ridge are adjacent to and where they are overlain by rocks of the Ocoee Supergroup in the Great Smoky thrust sheet. Furthermore, the magnetic profiles across areas of Ocoee rocks show little, if any, magnetic changes where the rock units range from less than 1/2 km to more than 5 km in thickness. Therefore, cover-rock thicknesses, especially in the Valley and Ridge and the western part of the Great Smoky sheet, do not seem to have much of an effect upon aeromagnetic gradients.

In areas where the basement is thickly mantled with cover rock of the Valley and Ridge and rocks of the Ocoee Supergroup in the Great Smoky sheet magnetic profiles show broad wavelength anomalies with broad gentle gradients (LKB Resources Inc., 1979; fig. 4). However, in the eastern part of the Great Smoky sheet the profiles show irregular short wavelength anomalies, but because some anomalies have lower magnetic intensities than the contour intervals of the aeromagnetic maps (figs. 2 and 3) they do not always appear on the maps (figs. 2, 3, and 4). These short wavelength anomalies appear to correspond with rocks of the Murphy syncline, Proterozoic Y rocks, as well as those of the Hayesville sheet and Helen-Coweeta terrane farther to the east.

The imprint of regional metamorphism does not seem to have noticeably effected the broad wavelength magnetic trends shown in the northwestern part of the Great Smoky sheet (figs. 2 and 3). The geologic map (fig. 1) gives the isograd distribution for the metamorphic index minerals in the northern part of the Knoxville quadrangle and shows they have somewhat variable trends that range from northeast to east-northeast. North of the staurolite zone, where the isograds cross magnetic gradients and anomalies commonly at high angles, the magnetic patterns and trends do not appear

to be related to or affected by the isograds. South of the staurolite isograd most other isograds generally have northeast trends that are closer to the regional trend of the aeromagnetic gradients.

In the northwest part of the Great Smoky sheet, especially northwest of the staurolite isograd, structurally imposed changes in the strikes of rock units, significant changes in rock thicknesses, or varying metamorphic grades do not seem to have any apparent effect on the magnetic gradient trends. Therefore, we interpret these aeromagnetic trends to reflect structural trends of magnetic source rocks in the deeply buried Proterozoic Y basement.

Magnetic features associated with the terrane between the Clingman lineament and the New York-Alabama lineament (fig. 3) reflect trends of magnetic source rocks in the deeply buried basement and, as such, probably represent lithologic or structural trends in the basement. Therefore we believe that lithologic units or structures in the basement in the northwest part of this terrane trend N15°E and then, as the Clingman lineament is approached, structures assume a more southwest- northeast trend to correspond with the magnetic trends. Similarly, on the southeast side most of the lithologic units or structures trend N45°E.

King and Zietz (1978) indicate that the New York-Alabama lineament represents a major crustal break, perhaps a strike-slip fault in the basement beneath the Appalachian basin. They report that it extends 1,600 km from New York to Alabama and marks the southeast edge of a stable crustal block. The terrane southeast of the New York-Alabama lineament may represent a faulted fragment of the North American craton or possibly a part of an ancient accreted terrane. The Clingman lineament may represent a subsidiary fault similar to the proposed fault of King and Zietz or a major Proterozoic Y lithologic boundary, possibly a Precambrian boundary of an accreted terrane.

## HAYESVILLE THRUST SHEET

### General Geology

Several major rock assemblages and some minor Proterozoic Y basement rocks, make up the Hayesville thrust sheet (fig. 1). These include: the Tallulah Falls Formation (Galpin, 1915; Hatcher, 1971a, and b, 1974), that occupies most of the eastern part, and the Richard Russell Formation of Gillon (1982), which occupies most of the western half of the sheet. Rocks of the Richard Russell Formation are probably equivalent to the Tallulah Falls Formation (Hatcher, oral commun., 1979), but these rock units are separated by the Helen-Coweeta terrane which divides a part of the Hayesville thrust sheet into its eastern and western halves (fig. 1). Two windows of the Great Smoky thrust sheet are present near the northwestern edge of the Hayesville thrust sheet (fig. 1).

The principal rock types forming the Hayesville thrust sheet are metagraywacke, metaquartzite, meta-arenite, biotite schist and gneiss, and amphibolite. In addition, a wide variety of ultramafic and mafic rocks are present as small discontinuous outcrop-size pods as well as some large units covering many acres (Hadley and Nelson, 1971). These rocks are chiefly serpentinite, dunite, pyroxenite, gabbro, and amphibolite (Hartley, 1973). Locally, some of these rocks are rich in magnetite. The mafic and ultramafic rocks are found only on the southeast side of the Hayesville fault (fig. 1) in the Hayesville thrust sheet. They are especially common northeast from Brasstown Bald (fig. 1) for about 120 km. In fact, they continue on the southeast side of the fault and its northeasterly extension into Newfoundland (Rankin, 1975, Williams, 1978). Numerous granitic, granodioritic, quartz monzonitic, and tonalitic gneisses are also present in the Hayesville thrust sheet.

Although the mafic and ultramafic rocks are present within the Hayesville thrust sheet, their relationship to the sheet is uncertain. They have chemical affinities with mantle rocks (Hartley, 1973, p. 59) and as such may represent fragments of oceanic crust (dismembered ophiolites) caught up in the Hayesville thrust sheet. Locally some of these rocks may actually be underneath rather than part of the Hayesville sheet. If so, they would be interpreted as a small, separate thrust slice of oceanic crust.

Rocks of the Hayesville thrust sheet are polydeformed. Bedding is seldom

preserved and the most prevalent structure is a discontinous compositional layering that is probably the result of metamorphic differentiation and transposition of bedding into the regional foliation (Hatcher, 1976, p. 17). Hatcher (1976, p. 14; oral commun., 1979) reports six phases of folding in some rocks of the Tallulah Falls Formation. Throughout most of the sheet, the rocks are of kyanite to sillimanite grade.

### Aeromagnetic Features and their Relation to the Geology

Because of the small scale of the maps (figs. 1 and 2) and the inconsistent relation between specific rock types and their magnetic susceptibilities, only the general magnetic character of the Hayesville sheet, and later the Helen-Coweeta terrane, will be discussed. For example, within both the Hayesville sheet and the Helen-Coweeta terrane, not all meta-arenites and mica schists correlate with magnetic low areas nor do all amphibolite units relate to magnetic high areas. Daniels (oral commun., 1981) made nonquantitative magnetic susceptibility readings on selected samples from both the Hayesville sheet and the Helen-Coweeta terrane that showed some amphibolites are nonmagnetic, whereas some meta-arenities and mica schists are magnetic. Although parts of the Hayesville thrust sheet have widely spaced magnetic contours, the thrust sheet characteristically has numerous small areas where northeast-trending short-wavelength anomalies are present. In general, most of the magnetic anomalies seem to correspond to groups of rock, as for example where undivided magnetite-bearing amphibolites are relatively abundant in an interlayered assemblage of only slightly magnetic metagraywacke, metasandstone, and schist. The Hayesville and Great Smoky thrust sheets have contrasting lithologic assemblages, and the magnetic intensities for the area of the Hayesville are generally higher and more variable than those associated with the Great Smoky sheet (fig. 2). Lithologic units in the Great Smoky thrust sheet are generally nonmagnetic or only slightly magnetic, whereas many of the Hayesville rock units are locally rich in magnetite and have relatively higher magnetic intensities. In addition, mafic-ultramafic rocks which are also locally rich in magnetite are present as undivided rocks throughout the Hayesville thrust sheet. On the southeast side of the Helen-Coweeta terrane, an incompletely mapped granitic gneiss and migmatite appears to correlate with a positive magnetic anomaly. East-west magnetic profiles across the Hayesville thrust sheet characteristically show many short wavelength anomalies with steep gradients, whereas profiles across the Great Smoky thrust sheet and the Valley and Ridge generally have smooth curves with gentle gradients (LKB Resources, Inc., 1979; fig. 4).

Although the Hayesville fault separates the terranes of the Great Smoky and Hayesville thrust sheets, it does not show up as a distinct lineament on the aeromagnetic map (fig. 2) except for a small area in the southern part of the Knoxville quadrangle where the fault roughly coincides with a magnetic low. This probably occurs because a relatively thin wedge of the Hayesville thrust sheet rests on the thicker section of the weakly magnetic Great Smoky thrust sheet near and along the east-dipping fault and because magnetite-rich Hayesville rocks are not present along all parts of the fault trace.

The eastern border of the Hayesville thrust sheet is the Brevard zone. Although it is a geologically significant feature, this fault zone is not particularly well defined on the aeromagnetic map (figs. 1 and 2).

## THE HELEN-COWEETA TERRANE

### General Geology

Rocks from the Helen Group (Gillon 1982) and the Coweeta Group (Hatcher 1979) form the Helen-Coweeta terrane (fig. 1), which extends northeast from near Dahlonega in the Greenville quadrangle. This terrane has a variable width and it divides the Hayesville thrust sheet into two main areas (fig. 1). The Helen Group consists of metagraywacke that is locally sulfidic, meta-arenite that is locally conglomeratic, metaquartzite, mica schist, graphite schist, amphibolite and hornblende gneiss. Commonly these lithologic units, which are not divided on the geologic map (fig. 1), are distinctly layered and continuous over relatively long distances, and, although these

rocks are transposed, evidence for extensive transposition is lacking. Several granitic gneiss bodies as well as some small mafic and ultramafic bodies are also present. From the Dahlonega area northeast toward Burton Lake the rocks of the Helen Group range from staurolite to kyanite grade, whereas the adjoining rocks of the Hayesville thrust sheet are at sillimanite grade (Gillon, 1982). Although prograde metamorphic rocks form most of the Helen Group, some rocks are retrograded.

Rock assemblages of the Coweeta Group (Hatcher, 1979) are principally exposed near the Georgia-North Carolina border. These rocks include feldspar-quartz-biotite gneiss, aluminous schist, garnetiferous biotite schist, metasandstone, metaquartzite, and minor amphibolite. These rocks range from staurolite-kyanite to sillimanite grade, but locally they are retrograded.

The Helen-Coweeta terrane has been intensely deformed by both brittle and ductile faulting. The southeast side of the belt near Dahlonega (fig. 1) is bounded by a fault that has been referred to as the Dahlonega shear zone (Fairly, 1973, p. 693; and Crickmay, 1952, p. 48). The northwest side of the terrane is bounded by the Shope Fork fault that was mapped by Hatcher (1979) near the Georgia-North Carolina boundary. Recent geologic mapping shows that the Shope Fork fault extends southwestward toward Dahlonega (Gillon, 1982). The Shope Fork fault appears to join the Hayesville fault southwest of the Greenville quadrangle.

## Aeromagnetic Features and their Relations to the Geology

Closely spaced long linear short wavelength anomalies parallel the northeast striking rock units of the Helen-Coweeta terrane (figs. 1 and 2). Although these anomalies are generally closer spaced than similar anomalies in the adjoining Hayesville thrust sheet, magnetic profiles (fig. 4) from both lithotectonic units show they have about the same range of magnetic intensities. Some closely spaced anomalies, which are present in the adjacent Hayesville sheet, may be in part due to magnetic source rocks of the Helen-Coweeta terrane that structurally underlies the Hayesville sheet (fig. 4). The short wavelength anomalies and associated lineaments, which are present throughout much of the terrane, extend southwestward beyond the study area into the Rome quadrangle (fig. 2).

The magnetic lineaments in the southern part of the Helen-Coweeta terrane appear to be on strike with both fault and shear zones described by Bowen (1961) farther to the southwest. Therefore, we suggest that the faults and shear zones in the terrane also extend southwestward to form part of a larger fault or shear zone in north Georgia. Aeromagnetic lineaments shown on the Rome aeromagnetic map may help define the proposed fault zone and the southwest continuation of the Helen Group.

## CONCLUSIONS

1. In the Knoxville quadrangle rocks forming the Valley and Ridge and the western part of the Great Smoky thrust sheet are non or only slightly magnetic.
2. Large wavelength magnetic anomalies over the Valley and Ridge, and adjacent parts of the Blue Ridge reflect trends of deeply buried magnetic source rocks in the Proterozoic Y basement.
3. The Clingman lineament probably represents a structural discontinuity, possibly a fault, in the concealed Proterozoic Y basement.
4. Rocks of the Hayesville sheet and the Helen-Coweeta terrane have magnetic intensities that are more variable and generally higher than those associated with rocks in the southeastern part of the Great Smoky sheet. Magnetic profiles across the Great Smoky sheet generally have smooth curves with gentle gradients, whereas profiles across the Hayesville sheet and the Helen-Coweeta terrane characteristically show many short wavelength anomalies with steep gradients.

## ACKNOWLEDGEMENTS

The authors wish to thank J. K. Costain, R. D. Hatcher, Jr., D. S. Harwood, R. G. Simpson, L. S. Wiener for their critical reviews which were most helpful and resulted in considerable improvement of the manuscript. We are grateful for the

helpful informal discussions with E. R. King, and D. L. Daniels.

## REFERENCES CITED

Bass, M. U. 1960, Grenville boundary in Ohio: Journal. Geology, v. 68, p. 673-677.

Bowen, Boone Moss, Jr., 1961, The structural geology of a portion of southeastern Dawson County, Georgia: Unpublished M.S. thesis, Emory University, 45 p.

Cook, Frederick A., Albaugh, Dennis S., Brown, Larry D., Kaufman, Sidney, Oliver, Jack E., and Hatcher, Robert D., 1979, Thin-skinned tectonics in the crystalline southern Appalachians, COCORP seismic reflection profiling of the Blue Ridge and Piedmont: Geology, v. 7, p. 563-567.

Crickmay, G. W., 1952, Geology of the crystalline rocks of Georgia: Georgia Geological Survey Bull. 58, 54 p.

Fairley, W. M., 1973, Correlation of stratigraphic belts of northwest Georgia Piedmont and Blue Ridge: American Journal Science., v. 273, no. 8, 686-697.

Galpin, S. L., 1915, A preliminary report on the feldspar and mica deposits of Georgia: Georgia Geological Survey Bulletin 30, 190 p.

Gillon, K. A., 1982, Stratigraphic, structural and metamorphic geology of portions of the Cowrock and Helen Georgia 7 1/2' quadrangles: Unpublished M.S. thesis, Univ. of Georgia, Athens, Georgia, 236 p.

Hadley, J. B., and Goldsmith, Richard, 1963, Geology of the Great Smoky Mountains, North Carolina and Tennessee: U. S. Geological Survey Professional Paper, 349-B, 118 p.

Hadley, J. B., and Nelson, A. E., 1971, Geologic map of the Knoxville quadrangle North Carolina, Tennessee, and South Carolina: U. S. Geological Survey Miscellaneous Geologic Investigation Map I-654, scale 1:250,000.

Harris, Leonard D., Harris, Anita G., de Witt, Wallace, Jr., 1981, Evaluation of southern eastern overthrust belt beneath the Blue Ridge-Piedmont thrust: American Association Petroleum Geologists Bulletin v. 65, no. 12, 9 p.

Harris, Leonard D., and Bayer, Kenneth C., 1979, Sequential development of the Appalachian orogen above a master decollement - A hypothesis: Geology, v. 7, p. 568-572.

Hartley, M. E., III, 1973, Ultramafic and related rocks in the vicinity of Lake Chatuge: Georgia Geological Survey Bulletin 85, 61 p.

Hatcher, R. D., Jr., 1971a, Geology of Rabun and Habersham Counties, Georgia: a reconnaissance study: Georgia Department of Mines, Mining, and Geology Bulletin 83, 48 p.

_____1971b, Stratigraphic, petrologic, and structural evidence favoring a thrust solution to the Brevard problem: American Journal Science v. 270, no. 3, p. 177-202.

_____1972, Development model for the southern Appalachians: Geological Society America Bulletin, v. 83, p. 2735-2760.

_____1974, Introduction to the tectonic history of northeastern Georgia: Geological Survey Guidebook 13-A, 59-60 p.

_____1976, Introduction to the geology of the eastern Blue Ridge of the Carolinas and nearby Georgia: Carolina Geological Society Guidebook, 53 p.

_____1978, Tectonics of the western Piedmont and Blue Ridge, southern Appalachians: Review and Speculations: American Journal Science, v. 278, p. 276-304.

_____1979, The Coweeta Group and Coweeta Syncline: Major features of the North Carolina-Georgia Blue Ridge: Southeastern Geology, v. 4, no. 1, p. 17-29.

_____1982, Southern and central Appalachian basement massifs: Geological Society America Abstracts with programs, p. 24.

Higgins, M. W., and Zietz, Isidore, 1975, Geologic interpretation of aeromagnetic and aeroradioactivity maps of northern Georgia: U.S. Geological Survey Miscellaneous Geological Investigation Map I-783.

Keller, G. R., 1979, Simple Bouger gravity map, in Seay, W. H., Southern Appalachian tectonic study: Tennessee Valley Authority, Division of Water Management, Geological Services Branch, 66 p.

King, P. B., 1964, Geology of the central Great Smoky Mountains, Tennessee: U. S. Geological Survey Professional Paper 349-C, 148 p.

King, Elizabeth R., and Zietz, Isidore, 1978, The New York-Alabama lineament: geophysical evidence for a major crustal break in the basement beneath the Appalachian basin: Geology, v. 6, p. 312-318.

Lidiak, Edward G., Marvin, R. F., Thomas, H. H., and Bass, M. U., 1960, Geochronology of the midcontinent region, United States: Pt. 4, eastern area: Journal Geophysical Research, v. 71, p. 5427-5438.

LKB Resources, Inc., 1979, NURE aerial gamma ray and magnetic reconnaissance survey. (No. 57-79), Blue Ridge area, v. 2, Knoxville N1 17-1 quadrangle: Huntington Valley, Pa., (n.p.).

Neuman, R. B., and Nelson, W. H., 1965, Geology of the western part of the Great Smoky Mountains, Tennessee and North Carolina: U. S. Geological Survey Professional Paper 349-D, 81 p.

Rankin, D. W., 1975, The continental margin of eastern North America in the southern Appalachians: the opening and closing of the Proto-Atlantic Ocean: American Journal Science., v. 275-A, p. 298-336.

Rodgers, John, 1953, Geologic map of east Tennessee with explanatory text: Tennessee Division Geological Bulletin 58, 168 p.

Shellebarger, J. E., 1980, A preliminary report on the geology of the Coosa Bald and Jack's Gap quadrangles, Georgia: Unpublished M.S. thesis, Univ. Georgia, Athens, 209 p.

Williams, Harold, 1978, Tectonic lithofacies map of the Appalachian Orogen: St. John, Newfoundland Memorial University, scale 1:1,000,000.

Wooten, R. M., 1979, Geology of the southern half of the Hayesville quadrangle, North Carolina: Unpublished M.S. thesis, University. Georgia, Athens.

Zen, E-an, 1981, An alternative model for the development of the Allochthonous southern Appalachian Piedmont: American Journal Science, v. 281, 11 p.

Zietz, Isidore and Gilbert, Francis, 1980, Aeromagnetic map of part of the southeastern United States: in color: U. S. Geological Survey Geophysical Investigation map, GP. 936.

Zietz, Isidore, 1982, Composite magnetic anomaly map of the United States Part A: Conterminous United States: U. S. Geological Survey Geophysical Investigation map, G. P. 954 A.